SEDIMENTOLOGY AND STRATIGRAPHY OF THE CAMPANO – MAASTRICHTIAN SUCCESSION, NORTHEAST OF IDAH TOWN, NORTHERN ANAMBRA BASIN.

BY

Lukman Musa ADAMU

(P13SCGL8004)

A DISSERTATION SUBMITTED TO THE SCHOOL OF POSTGRADUATE STUDIES, AHMADU BELLO UNIVERSITY, ZARIA

IN PARTIAL FULFILMENT OF THE REQUIREMENTS FOR THE AWARD OF A MASTER OF SCIENCE DEGREE IN GEOLOGY.

DEPARTMENT OF GEOLOGY

FACULTY OF PHYSICAL SCIENCE

AHMADU BELLO UNIVERSITY, ZARIA

NIGERIA.

APRIL, 2017.

SEDIMENTOLOGY AND STRATIGRAPHY OF THE CAMPANO – MAASTRICHTIAN SUCCESSION, NORTHEAST OF IDAH TOWN, NORTHERN ANAMBRA BASIN.

BY

Lukman Musa ADAMU

(P13SCGL8004)

A DISSERTATION SUBMITTED TO THE SCHOOL OF POSTGRADUATE STUDIES, AHMADU BELLO UNIVERSITY, ZARIA

IN PARTIAL FULFILMENT OF THE REQUIREMENTS FOR THE AWARD OF A MASTER OF SCIENCE DEGREE IN GEOLOGY.

DEPARTMENT OF GEOLOGY

FACULTY OF PHYSICAL SCIENCE

AHMADU BELLO UNIVERSITY, ZARIA

NIGERIA.

APRIL, 2017.

DECLARATION

I declare that the work in this dissertation entitled "**Sedimentology and Stratigraphy of the Campano-Maastrichtian succession northeast of Idah Town, northern Anambra Basin**" has been carried out by me and is a record of my own research work under the supervision of Professor H. Hamza and Dr. I. Hamidu. All the information derived from literature has been duly acknowledged in the text and a list of references provided. No part of this dissertation was previously presented for another degree or diploma at this or any other institution.

Name of Student	Signature	Date

CERTIFICATION

This dissertation entitled "Sedimentology and Stratigraphy of the Campano-Maastrichtian succession northeast of Idah Town, northern Anambra Basin" by ADAMU, Lukman Musa meets the regulations governing the award of master's degree in Geology (Petroleum Geology) of the Ahmadu Bello University, and is approved for its contribution to knowledge and literary presentation.

Chairman, Supervisory Committee	Signature	Date
Member, Supervisory Committee	Signature	Date
Head of Department	Signature	Date
Dean, School of Postgraduate Studies	Signature	Date

ACKNOWLEDGEMENTS

I thank Almighty Allah for his love, protection, knowledge and inspiration throughout this research work.

My profound gratitude goes to my supervisors Professor H. Hamza and Dr. I. Hamidu who had the time from out of their tight schedules to supervise this research as well as putting me through when I am faced with challenges. Their criticism, excellent and precise suggestions made this work a reality.

Many thanks to my lecturers such as Professor U.A. Danbatta, Professor S.A. Alagbe, Dr. A. E. Ikpokonte, Dr. .E.O. Obiosio, Dr. T. Najime, Dr. S.A. Arabi, Dr. I.Y. Abubakar, Dr. B. A. Jolly, Dr. S. S. Magaji and the non – academic staff such as Mr. E. Animashawun, Mr. O. Onyeamechi, Mallam Muhammed, Mallam Yashe and Mr. Kwaru. To all lecturers not mentioned and staff of Geology Department who have contributed or assisted me in the course of this research I say a big thank you.

My sincere gratitude goes to my parents and guardians Late Alhaji Adamu Musa, Hajiya Khadijat Adamu, Mrs Habibat Adams, Professor N.G Obaje, Mr Adams Tahiru and Dr. O. Atabo for their immense contribution towards the success of this work. I specially acknowledge the encouragement given to me by my ever supporting siblings, Adama Ali, Adama Murtala, Adama Ramotu, Umoru Ramotu, Adama Amina, Adama Ibrahim, Adama Muhammed, Adama Abdul, Adama Abbas, Umoru Iyadi, Adama Abubakar, Brother Shehu (Imam), Ademu Lawal, Haleema Alhassan. The entire family of ADAMA MUSA and UMORU KOSHE, wife, Mrs. Adejoh Nefisat Lukman and daughters, Lukman Nadia and Lukman Na'eemah. I love you all.

I would like to thank and appreciate the companionship, contribution and understanding of my friends and colleagues particularly Mr. H. Abdulmalik, Mr. A. Abdullahi, Mr. M. Kovona, Mr. I. Waziri, Mr. M. Kitha, Mr. A. Usman, Mr. S. Adedeji, Mr. J. Jonathan, Mr. S. Abbah, Mr. H. Grema, Mr. A. M. Yahuza, Miss. A. Joy, Miss. H. Serah, Miss. Hauwa M. Mshelia, Miss. Brenda Agidi, Miss. Kwatam (Engr), Mr. A. Jarumi, Mr. E. Kundila, Mr. O. Bernard, Mr. A. Umaru, Mr. A. Abubakar, Mr. E. Charlse, Mr. A. Femi (Geosolutionz). For all your contributions and support I remain grateful.

To those not mentioned, you are equally important and appreciated. I remain loyal.

DEDICATION

This Dissertation is dedicated to my children (Nadia and Na'eemah) and parents/guardians Mrs Habibat A. A.

ABSTRACT

The Campano-Maastrichtian successions in the northern Anambra Basin comprises the Nkporo Formation, Mamu Formation and Ajali Sandstone. An extensive geological field work was carried out, where lithostratigraphic sections were studied and described. Features such as textures, physical and biogenic sedimentary structures (facies variations and associations) were documented. Some selected representative samples of the sedimentary depositional facies were also subjected to grain size analysis. The Nkporo Shale is made up of sandy shale, silty clay, grey mud, bioturbated siltstone which graded into Mamu Formation which is made up of cross-massive bedded sandstone with bioturbation structures, siltstone, dark grey to light grey fissile shale, mudstone and milky white claystone which often displays a fining upward trend. It passes upward into Ajali Sandstone which is made up of fine to coarse-grained, cross-bedded sandstone and fissile shale with bioturbation structures. The sandstone facies of the Mamu Formation is coarse to fine-grained, poorly to moderately sorted, leptokurtic and negatively skewed possibly deposited from fluvial source. The bioturbated lower sandstone beds contain burrows of *Ophiomorpha* which belong to skolithos ichnofacies that typifies littoral environment while the Ajali Sandstone is pebbly coarse to medium-grained, poorly to moderately sorted, predominants mesokurtic to platykurtic or very platykurtic and negative to near symmetrical. The linear discriminate function scatter plots results reveal shallow marine deposits for the sandstone facies of Mamu Formation and Ajali Sandstone.

The fissility of shale suggests that it was deposited in a low energy environment. However, the textural studies of the Nkporo Formation and the siltstone facies of the Mamu Formation suggests the sediments to be deposited in a low energy environment which favoured deposition of fine to medium size sediments, that is, delta plain to prodelta environment. Field and textural studies of the sandstone facies of the Mamu Formation suggest the sediments to be deposited in a relatively high energy environment with tidal influence of transport and deposition with two main facies association, that is, subtidal and intertidal. The cross-beddings, unimodal paleocurrent of Ajali Sandstones also indicates fluvial or fluvial-dominated deltaic environment while the bimodal oblique paleocurrent pattern obtained for Mamu Formation shows that the formation was deposited in environment such as shoreline (beach) or fluvio-deltaic where tidal effect is significant. Paleocurrent studies and textural characteristics indicate that the paleocurrent direction is northeast while the provenance is southwest suggesting that the sediments were mainly sourced from the Santonian Okigwe-Abakaliki Anticlinorium and partly from the nearby Oban Massif for the Ajali Sandstone in the study area while the sediments of the sandstone facies of Mamu Formation were sourced from more than one source. The results obtained from the textural, structure and statistical analyses revealed that the sediments in the study area were deposited in fluvial, delta front through delta plain to prodelta in shallow marine environment.

TABLE OF CONTENTS

Title page - - - - - - - - - - i

Declaration - - - - - - - - - - ii

Certification - - - - - - - - - - iii

Acknowledgement - - - - - - - - - - iv

Dedication - - - - - - - - - - v

Abstract - - - - - - - - - - vi

Table of contents - - - - - - - - - vii

List of Figures - - - - - - - - - xi

List of Tables - - - - - - - - - - xiii

List of Plates - - - - - - - - - - xiv

List of Appendices - - - - - - - - - xvi

CHAPTER ONE: INTRODUCTION

1.1 Introduction - - - - - - - - - 1

1.2 Statement of research problem - - - - - - 1

1.3 Justification - - - - - - - - - 2

1.4 Aim and Objectives - - - - - - - - 3

1.5 Location and accessibility of the study area - - - - - 3

1.6 Scope and limitation of the study - - - - - - 3

1.7 Climate and Vegetation - - - - - - - 4

1.8 Relief and Drainage - - - - - - - - 5

CHAPTER TWO: LITERATURE REVIEW

2.1 Introduction - - - - - - - - - 6

2.2 The Anambra Basin Territory - - - - - - 8

2.3 Regional Tectonics and Stratigraphic Setting of the Anambra Basin - 11

2.4 Origin and Structure of the Companian- Maastrichtian Succession in the Anambra Basin - - - - - - - - - - 14

2.5 Stratigraphic Setting of the Late Campanian – Maastrichtian Succession of the Anambra Basin - - - - - - - - 18

2.6. Systematic lithostratigraphy of the Late Companian- Maastrichtian Succession of the Anambra Basin - - - - - - - - 20

2.6.1 Nkporo Group - - - - - - - - - 20

2.6.1.1 Nkporo Shale - - - - - - - - - 21

2.6.1.2 Owelli Sandstone - - - - - - - - 22

2.6.1.3 Enugu Shale - - - - - - - - - 24

2.6.2 Coal Measures- - - - - - - - - 26

2.6.2.1 Mamu Formation - - - - - - - - 26

2.6.2.2 Ajali Sandstone - - - - - - - - 27

2.6.2.3 Nsukka Formation - - - - - - - - 29

CHAPTER THREE: METHODOLOGY

3.1 Introduction - - - - - - - - - 32

3.2 Desk study - - - - - - - - - 32

3.3 Field Work - - - - - - - - - 32

3.4 Laboratory Sample Preparation and Analysis - - - - 32

3.4.1 Granulometric Analysis - - - - - - - 32

3.4.2 Paleocurrent Analysis - - - - - - - 34

3.4.3 Data Processing and Compilation of Report - - - - - 34

CHAPTER FOUR: RESULTS

4.1 Introduction - - - - - - - - - 37

4.2 Lithostragraphic sections - - - - - - - 37

4.2.1 Nkporo Shale - - - - - - - - - 37

4.2.2 Mamu Formation - - - - - - - - 41

4.2.3 Ajali Sandstone - - - - - - - - 54

4.3 Granulometric Studies - - - - - - - 60

4.3.1 Grain size and statistical parameters - - - - - - 60

4.3.2 Univariate grain size parameters - - - - - - 63

4.3.3 Linear discriminate function - - - - - - - 65

4.3.4 CM pattern - - - - - - - - - 68

4.4 Paleocurrent Studies - - - - - - - - 69

CHAPTER FIVE: DISCUSSION

5.1 Sedimentology, Facies description and Depositional Environments of the Campanian – Maastrichtian Succession in the study area - - - - - 76

5.1.1 Nkporo Shale - - - - - - - - - 76

5.1.2 Mamu Formation - - - - - - - - 77

5.1.3 Ajali Sandstone - - - - - - - - 84

5.2 Lithostratigraphic Overview of the Study Area - - - - 86

5.3 Paleocurrent Studies - - - - - - - - 87

5.3.1 Ajali Sandstone - - - - - - - - 87

5.3.1 Mamu Formation - - - - - - - - 88

5.4 Depositional History - - - - - - - - 89

CHAPTER SIX: CONCLUSION AND RECOMMENDATION

6.1 Summary and Conclusion - - - - - - - 91

References - - - - - - - - - - 93

Appendices - - - - - - - - - - 104

LIST OF FIGURES

Figure 1.1: Location and Accessibility map of the study area. - - - 4

Figure 2.1: Geological map of Nigeria showing the northern Anambra Basin (Modified after Obaje, 2009). - - - - - - - 7

Figure 2.2: Campanian – Maastrichtian Stratigraphic Succession of the Anambra Basin. - - - - - - - - - 9

Figure 2.3: Summarized Stratigraphic successions in the Benue Trough, Anambra Basin and the Nigerian sector of the Chad Basin. - - - - 11

Figure 2.4: Geological sketch map of the Anambra Basin (After Obaje, 2009). - 12

Figure 3.1: Organogram showing the sequence (algorithm) of the methods from the beginning to the end of the research. - - - - - 36

Figure 4.1: Geological map of the Area around Idah, Ajaka, Ugwolawo and environs. 38

Figure 4.2: Lithostratigraphic section of the Nkporo Formation exposed north of Ukunube town 07^0 21' 15.1"N, $06^0$47' 06.2"E. - - - - - 39

Figure 4.3: Lithostratigraphic section of siltstones and clay of Nkporo Shale exposed near Achago village (7°19'48.1"N 6°47'02.8”E). - - - - 40

Figure 4.4: Lithostratigraphic section of the Mamu Formation exposed southwest of Ojodu town 07^0 20' 44.9"N, 06^0 55' 09.2"E. - - - - 42

Figure 4.5: Lithostratigraphic section of the Mamu Formation exposed west of Ugbabo town 07^0 20' 59.1"N, 06^0 53' 58.2"E. - - - - - 43

Figure 4.6: Lithostratigraphic section of the Mamu Formation exposed southsouth of Ojodu town 07^0 20' 47.7"N, 06^0 55' 16.9 "E.- - - - - 45

Figure 4.7: Lithostratigraphic section of siltstones and clay of Mamu Formation exposed south of Ojodu town. 07^0 20' 49.9"N, 06^0 56' 00.3 "E. - 46

Figure 4.8: Lithostratigraphic section of siltstones of Mamu Formation exposed near Aya village (7°14'59.4"N, 6°48'02.7"E). - - - - - 48

Figure 4.9: Lithostratigraphic section of sandstones of Mamu Formation exposed near Ocheche River at Idah 07°07'27"N, 06°44'20.6"E. - - - 53

Figure 4.10: Lithostratigraphic section of Mamu Formation exposed northwest of Ojuwo Omachi town 07^0 20' 35.0"N, 06^0 56' 14.8 "E. - - - 55

Figure 4.11: Lithostratigraphic section of lateratized shale of Ajali Sandstone exposed at Ikare Road, south of Ajaka town 07°10'02.2"N and 06°50'12.8"E. - 56

Figure 4.12: Lithostratigraphic section of Ajali Sandstone exposed at Ogbogba Hill 07°12'31.5"N and 06°52'22.2"E. - - - - - 60

Figure 4.13: Average values of grain size statistical parameters of the study area: (a) mean; (b) sorting; (c) skewness and (d) kurtosis. - - - - 67
Figure 4.14: Linear Discriminate Function (LDF) values plot for the sandstone facies of Mamu Formation and Ajali Sandstone in the study area. - - 70
Figure 4.15: CM diagram for sandstone facies samples in the study area. - - 71
Figure 4.16: Paleocurrent pattern from cross bed azimuths in the Ajali Sandstone showing a unimodal high variability pattern in the SW direction in fluvial environment. - - - - - - - - - 73
Figure 4.17: Paleocurrent pattern from cross bed azimuths in the Sandstone beds of the Mamu Formation showing a bimodal pattern in the NW and NE direction in tidal environment. - - - - - - - 73
Figure 4.18: Paleocurrent map of the Campanian to Maastrichtian Mamu Formation and Ajali Sandstone in the study area. - - - - - 74

LIST OF TABLES

Table 4.1: Percentile value from cumulative curve plots of sandstones samples in the study area. - - - - - - - - 61

Table 4.2a: Grain size distribution and quantitative parameters of samples of Ajali Sandstone in the study area. - - - - - - 62

Table 4.2b: Grain size distribution and quantitative parameters of samples of the sandstone facies of Mamu Formation in the study area. - - 63

Table 4.3: Linear discriminate function (After Sahu, 1964) of sandstone facies of Mamu Formation and Ajali Sandstone in the study area. - - - 69

Table 4.4: Azimuthal readings and statistical table for the sandstone facies of Ajali Sandstone in the study area. - - - - - - 72

Table 4.5: Azimuthal readings and statistical table for the sandstone facies of Mamu Formation in the study area. - - - - - - 73

LIST OF PLATES

Plate I: Npkoro Shale exposed near Achago village 7°19'48.1"N 6°47'02.8"E. 39

Plate II: Nkporo Shale exposed north of Ukunube town 07^0 21' 15.1"N, $06^0$47' 06.2"E. - - - - - - - - - 40

Plate III: Mamu Formation exposed southwest of Ojodu town 07^0 20' 44.9"N, 06^0 55' 09.2"E. - - - - - - - - 42

Plate IV: Mamu Formation exposed west of Ojuwo olijo town 07^0 20' 59.1"N, 06^0 53' 58.2"E. - - - - - - - - 43

Plate V: Mamu Formation exposed west of Ajegwu town 07^0 20' 47.7"N, 06^0 55' 16.9 "E. - - - - - - - - - 44

Plate VI: Mamu Formation exposed west of Ojodu town 07^0 20' 49.9"N, 06^0 56' 00.3 "E. - - - - - - - - - 46

Plate VII: Mamu Formation exposed near Aya village 07°14'59.4"N, 06°48'02.7"E. 47

Plate VIII: Mamu Formation exposed along Ocheche River near Idah. - - 49

Plate IX: Mamu Formation exposed along Ocheche River near Idah. Photograph showing the coarse grained tabular cross bedded sandstone with reactivation surfaces. - - - - - - - - 50

Plate X: Mamu Formation exposed along Ocheche River near Idah. Photograph showing coarse grained cross – bedded sandstone with wave ripples 07°07'27"N, 06°44'20.6"E. - - - - - - 50

Plate XI: Mamu Formation exposed along Ocheche River near Idah. Photograph showing medium grained tabular cross bedded sandstone with bedding planes. - - - - - - - - - 51

Plate XII: Mamu Formation exposed along Ocheche River near Idah. Photograph showing vertical section of intercalation of white and grey, medium to coarse grained, moderately sorted, bioturbated, tabular cross – bedded sandstone with erosional surfaces. - - - - - - - 51

Plate XIII: Mamu Formation exposed along Ocheche River near Idah. The arrows showing vertical (*Ophiomorpha*) burrows **07° 07' 27"N, 06° 44' 20.6"E.** 52

Plate XIV: Mamu Formation exposed along Ocheche River near Idah. Photograph showing fine to medium grained trough (TrB), tabular (TB) and herringbone cross – bedded (HB) sandstone with lens of reworked clay (RC) and sinuous crested dunes. - - - - - - - - 52

Plate XV: Mamu Formation exposed northwest of Ojuwo Omachi town. 07^0 20' 35.0"N, 06^0 56' 14.8 "E. - - - - - - - 54

Plate XVI: Ajali Sandstone exposed at Ikare Road, south of Ajaka town. 7°10'02.2"N and 6°50'12.8"E. - - - - - - - - 56

Plate XVII: Ajali Sandstone exposed at Ogbogba Hill northwest Ogbogba town. Photograph showing planer cross – bedded sandstone as described **7°12'31.5"N, 6°52'22.2"E.** - - - - - - 58

Plate XVIII**:** Ajali Sandstone exposed at Ogbogba Hill northwest Ogbogba town. Photograph showing planar cross bedding, reactivation surfaces and herringbone cross bedding as described **7°12'31.5"N, 6°52'22.2"E.** 59

Plate XIX: Ajali Sandstone exposed at Ogbogba Hill northwest Ogbogba town as described **7°12'31.5"N, 6°52'22.2"E.** - - - - 59

LIST OF APPENDICES

Appendix I: Cumulative curve plots and tables for data obtained from granulometric analysis. - - - - - - - - - - 107

Appendix II: Histogram plots and tables of samples analysed. - - - 123

Appendix III: Calculation of Linear Discriminate Function (Sahu, 1964). - - 126

CHAPTER ONE

INTRODUCTION

1.1 INTRODUCTION

The study focused mainly on the sedimentology and stratigraphy of the Late Campanian to Maastrichtian successions in the area northeast of Idah town in the northern Anambra Basin, wherein stratigraphic setting is thus conveniently divided into two – the Nkporo Group (Nkporo Shale) and the Coal Measures (Mamu Formation and Ajali Sandstone).

1.2 Statement of Research Problem

Previous research work carried out in the Anambra Basin began with the establishment of the Mineral Survey of Southern Nigeria in 1903 by the British Secretary of State for the Colonies. Much geological information became available following the discovery of several industrial minerals especially coal (Bain, 1924; Simpson, 1954). The strata exposed by the construction of the eastern railway were systematically studied (Wilson, 1925). Geomorphological and environmental studies had also been carried out by the Geological Survey of Nigeria (Grove, 1951). More geological information came to light as the geologist of Shell-D'Arcy Petroleum Company began extensive surface mapping and geophysical investigations in the more easily accessible areas of southern Nigeria, which turned out to be the Cretaceous sediment underlying the Cenozoic Niger Delta. Exploratory drilling was first carried out in 1951 at Ihuo, 15 km northeast of Owerri and encountered Cretaceous stratigraphic units. A lot of information contained in 1:250,000 geological maps made by Shell-BP for the Geological Survey of Nigeria starting from 1957. Systematic geological mapping by the Geological Survey of Nigeria also contributed substantial amount of information. Further work, specifically on the stratigraphy and paleoenviromental reconstruction had been done by several authors including Rayment (1965), Murat (1972), Dessauvagie (1974), Petters (1976), Avbovbo and Ayoola (1981) and Agagu *et al*. (1985).

Analysis of information from surface mapping and other oil exploration activities by authors such as Burke *et al*. (1972), Murat (1972) and Whiteman (1982) has shown that the sedimentary rocks of southern Nigeria belong to several distinct basins. Reyment (1965) had inferred them all to one large single basin extending eastward to Douala in Cameroon and westword to Benin Republic.

Later stratigraphic/sedimentological studies of smaller specific locations within the basin (e.g. Nwajide and Reijers, 1996a and 1996b) have contributed to the present understanding of the characteristics of most of the component lithostratigraphic units of the basin. Reyment (1965), Murat (1972), Adeleye (1975), Peters (1978), Whiteman (1982), Hoque and Nwajide (1984), Agagu *et al*. (1985), Onuoha (1986) predicted the history of the basin using data from the Akukwa – 2 exploratory well. A sequence stratigraphic model for the group was developed by Nwajide and Reijers (1996c) on the basis of stratigraphic analysis of a composite section located at Leru near Okigwe. Nwajide (2005), Adeigbe and Salufu (2009) and Ojo *et al*. (2010) have studied the Enugu and Mamu Formations with respect to their lithostratigraphy, age relations, biostratigraphy, sequence stratigraphy, coal geology and petroleum geology. To the best of my knowledge, little or no work have been carried out in the present area of study, and this prompted me to carry out this research.

1.3 Justification

The present research attempts to fill the gaps and update the knowledge on the lithostratigraphy, structure, paleoenvironment and sedimentology of the Late Campanian to Maastrichtian successions in the northeast of Idah town, northern part of the Anambra Basin.

This research will attempt to evaluate the sedimentology and stratigraphy of the Late Campanian to Maastrichtian successions in the study area using data obtained from outcrops

in the field and interpret the depositional environments of the succession based on the sedimentary structures, lithofacies (or lithofacies association) and linear discriminate function.

1.4 Aim and Objectives

This research is aimed at producing a detailed geological map of the area and to study the Campanian – Maastrichtian lithostratigraphic successions in the area. The objecves are to:

- **(i)** Carry out geological fieldwork in the study area in order to generate a geological map of the area.
- **(ii)** Interpret the paleoenvironment of deposition of the Campano-Maastrichtian successions in the study area.
- **(iii)** Deduce depositional mechanism leading to deposition of the studied succession in the area, and
- **(iv)** Determining the principal paleocurrent direction relative to provenance of the sediment source area.

1.5 Location and Accessibility of the Study Area

The study area is located in Kogi State, north central Nigeria within the coordinates of latitudes 7° 06' 00"N to 7° 21' 00" N and longitudes 6° 43' 00" E to 6° 58' 00"E, with a total area of seven hundred and seventy square kilometres (770 km^2). The area is accessible via footpaths, major and minor roads that link the villages (Figure 1.1).

1.6 Scope and Limitation of the Study

This research work is limited to the lithostratigraphic and sedimentological analysis of sediments in the northeast of Idah town, northern Anambra Basin, wherein good sections are exposed due to the road cuts and River channels. These sections were logged, taking into account the different textural characteristics, colour, structure and fossil content which form basis for recognition of facies and subfacies, and even facies association.

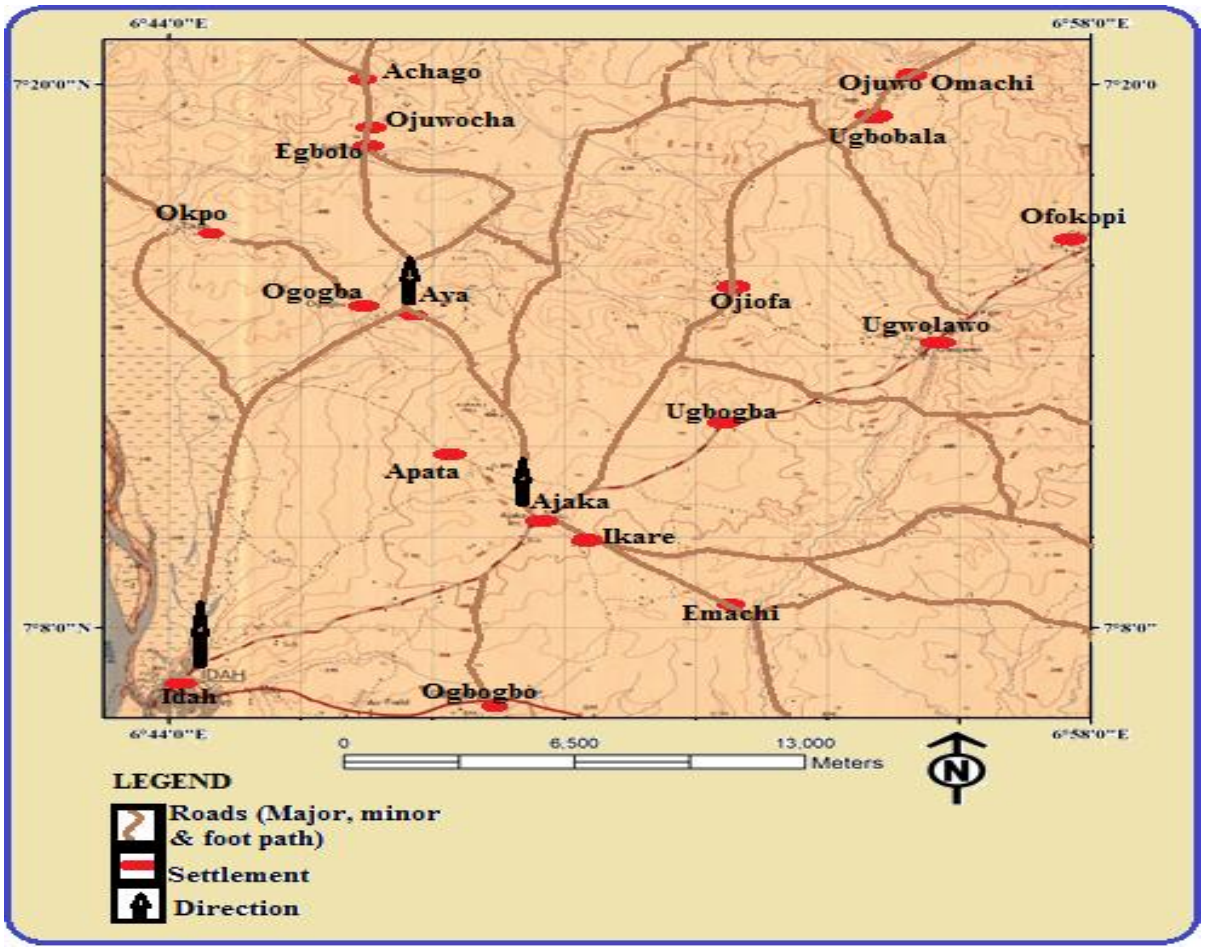


Figure 1.1: Location and Accessibility map of the study area (Nigeria geological survey, Kaduna).

1.7 Climate and Vegetation

The northern Anambra Basin lies within the tropical climate marked by wet and dry seasons. The dry season sets in during November and lasts until March. It is followed by a wet or rainy season from April to October with maximum rainfall in July to September. The annual amount of rainfall within the area is between 1200 and 1500 mm. The annual temperature range between 16°C and 37°C. During the rainy season, the area is under the influence of moisture-laden southwest trade winds which give way to the dry and sometimes dusty northeast winds (harmattan) during the dry season.

The northern Anambra Basin lies within the rainforest vegetation belt with rich deciduous and occasional stunted trees including palms, Iroko, mahogany, akeeapple and other towering trees in sparsely settled area.

These are green in the rainy season with fresh leaves and tall grasses, but the land is open during the dry season, showing charred trees and the remains of burnt grasses. The trees which grow in clusters are up to nine metres tall, interspersed with grasses which grow up to about three metres. There are heavy forests along the river valleys. However, the original vegetation has been, in most cases, tempered with through human activities.

Examples of trees in the study area include *Afezilia africana*, *Uapacatogoenesis, Daniella oliveri (*locust bean*), Buttryospenum paradoxim, (*sheabutter*),* oil bean, *Montes kerstingi* and *Isoberlina dalzieli*. The dominant grasses include Elephant grass (*Axonopus compressors),* Pine grass, species of Devil bean stems with delicate, offensive, adhesive hairs that produce unpleasant irritation when in contact with the skin are also common.

1.8 Relief and Drainage

The area is generally an undulating land to flat plains with a few isolated hills. The highest point is 246.0 m and the lowest point is 131.0 m above mean sea level. The drainage pattern in the area is dentritic. The area is well drained with major rivers such as Ocheche, Inachalo, Ofu, Emachi and Ega among others and streams occupying rather wide valleys. The rivers eventually drain into the River Niger. The tributaries are mostly seasonal having their sources mainly within the area. This drainage configuration is thought to be the result of substantial degree of evolution from the primeval setting, i.e. the paleodrainage (Nwajide, 2014).

CHAPTER TWO

LITERATURE REVIEW

2.1 INTRODUCTION

Wright *et al*. (1985) defined the Anambra Basin as "the upper Senonian to Palaeocene depositional area located at the southern end of the Benue Trough, within which the Nkporo Group and younger sediments accumulated and which extended towards the southwest as the Niger Delta Basin". This definition lumps the lithofacies of three distinct basins into one continuous series simply on the basis of contiguity. Akande and Erdtmann (1998) and Obaje *et al*. (1999) consider the Anambra Basin a part and parcel of the Benue Trough on the premise that it is a consequence of the compressional history/stage of the trough. The genetic relationship notwithstanding, the basins are treated as separate entities. The perspective here is that the Anambra Basin is a distinct lithostratigraphic entity overlying the southern Benue Trough and is in turn overlain in its southern reaches by the Niger Delta Basin (Figure 2.1).

Anambra Basin refers to the sedimentary succession that directly overlies the facies of the Lower Benue Trough (Figure 2.1) and consists of Campanian to Early Palaeocene (Danian) lithofacies. These correspond to the facies of the Nkporo Group and the Coal Measures. It has been a common practice to lump up the lithostratigraphic units belonging to three individual basins – southern Benue Trough, Anambra Basin and the Niger Delta – and refer them to the Lower Benue Trough. In discussing the stratigraphy of southeastern and northeastern Nigeria, it should be clear that there is a stacking or tiering of basins. This approach may appear contrary to the common practice of naming an area using only the basin bearing the outcropping facies. Progress in the acquisition of both outcrop and subsurface data has enabled a better knowledge of the origin of several Nigerian basins. For instance, we now know that the Anambra Basin and its lithic fill were not in existence prior to the Santonian thermotectonic event, which involved the Awgu Formation. It is now clear that the extensive transgression that deposited the Imo Formation marked the termination of the Anambra Basin regime and heralded the Niger Delta of which the formation is the oldest lithostratigraphic unit (Nwajide, 1990).

The so – called "Afikpo Basin" is considered a part of the Anambra Basin. The basis for this position is that it is the result of the same Santonian thermotectonic event in the southern Benue Trough. Besides, there is really no physical separation or barrier between the two areas; there does not appear to be any tectonic definition of that area into a depression separate from the area to the northwest Nwajide (2014). The sediment packages are both common and continuous southeastwards across the Afikpo area towards Calabar. There is therefore no clear justification for Afikpo area the status of a basin distinct from the Anambra Basin (Nwajide, 2014 and Obaje, 2009).

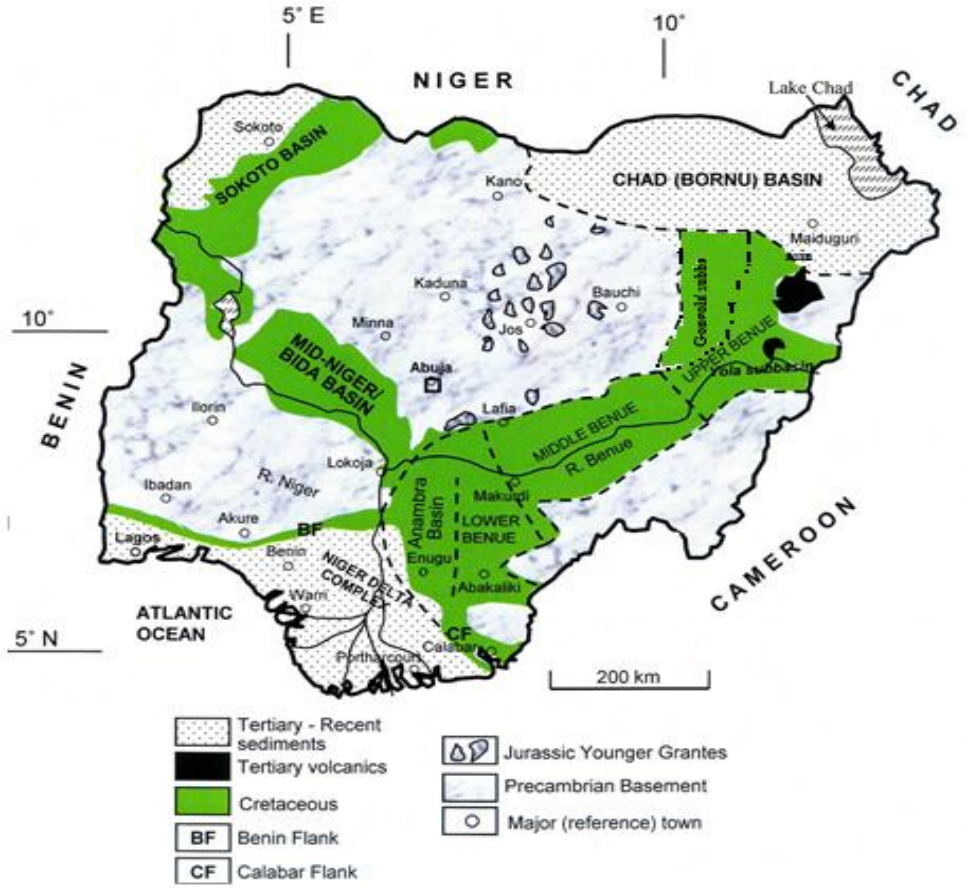


Figure 2.1: Geological map of Nigeria showing the northern Anambra Basin (Modified after Obaje, 2009).

2.2 The Anambra Basin Territory

In territorial terms, the outcropping area of the Anambra Basin has a roughly triangular outline, with a doubly indented base (Nwajide, 2014). The western boundary should be taken

as the Okitipupa Ridge, a tectonic feature that demarcates the Dahomey Basin from the Lower Benue Trough, even though the two depressions originated from the same event, i.e. the separation of the African Plate from the South American Plate. To the northwest the basin directly overlies the basement complex, as seen between Auchi and Igarra in the basement area in the northern part of Edo State, as well as the sediment/basement contact between Itobe and Anyigba in Kogi State. The occurrence of numerous outliers of sedimentary facies on the basement area north of Auchi as reported by Hockey *et al.* (1986) suggests that this boundary has been shifting southwards. The boundary with the Bida Basin is not sharp. Rather, there is an interfingering relationship and thus the cartographic demarcation has to be arbitrary. The northern boundary is with the Basement Complex of Keffi – Wamba area, intruded by the Younger Granites. The lower basin boundary, i.e. the demarcation from the facies of the central and southern Benue Trough is an onlap marked by an angular unconformity between Awgu Formation and Nkporo Shale. The top boundary is also regarded as an unconformity between the Nsukka and the Imo Formations (Avbovbo and Ayoola, 1981) while other authors did not indicate unconformity between Nsukka Formation and Imo Shale (Figure 2.2).

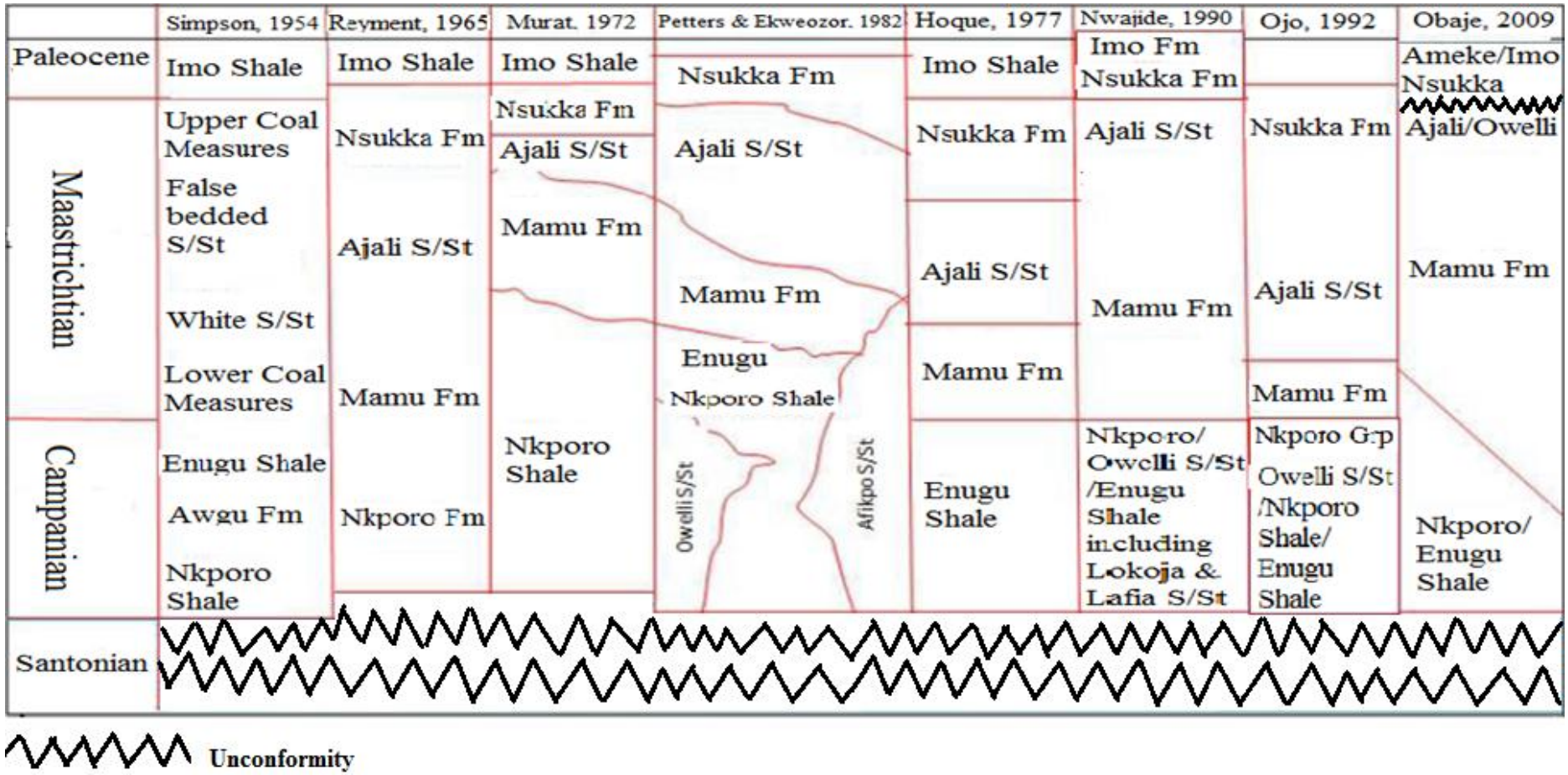


Figure 2.2: Campanian – Maastrichtian Stratigraphic Succession of the Anambra Basin After Simpson, (1954), Reyment (1965), Murat (1972), Petters & Ekweozor (1982), Hoque (1977), Nwajide (1990), Ojo (1992) and Obaje (2009) .

2.3 Regional Tectonic and Stratigraphic Setting of the Anambra Basin

The origin of the Anambra Basin is intimately related to the development of the Benue Rift. The Benue Rift was known as the failed arm of a trilate fracture (rift) system, during the breakup of the Gondwana supercontinent and the opening up of the southern Atlantic Ocean in the Jurassic (Burke *et al*., 1972; Olade, 1975; Benkhelil, 1982, 1989; Hoque and Nwajide, 1984; Fairhead, 1988). The initial synrift sedimentation in the embryonic trough occurred during the Aptian to early Albian and comprised of alluvial fans and lacustrine sediments of the Mamfe Formation in the southern Benue Trough. Two cycles of marine transgressions and regressions from the middle Albian to the Coniacian filled this ancestral trough with mudrocks, sandstones and limestones with an estimated thickness of 3,500 m (Murat, 1972; Hoque, 1977). These sediments belong to the Asu River Group (Albian), the Odukpani Formation (Cenomanian), the Ezeaku Group (Turonian) and the Awgu Shale (Coniacian) (Table 2.2). During the Santonian, epeirogenic tectonics, these sediments underwent folding and uplifted into the Abakaliki- Benue Anticlinorium (Murat, 1972) with simultaneous subsidence of the Anambra Basin and the Afikpo sub- basins to the northwest and southeast of the folded belt respectively (Murat, 1972; Burke, 1972; Obi, 2000; Mode and Onuoha, 2001). The Abakaliki Anticlinorium later served as a sediment dispersal centre from which sediments were shifted into the Anambra Basin and Afikpo Syncline. The Oban Masif, southwestern Nigeria basement craton and the Cameroon basement complex also served as sources for the sediments of the Anambra Basin (Hoque and Ezepue, 1977; Amajor, 1987; Nwajide and Reijers, 1996a and b). Figure 2.3 is the summarized stratigraphy of the lower Benue Trough and the Anambra Basin. After the development of the Anambra Basin following the Santonian epeirogeny, the Campanian- early Maastrichtian transgression deposited the Nkporo Group (i.e the Enugu Formation, Owelli Sandstone, Nkporo Shale, Afikpo Sandstone, Otobi Sandstone and Lafia Sandstone) as the basal unit of the basin,

unconformably overlying the Awgu Formation. This was followed by the Maastrichtian regressive event during which the coal measures (ie the Mamu, Ajali and Nsukka Formations) were deposited. Figure 2.4 is the geologic map of the southeastern Nigeria indicating the Anambra area.

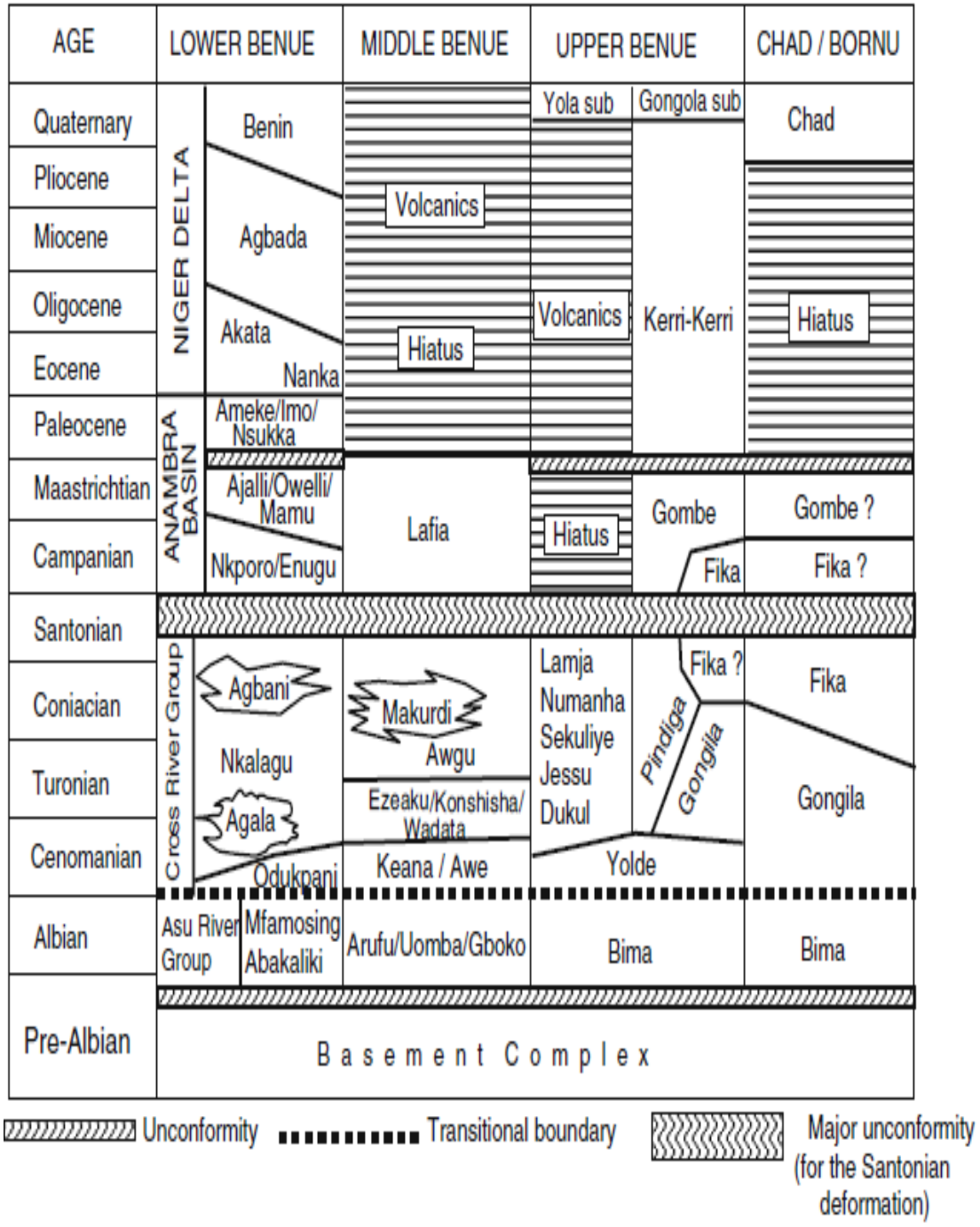


Figure 2.3: Summarized Stratigraphic successions in the Benue Trough, Anambra Basin and the Nigerian sector of the Chad Basin (After Obaje, 2009).

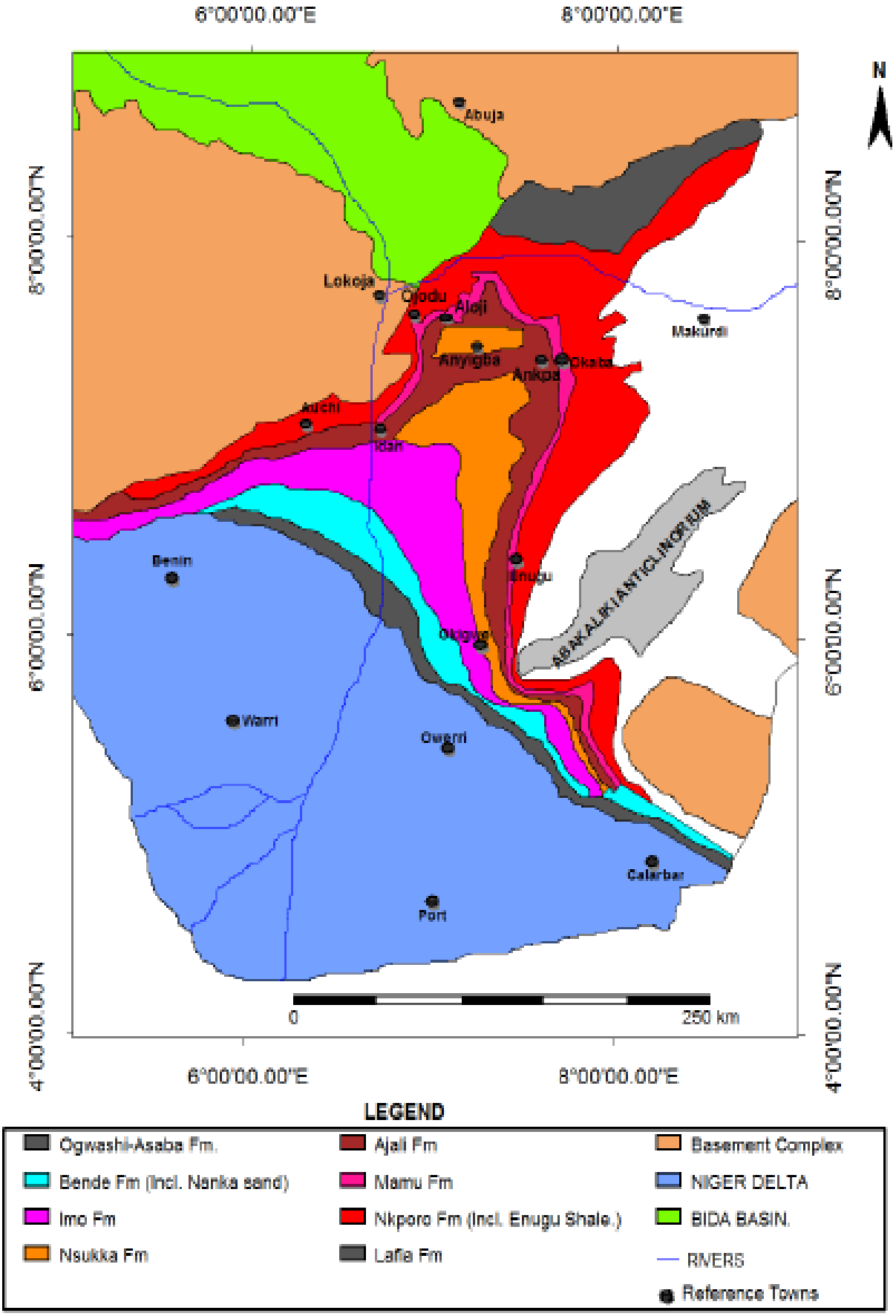


Figure 2.4: Geological sketch map of the Anambra Basin (After Obaje, 2009).

2.4 Origin and Structure of the Campanian – Maastrichtian Succession in the Anambra Basin

The major factor widely believed to have controlled the stratigraphic evolution of the Anambra Basin was the continued asymmetrical subsidence along the landward extension of the Atlantic Chain fracture associated with the initial opening of the Benue Trough (Benkhelil, 1982; Obi *et al*., 2001). The subsidence was in response to post-Benue rift thermal contraction of the lithosphere (Popoff, 1990; Binks and Fairhead, 1992).

As recognised by Murat (1972), the megatectonic setting in the southern domain of the Benue Trough was a longitudinally faulted crest whose eastern half subsided preferentially to become the Abakaliki sub – basin (or the Lower Benue Trough). The western fragment remained a stable platform up to the Santonian. Thus, the subsided eastern part became an important depocentre relative to the platform which received only a veneer of clastic and chemical sediments. Following the Santonian folding and uplift, the main depocentre in the Lower Benue Trough, i.e. the Abakaliki area, became flexurally inverted, displacing the depocentre to the west and northwest. This created the Anambra Basin.

Ojoh (1990) had noted that basin subsidence in the Lower Benue Trough was spasmodic, being a high rate in pre – Albian time, low in the lower Cenomanian, and very high in the Turonian, which was related to the important phase of platform subsidence. This is thought to be the actual time of initiation of the Anambra Basin creation, a process that gained momentum in the Coniacian and climaxed during the Santonian thermotectonic event Nwajide (2014). Thus the localised subsidence on the western reach of the Lower Benue Trough and the continued sea level rise into the Coniacian, led to the development of the Anambra Basin (Ojoh, 1990). It should be noted however, that sedimentation started as far back as Turonian or even earlier on the submerged Anambra Platform. The rate of westward

migration of the depo axis was of the order of 10 km/My or 1 cm/year, and gradually effected the tectonic inversion between the Abakaliki region and the Anambra Basin (Nwajide, 2014).

The Upper Campanian to Maastrichtian succession – renewed rifting produced the main post – Santonian depocentre, the Anambra Basin (Zaborski, 1998). Close to the northwestern margin of the basin, Jones (1958) identified a series of parallel monoclinal folds in the sedimentary cover dipping steeply ESE suggesting step – faulting of the underlying basement. Allix (1987) regarded the Anambra Basin as bounded by NE – SW trending fracture or flexure zones which Allix *et al*. (1984) correlated with the onshore extensions of the Chain and Charcot fracture zones. Popoff *et al*. (1988) reported synsedimentary normal faults along the eastern margin of the basin and subsidence rates of about 58 m My-1 for the Late Campanian to Maastrichtian. Magmatic activity at this time was subdued but intrusive bodies formed during the Late Maastrichtian to Eocene phase of activity occur around the margin of the Anambra Basin and the Afikpo Syncline (Zaborski, 1998). According to Baudin (1991) and Maluski *et al*. (1995), they are related to underlying vertical flexure zones responding to tectonic readjustment and post – thermal relaxation of the lithosphere. Early activity (68 Ma) at Katyo, south of Gboko, was alkaline in nature but dolerites at Oturkpo (60 Ma) and in the Ugep – Afikpo area (55 Ma) are tholeiitic (Hossain, 1981). Dolerites (49 Ma) occurring southwest of Makurdi are the youngest known representatives of this phase (Maluski *et al*., 1995).

According to Agagu and Adighije (1983) the Anambra Basin can be divided into a main southern “Onitsha Basin” and a circular northern “Ankpa Basin”, the two being separated by the NW-SE trending “Nsukka High”. Benkhelil *et al.* (1988) indicated a somewhat different basin structure with a circular depocentre west of Nsukka, containing over 6 km of sediments partly separated from a sub-basin south of "Onitsha, containing over 12

km. According to Agagu and Adighije (1983), more than 8 km of the sediments in the later area may be of Cretaceous age with some 3 km being post-Santonian; in the Ankpa Basin 3 km of Pre-Santonian and 2 km of post-Santonian sediments were suggested. Subsurface data (Allix *et al*., 1984; Agagu *et al.,* 1985; Allix, 1987; Popoff *et al.,* 1988) confirm thicknesses of 2-3 km for the Campanian to Palaeocene infill of the Anambra Basin.

The other Post-Santonian depocentre in the Lower Benue Trough was the Afikpo syncline to the southeast of the Abakaliki uplift (Zaborski, 1998). According to de Swardt and Casey (1961) the Abakaliki anticlinorium itself continued to show gentle uplift during the latest Cretaceous, demonstrated by thinning of the Campano-Maastrichtian formations and lateral facies changes into sandy lithologies over its axis.

Murat (1972) envisaged the Campano-Maastrichtian cycle as beginning with a Late Campanian transgression during which dominantly argillaceous sediments accumulated, these beds extending southeast onto the Calabar Flank and to the northwest passing laterally into sediments in the Bida Basin. A conformable, succession comprising the Mamu Formation, Ajali Sandstone, and Nsukka Formation lies above. Murat regarded these formations as paralic and continental respectively. Other authors (Ladipo, 1988a; Courel *et al.,* 1991) have shown that the Anambra Basin was subjected to marine influence to a greater or lesser extent throughout the Late Campanian and Masstrichtian. Peak transgressive conditions, however, occurred at the beginning of the cycle. During the very late Campanian marine conditions probably affected the entire length of the Benue Trough, as well as parts of the Bida Basin.

The sediment – filled depression in the Afikpo area is considered a part of the Anambra Basin. The area was involved in tectonic inversion that produced the depocentre to the west of the Abakaliki Anticlinorium. Sedimentation in that area, which is centred to the south of

southeast of Abakaliki, is dated to have commenced in the Santonian into the Campanian, using the *palynofloral syncolporites lisamae subtilis* and *Auriculidites sp.* (Ojoh, 1990).

In the southern Nigeria stack the Anambra Basin is sandwiched between the Benue Trough and the Niger Delta. The main implication of this is that, after the Santonian thermotectonic event, there must have been a thermal decay that produced a sag on which at least part of the Anambra Basin became superimposed (Nwajide, 2014). In the same manner, the establishment of the Niger Delta sedimentary regime from the Palaeocene must have taken advantage of a continued thermal sag. According to McKenzie (1978), there is usually a distinct thermal sag stage involved in post – rift basin formation in response to the cooling and contraction of the lithosphere and the asthenosphere that were thermally perturbed during the earlier rifting process. The isostatic response to such cooling is a flexural subsidence of the crust, such that magmatism would rapidly decrease and then cease altogether, such as developed along the western margins of the Benue – Gongola – Bornu fold zone (Benkhelil and Robineau, 1983; Guiraud *et al.,* 1992).

The resulting basin has an apparently simple structural configuration, being a broad syncline plunging gently south of southwest beneath the Niger Delta. However, Benkhelil and Robineau (1983) observed that in the Anambra Basin there are lineament trends ranging from 017° to 040°, thought to be comparable to those in the Gongola sub – basin of the northern Benue Trough. Fractures within the Anambra Basin trend may have acted as transverse faults to the Benue Trough sinistral faults for the opening of the rhomb basins (pull – apart basins). It is also likely that the same faults may have been active during the compressional phases that determined the folding along the trough still in connection with the sinistral shear movements along the BenueTrough trend fracture zones.

In addition to the Benue Trough fracture trend, there are subsidiary concentrations of linear fractures, notably the lineaments trending between 107° and 163°. Thus in the southeastern part of the Benue Trough, this trend seems strictly related to the Calabar Flank in the Lower Benue Trough, which coincides with the Bida Basin and Mamfe embayment. In the Anambra Basin the features of this trend may have influenced sedimentation, both as distribution of facies and as continuities along which sedimentary faults may have developed (Nwajide, 2014). There are also numerous normal faults whose trends are consistent with the trend of the lineaments identified by Benkhelil and Robineau (1983), and those en echelon with the Niger Delta Hinge line.

2.5 Stratigraphic Setting of the Late Campanian – Maastrichtian Succession of the Anambra Basin

The filling of the Anambra Basin took place within the time interval from Santonian to Early Palaeocene (Danian), i.e. an absolute time span of 60Ma. There were two marine transgressions – a major one (the Nkporo transgression) and a less extensive one (the Nsukka transgression). Stratigraphic packaging is thus conveniently divided into two – the Nkporo Group and the Coal Measures. The former is so called because the Nkporo Shale as a formation that has several lateral (age) equivalents. Sedimentation in the basin started with the late Campanian Nkporo Group (Reyment, 1965; Zaborski, 1983). The latter is separated from the Pre-Campanian strata of the adjacent Abakaliki Basin by a type-1 sequence bounding angular unconformity (Nwajide and Reijers, 1996b). The Nkporo Group consists of:

(i) the basal Nkporo Shale (Petters, 1980; Arua, 1988);

(ii) the Owelli Sandstone, and

(iii) the Enugu Shale

To demonstrate how far – reaching and all – inclusive the usage "Nkporo Shale" is, Reyment's (1965) correlation of formations around Nigeria shows it to range from Lower

Maastrichtian to Danian in the western coast of Nigeria, and further inland rests on the basement and is equivalent to the basal part of the Abeokuta Group, which is in turn equivalent to the Ajali and the Nsukka Formations. In eastern Nigeria, Reyment (1965) shows that the Nkporo Shale to be Lower Campanian overlain by the Mamu Formation, which is Lower Maastrichtian. This correlation assumes continuity in paleogeographic conditions across the entire southern part of Nigeria during the Cretaceous. In southeast of Nigeria, Reyment (1965) observed that "it seems that Nkporo Shale was deposited during the whole of Campanian time and that the coal – cycle beds are time – equivalents of the upper part of the Nkporo Shale".

The Nkporo Group is succeeded by the marginal marine mudstones and sandstones of the Mamu Formation (Maastrichtian), which in the area north of Awgu, contains about five coal-bearing tidal-intertidal cycles that reflect the infilling of the bay head of an estuary (Reyment, 1965; Nwajide and Reijers, 1996c). In the more distal basinal areas south of Awgu, the Mamu Formation is dominated by cycles of carbonaceous fissile shale–oncolitic mudstones–oolitic sandstone deposited in shallow shelf-shoreface environment (Akande and Mucke, 1993; Obi, 2000).

The Mamu Formation passes upward into profusely cross-bedded tidal channel/fluvial channel deposits that constitute the Maastrichtian Ajali Sandstone (Ladipo, 1986). At the top of the Campanian–Maastrichtian succession is the Nsukka Formation (Late Maastrichtian) which consists of carbonaceous mudrocks and sandstone similar in lithologic character to the Mamu Formation (Reyment, 1965). The Tertiary strata comprising the Imo Formation and Ameki Group unconformably overlie the Nsukka Formation. These stratigraphic units maintain a gentle offlapping arrangement, with younger units occurring successively to the southwest (Obi *et al.*, 2001).

2.6 Systematic Lithostratigraphy of the Late Campanian – Maastrichtian Succession of the Anambra Basin

The Late Campanian – Maastrichtian lithostratigraphical succession for the Anambra Basin has been established by various authors (for example Wilson, 1925; Tattam, 1944; Grove, 1951; Simpson, 1954 and 1955; Reyment and Barber, 1956; Reyment, 1965; Cratchley and Jones, 1965; Burke *et al.,* 1971; Murat, 1972; Dessauvagie, 1975; Offodile, 1976; Kogbe, 1981a; Ayoola, 1981; Ekweozo, 1982; Agagu *et al., 1*985; Hockey *et al*., 1986; Ojoh, 1990; Ladipo *et al.,* 1994; Agumanu, 1993; Nwajide and Reijers, 1996a and b; Nwajide, 2014) .

The Campanian sediment which overlies the Awgu Formation is known as the Nkporo Group which is made up of the Nkporo Shale, Owelli Sandstone, and the Enugu Shale. In the south these are marine shales (Offodile, 1976) but towards the southwest, they pass into the arenaceous Otobi Sandstones. The Nkporo Group unit is unconformably overlain by the Mamu Formation or Lower Coal Measures (Cratchley and Jones, 1965; Offodile, 1976; Kogbe, 1981a). The Mamu Formation is overlain by Ajali Sandstone (Offodile, 1976), or "False-Bedded Sandstones" (Simpson, 1955; Cratchley and Jones, 1965). Above the Ajali Sandstone, a thin coating of what has been widely accepted as the latest sediments in the Lower Benue area was deposited. This is the Nsukka Formation, or the Upper Coal Measures.

2.6.1 The Nkporo Group

After the folding and uplift of the initial axis of subsidence in the Santonian, deltaic sedimentation and formation of coal swamps became prevalent during the final Campanian – Maastrichtian infilling of the basin (Petters, 1982). In general, the Nkporo Group (Nkporo Shales and its lateral/stratigraphic equivalents) overlies the Awgu Formation with an angular unconformity. The group comprises the lowest stratigraphic units of the Anambra Basin. Its lithofacies characteristically form low – lying topographic forms, and are of shallow water origin. Locally there are gypsiferous thin sandstones, shelly limestones and impersistent coals.

2.6.1.1 Nkporo Shale

The lowermost sediments of the Campano-Maastrichtian cycle in the southern part of the Anambra Basin and in the Afikpo Syncline belong to the Nkporo Shale (Tattam, 1944, after Shell-BP) for which Reyment (1965) estimated a maximum thickness of 1000 m; Agagu *et al*. (1985) reported a maximum of over 350 m in the subsurface of Anambra Basin.

The Nkporo Shale documents the transgressive event that followed the Santonian deformation in the Anambra Basin (Murat, 1972; Obi, 2000; Obi and Okogbue, 2004). The coarse-grained sandstone at the base of the Nkporo Shale is interpreted as paleovalley because it clearly cuts erosionally into the older, genetically unrelated Awgu, Ezeaku and Asu River Groups (Shirley and Gordian, 2013). The basal contact is therefore an erosional unconformity (type-1 sequence boundary) formed by subaerial exposure and fluvial incision during a fall of relative sea level (Weimer, 1984; Van Wagoner *et al.,* 1990), which is coincident with the regional Santonian deformation. Evenly laminated and sparsely burrowed black shale, thinly intercalated with silt, sand and lime mud reflects deposition in a quiet water/muddy shelf (Davis *et al.,* 1989; Walker and Plint, 1992).

The formation consists primarily of dark grey fissile shales and mudstones, often pyritic or gypsum-bearing (Zaborski, 1998). A variety of subordinate lithologies occur including sandy shales, shelly limestones or calcareous noddle beds, ripple-marked fine-grained sandstones, coarser-grained sandstones with *Ophiomorpha* and chamositic or limonitic oolitic ironstones (Simpson, 1954; Arua, 1988; Okoro and Arua, 1989; Mode, 1991). In contrast to contemporaneous shales in the Benin Basin, benthonic foraminifers predominate over planktonic. A variety of *gastropods* and *bivalves,* including inoceramids, were reported by Simpson (1954) and Reyment (1955b). The crab *Costacopluma* is common in horizons that also contain *ammonites* (Collins and Morris, 1975). Agagu *et al*. (1985) regarded the Nkporo Shale as a shallow-water deposit but depths clearly varied considerably.

The Late Campanian ammonite *Libycoceras afikpoense* occurs in the lower Nkporo Shale in the Afikpo syncline (Reyment, 1955a). At Lokpauku, where the Nkporo Shale oversteps the nose of the Abakaliki anticlinorium, the upper part of the formation contains *L. dandense* (Howarth) and *heteromorph ammonites* indicating an age very close to the Campanian-Maastrichtian boundary (Zaborski, I990). The top of the Nkporo Shale is diachronous; in the Calabar Flank the formation ranges into the middle part of the Maastrichtian. Foraminiferal and palynomorph assemblages from the Anambra Basin and Afikpo syncline suggest a Late Campanian to Maastrichtian age for the Nkporo Shale (Petters, 1980; Agagu *et al*., 1985; Mode, 1991; Edet, 1992).

In the axial part of the Afikpo Syncline the Nkporo Shale encloses major lensoid sandstone bodies, the Afikpo Sandstone (Reyment, 1964). Pebbly or conglomeratic, Coarse-grained sandstones with erosive bases and epsilon cross-bedding occur here, as do thin coal seams associated with shales (de Swardt and Casey, 1961). The Afikpo Sandstone appears to represent a local fluvio-deltaic development. Reyment (1965) reported marine *ostracods, foraminifers, gastropods* and *bivalves* from calcareous parts of the unit.

2.6.1.2 Owelli Sandstone

Around Awgu and Ogugu the lower part of the Nkporo Shale passes laterally into the Owelli (Owelle) Sandstone (Reyment, 1964) [= Awgu Sandstones of 'Grove (1951), Simpson (1954)].

This unit has been described by Simpson (1954), de Swardt and Casey (1961), Agagu *et al.* (1985) and Agumanu (1993). Prominent, 3-10 m-thick, often ferruginous sandstones

displaying trough or planar cross-bedding with sets up to 2 m thick are present. Foreset inclinations indicate a westerly to southwesterly-inclined palaeoslope. Quartz pebble or clay clast conglomerates occur at the bases of these units which pass upwards into laminated and ripple-bedded sandstones associated with kaolinitic clays (Zaborski, 1998). Large-scale channel-filling sandstone bodies also occur. Towards the top of the Owelli Sandstone interbedded fine-grained sandstone, siltstone and shale successions appear; the shales contain poorly preserved gastropods, wood and leaf fragments and enclose thin coals (Zaborski, 1998). Agumanu (1993) regarded the Owelli Sandstone as formed within a meandering river system draining source areas within the Precambrian basement rocks of the southern Adamawa highlands and the eroded sedimentary rocks of the Abakaliki anticlinorium.

The stratigraphic relationship with the open marine Nkporo Shale and the presence of sharp-based progradational parasequences are consistent with deposition in estuarine channels (Allen, 1993). Shallow marine *bivalves*, *gastropods* and *Ophiomorpha nodosa*, are typical of near shore, possibly lower shoreface conditions (Curran and Frey, 1977; Frey and Howard, 1985; Martino and Curran, 1990). The observed high-angle cross stratification results from the migration and aggradation of moderate-scale bed forms and is consistent with deposition from strong, dominantly unidirectional currents on bars in a channel (Miall, 1992). Herringbone cross-bedding and reactivation surfaces provide evidence of bidirectional flows in a subtidal setting (Smith, 1988). These features and the association with *Ophiomorpha verticalis*, which provides a more conclusive evidence of brackish water and tidal influence (Bowen and Weimer, 2004), suggest that this part of the Owelli Sandstone was formed as a sandy bar within a channel located in the freshwater-dominated upper portion of an estuary. Association of rhythmic alternation of mudstone and thin lenses of sandstone with wave ripple lamination, lenticular bedding and planar bedding, is typical of sedimentation in subtidal and intertidal systems (Boersma and Terwindt, 1981; Prothero and Schwab, 1996; Oboh-Ikuenobe

et al., 2005). The stratigraphic relationship of the Enugu Shale and the underlying tidally influenced Owelli facies is consistent with a relative rise in sea level and the establishment of estuarine conditions (Reineck and Singh, 1980; Dalrymple, 1992).

No direct dating is available for the Owelli Sandstone; it contains no known microfauna (Agagu *et al.*, 1985). On the basis of its stratigraphical position a Late Campanian (to Early Maastrichtian?) age is probable. A minimum exposed thickness of 80 m was reported by Agumanu (1993). Agagu *et al.* (1985) estimated the thickness of about 50 m in outcrop but increasing to around 400 m in the subsurface to the west. Allix (1987) identified major southwesterly prograding Delta Front deposits, over 1500 m thick, overlying shales with thin limestone in the subsurface Anambra Basin to the west of the outcropping Owelli Sandstone. It is possible that this Delta Front represents the distal part of the latter unit prograding over subsurface equivalents of the Nkporo Shale (Zarborski, 1998).

In the Mpu Hills, some 20 km east of Awgu, 300-400 m of coarse to fine-grained, cross-bedded ferruginized sandstones with pebbly beds, shaly sandstones, occasional shales and an impure coal about 1.5 m thick overlie folded Pre-Santonian shales. Simpson (1954) described 20-30 m of breccia comprising sandstone and shale fragments set in a carbonaceous matrix at the base of this succession (see also Ojoh, 1990). Agumanu (1993) regarded this as a channel lag deposit lying upon an erosional surface. Simpson (1954) considered the Mpu Hills beds as an outlier of either the Mamu Formation or the Owelli Sandstone. Agumanu (1993) favoured the latter suggestion, while Ojoh (1990) referred them to a separate Mpu Hills Formation; he recovered a palynoflora indicative of a Maastrichtian age along with *dinoflagellates* and marginal marine *arenaceous foraminifers*.

2.6.1.3 Enugu Shale

To the north of Agbani the Owelli Sandstone passes laterally into a further argillaceous facies, the Enugu Shale (Grove, 1951). The formation comprises grey-blue to dark grey

mudstones, shales and silty shales, often carbonaceous or gypsum-bearing. Occasional white fine-grained sandstones, siltstones and sandy shales occur as well as septarian nodules, ironstone horizons and rare thin coals (Simpson, 1954). Plant remains have been described by Slopes (1914) and Seward (1924) while Newton (1924) and Simpson (1954) recorded a number of marine *bivalves* and *gastropods*. *Libycoceras afikpoense* occurs in the lower part of the formation northeast of Enugu (Reyment, 1955). Foraminifers are rare or absent (Agagu *et al.,* 1985). The palynoflora is diverse and of similar composition to that of the Nkporo Shale (Edet, 1992). Dinoflagellates occur in some abundance (Mebradu, 1990, Courel *et al.,* 1991). Although the lower part of the Enugu Shale contains marine molluscs including *inoceramids*, the other part of the formation was deposited under less open marine conditions than the Nkporo Shale. Courel *et al.* (1991) regarded the Enugu Shale as of prodeltaic origin passing at the top into lower delta plain deposits.

In the northern part of the Anambra Basin [Ankpa Basin of Agagu and Adighije (1983)] the Enugu Shale passes laterally into largely arenaceous facies which include the Otobi Sandstone and Ekeh Sandstone (Simpson, 1954; Reyment, 1965). The Nkporo Shale and Enugu Shale pass transitionally upwards into the Mamu Formation (Reyment, 1964) ["Lower Coal Measures" of Tattam (1944), Simpson (1954), de Swardt and Casey (1961)] which reaches a maximum thickness of over 300 m in the Enugu area, thinning to 90 m in the north of the Anambra Basin and 80 m in the south (Ladipo, 1988). Around Enugu it is made up of a laterally variable succession of fine to medium-grained well-bedded sandstones, shales, mudstones and sandy shales, frequently bioturbated. Carbonaceous shales and sandstones are common. Shale units reach greater thicknesses to the north of Enugu. Shale and sandstone may alternate rapidly; oxidized parts of such lithologies comprise the "White Sandstones" of Simpson (1954). Cross-bedded sandstones and channel-filling sands occur only rarely. Synsedimentary slumps or convolute bedding are common (de Swardt and Casey,

1961; Ladipo, 1988; Courel *et al.* 1991). Coarsening-upwards sequences, each some 10 m thick, were reported by Courel *et al.* (1991).

2.6.2 The Coal Measures

Centred in Enugu but extending far north to the Owukpa area north of Nsukka, the coal measures represent an extensive Maastrichtian interval and document a period of non – marine alternating with shallow marine sedimentation in the Anambra Basin. The facies attain over 900 m in thickness. The basal 100 m is the Mamu Formation. The top 400 m is the Ajali Formation which is in turn succeeded by a further 300 m Nsukka Formation, also referred to as the Upper Coal Measures.

2.6.2.1 Mamu Formation

Sub-bituminous coals occur in the Mamu Formation in the central and northern parts of the Anambra Basin. The seams are generally laterally impersistent and vary in thickness from a few cm to about 4 m. In the Enugu area five seams occur in a succession showing rhythmic sedimentation (de Swardt and Casey, 1961); the middle coal is the thickest of about 2 m. Courel *et al.* (1991) reported significant numbers of *dinoflagellates* below the coal-bearing part of the Mamu Formation, inferring a lower delta plain environment of deposition for these beds. *Dinoflagellates* also occur immediately below, above and exceptionally within the coals indicating the proximity of marine environments throughout. They regarded the coal-bearing sequences, containing seat earths in places, to have formed after the infilling of the prodeltaic system represented by the Enugu Shale. Repetitive, coarsening-upwards sequences were interpreted as the result of shallowing into conditions intermediate between swamp and lagoon when coal formation took place. These low-lying environments were then inundated by the sea; *Ophiomorpha* and *Thalassinoides* were reported from beds directly overlying coals. Retreat of marine environments was attributed to intervals of sediment infilling rather than general regression. Agagu *et al*. (1985) regarded the Mamu Formation as representing

strandplain to deltaic environments, evolving into more open strandplain systems, Ladipo (1988) suggested a variety of estuarine and shallow marine conditions with tidal flats present even in the most northerly part of the Anambra Basin. Akande *et al*. (1992a, 1992b) regarded the coals of the Mamu Formation as having accumulated in forest and marsh swamps within delta plain environments. Salami (1990) identified *palynomorphs* characteristic of freshwater swamps or marshes populated by ferns and fringed by shrubs and palms; they were thought to have been inundated on occasion by brackish waters. Arenaceous foraminifers occur sparsely in carbonaceous shales (Agagu *et al.*, 1985).

To the south of Enugu coals rapidly disappear and carbonaceous shales decrease in importance. Pebbly coarse grained sandstones, similar to those within the Owelli Sandstone, were reported from the subsurface west of Awgu by Agagu *et al.* (1985) as were shales with calcareous foraminifers. Where the Mamu Formation crosses the axis of the Abakaliki anticlinoriurn sandy facies dominate (Simpson, 1954; de Swardt and Casey, 1961). In its lower part, however, there is an interval of carbonaceous shales and thin limestones (Akande and Mucke, 1993) containing arenaceous and calcareous benthonic foraminifers indicative of "prodeltaic to lagoonal and interdistributary bay, brackish water to open marine environments (Gebhardt, 1998).

Owing to the lack of age-diagnostic faunas, precise dating of the Mamu Formation is difficult; but on the basis of its stratigraphical position, an Early Maastrichtian age is probable, though it may be diachronous, younging from north to south.

2.6.2.2 Ajali Sandstone

The Mamu Formation is overlain by the Ajali Sandstone (Reyment, 1964) [= "Falsebedded Sandstones" of Tattam (1944), Simpson (1954), de Swardt and Casey (1961)] which has an overall blanket-like geometry" (Ladipo, 1986; Allix, 1987). Its maximum

thickness in the central part of the Anambra Basin is some 500-600 m (Simpson, 1954; Allix, 1987). According to Simpson (1954), it thins to the south and about 200 m occurring where its outcrop crosses the axis of the Abakaliki anticlinorium though only a few tens of metres were reported from this area by Ladipo (1986). The formation mainly comprises friable, clean, medium to coarse-grained, subangular to subrounded, poorly sorted, white to grey, sometimes iron-stained quartz arenites [in contrast to the feldspathic nature of Pre-Santonian sandstones, those of Campano-Maastrichtian age are quartz arenites (Hoque, 1977)]. Cross-bedding is virtually ubiquitous; small-scale trough cross-bedding occurs but tabular varieties are predominant. Solitary units 1-2.5 m thick are present but in most cases there are superposed sets each 60 cm or less in thickness. Foresets are frequently marked by a grading of coarse and medium-grained sand. Pebble or granule beds also occur. White to pink laminated mudstones are a subordinate lithology; they frequently contain plant impressions (Rao and Kumaran, 1981). The Ajali Sandstone contains fine-grained and calcareous sandstones in the subsurface Anambra Basin; here there is a greater proportion of shale, often pyritic or carbonaceous and containing *ostracods* and arenaceous *foraminifers* (Agagu *et al*., 1985).

Murat (1972) regarded the Ajali Sandstone as continental in nature. Hoque and Ezepue (1977) interpreted it as a fluvio-deltaic deposit on account of its unimodal, westerly to southwesterly foreset inclinations, its poor to moderate sorting and the absence of fossils other than plant remains. A derivation from the Adamawa highlands was suggested. Banerjee (1979) found certain features consistent with a fluvial origin but preferred an intertidal sand bar and tidal channel point bar nature, noting in particular the presence of *Ophiomorpha* and *Skolithos* at a few horizons. Amajor (1984) and Ladipo (1986, 1987a, 1987b, 1988a, 1988b) described a number of features indicative of a tidal to shallow sublittoral palaeoenvironment: *Skolithos* and *Ophiomorpha*; bipolar-bimodal current azimuths; and reactivation surfaces of inferred tidal origin. Ladipo (1986, 1988a) suggested a subtidal to tidal origin for the Ajali

Sandstone with a gradation into more paralic deposits in the subsurface. Shoreline-parallel sand bodies intercalated with shelf muds were suggested with a dominantly southerly (ebb) current responsible for the large-scale cross-bedding. Intermittent storms produced coarse sediment lags. Allix (1987) regarded the Ajali Sandstone as fluvially-derived but reworked in a marine environment. Amajor (1984) suggested channelled intertidal flat environments grading landwards into continental deposits. The lack of age-diagnostic fossils precludes dating more precise than Maastrichtian for the Ajali Sandstone.

2.6.2.3 Nsukka Formation

The youngest of the Cretaceous formations in southeastern Nigeria is the Nsukka Formation (Reyment, 1964) [= "Upper Coal Measures" of Tattam (1944), Simpson (1954), de Swardt and Casey (1961)]. Surface occurrences of the formation are frequently deeply weathered (Hazell, 1958). Simpson (1954) reported an overall thickness of some 450 m in the western part of the Afikpo Syncline; Allix (1987) referred some 200 m of beds in the subsurface for Nsukka Formation. Lithologically the unit resembles the Mamu Formation. The following general succession outcrops in the central part of the Anambra Basin (du Preez, 1947; Simpson, 1954; de Swardt and Casey, 1961):

iv) at the top, a thick sequence of sandstones and dark coloured shales;

iii) 10-20 m of sandstones;

ii) 10 m of blue clays, fine-grained clay-rich sandstones, carbonaceous shales, and coal seams reaching thicknesses of nearly 2 m; and

i) at the bottom, about 15 m of fine-grained, white well-bedded sandstones with subordinate siltstones and coarser-grained sandstones.

Detailed accounts of the coal occurrences were provided by de Swardt and Casey (1961). Where the Nsukka Formation crosses the axis of the Abakaliki anticlinorium it comprises medium to coarse-grained yellow sandstones with subordinate shales or sandy shales. No coals occur here but thin oyster-rich limestones containing the bivalve *Veniella* occur in the upper part of the formation. In the Afikpo Syncline a few thin coals are again present and shelly limestones containing *ostracods* and *foraminifers* occur; especially to the east. In the subsurface Anambra Basin dark grey, pyritic, glauconitic and calcareous shales are present (Agagu *et al*., 1985).

In that part of the Anambra Basin west of the River Niger beds referred to the Nsukka Formation by Reyment (1965) [- "Coal Measures" of Hockey *et al*. (1986)] directly overlie the Precambrian basement. The Nsukka Formation here consists of sandstones, shales, calcareous sandstones, limestone containing Maastrichtian *foraminifers* and *ostracods* and sandy shales with plant remains. A basal conglomerate or pebbly sandstone is present and thin coal seams occur. From exposures northeast of Benin City, Reyment (1955a, 1957a) described the ammonite *Sphenodiscus studeri* (Reyment) and the bivalve *Endocostea coxi* (Reyment) and suggested a Late Maastrichtian age [*E. coxi* also occurs in the mid-Maastrichtian part of the Nkporo Shale in the Calabar Flank].

Simpson (1954) reported the presence of (unspecified) Palaeocene *foraminifers* in the upper part of the Nsukka Formation which therefore appears to contain the Cretaceous-Cenozoic boundary. On the basis of *dinoflagellate* and *ostracods* occurrences, Mbuk *et al.* (1985) and Kumaran and Rajshekhar (1992) suggested that the boundary lay within a conformable sequence of clays, shales, sandstones and limestones of inferred shallow sublittoral to tidal origin in the eastern Afikpo Syncline. Allix *et al.* (1984) reported an abrupt

turnover of palynofossils at the inferred Cretaceous-Cenozoic boundary in the subsurface Anambra Basin and suggested that a hiatus might exist at this level.

CHAPTER THREE

METHODOLOGY

3.1 INTRODUCTION

Field mapping was conducted within the period of November and December, 2015. Various stratigraphic sections were studied and samples collected from each section for granulometric analysis, directional structures were measured for paleocurrent analysis.

3.2 Desk Study

This involves literature review of both published and unpublished materials relevant to the present reseach in the study area.

3.3 Field Work

The fieldwork was conducted during the dry season using 1:50,000 topographic base maps of Idah Sheet 267 SE.

Traverses were taken, directional bearing were obtained with the aid of compass along major roads and minor footpaths while sampling of rock units was carried out concurrently

where there are exposures of surface outcrops. However, much attention was devoted to locating stratigraphic outcrop sections which are mainly exposed along river banks and road cuts. Along these river banks, it was easy to locate and describe geological contacts or boundaries. Because of the large area involved, it was necessary to use motor cycle between some outcrop locations.

Fresh samples were carefully collected from each section in order to avoid distortion of the result due to weathering. Vital information like location, sample number, horizon description such as; lithologies, colours, sedimentary structures from each unit and date of the sampling were clearly indicated on the sample bags and all the relevant data were written in field note book. Eleven sections were logged within the study area.

Samples of the various lithologic units were collected with the aid of geologic hammer and chisel. The thickness of each unit measured using measuring tape. Location of boundaries and elevation were obtained using the (Global Positioning System). The samples were well labelled and kept in separate sample bags for analysis in other to avoid contamination. Sedimentologic graphic logs were drawn for each section studied. The paleoenvironmetal interpretation was attempted based on facies association, sedimentary structure and textures, and granulometric analysis.

3.4 Laboratory Sample Preparation and Analysis

3.4.1 Granulometric Analysis

Granulometric analysis (sieve analysis) was carried out on samples from Mamu Formation and Ajali Sandstone in the Department of Geology, Kogi State University, Ayingba and Ahmadu Bello University, Zaria. The primary aim of sieve analysis is to determine particles size distribution and other grain size parameters like sorting, skewness, mean and

kurtosis. A total of 23 samples from Mamu Formation and Ajali Sandstone were selected from different locations for the sieve analysis.

The Samples were friable. The weights of the bottom pan and selected empty sieves with slot sizes of (2.0 mm, 1 mm, 500 µm, 250 µm, 125 µm and 63 µm) and 100g of each disaggregated samples were obtained by using electric weighing machine. The required sieves were arranged according to decreasing mesh sizes with the smallest opening at the bottom which collects the finest grain and the top is covered with a lid. The sieves and the bottom pan were fastened to the mechanical sieve shaker (R_o Top), and 100 g of the samples poured into the uppermost sieve. The machine was allowed to shake for ten (10) minutes. Sediment fractions on each of the sieves and the bottom pan were weighed and recorded.

During the process of the sieve analysis care was taken in the separation of the sieves to avoid the spillover or pouring away of the sediment fractions retained on the sieves after shaking. The results from the sieve analysis are presented in a tabular form (Table 4.1and Appendix I).

The cumulative frequency curves resulting from the analysis are shown in (Appendix 1). From the cumulative frequency curve, critical percentiles (φ5, φ16, φ25, φ50 φ75 φ84 φ95) were obtained and used in the calculation of grain size parameters such as graphic mean, sorting (graphic standard deviation), graphic skewness and graphic kurtosis; the results of these parameters for each of the samples were tabulated and shown under result section. The statistical parameters of the grain size frequency distribution were obtained and computed using the method of Folk and Ward (1957).

These were used as independent function or combined in multivariate analysis such as the LDF and CM pattern to interpret the depositional environments and processes. For the CM pattern, parameter C (one percentile of the grain size distribution) and M (the median) were

plotted with phi values of the C and M obtained from cumulative curves in phi and converted to microns using the standard formular μm= $2^{-\phi}$ x 1000 (Figure 4.14).

The following graphical parameters were obtained using Folk and Ward's (1957) formulae.

1 Graphic mean $(M) = \frac{\phi_{16}+\phi_{50}+\phi_{84}}{3}$

2. Graphic Standard Deviation (sorting) $(I) = \frac{\phi_{84}-\phi_{16}}{4} + \frac{\phi_{95}-\phi_{5}}{6.6}$

3. InclusiveGraphic Skewness $(Ski) = \frac{\phi_{84}+\phi_{16}-2\phi_{50}}{2(\phi_{84}-\phi_{16})} + \frac{\phi_{95}+\phi_{5}-2\phi_{50}}{2(\phi_{95}-\phi_{5})}$

4. Graphic Kurtosis $(K_G) = \frac{\phi_{95}-\phi_{5}}{2.44(\phi_{75}-\phi_{25})}$

M: Graphic mean standard values

Phi (ϕ) value	**Size class (Wentworth, 1922)**
-1.0 to 0.0	Very coarse grained sand
0.0 to 1.0	Coarse grained sand
1.0 to 2.0	Medium grained sand
2.0 to 3.0	Fine grained sand
3.0 to 4.0	Very fine grained sand
4.0 to 8.0	Silt
8.0 to 14.0	Clay

I: values Graphic phi standard deviation

Phi standard deviation	**Verbal sorting**
<0.35	Very well sorted
0.35 to 0.50	Well sorted
0.50 to 0.70	Moderately well sorted
0.70 to 1.00	Moderately sorted
1.00 to 2.00	Poorly sorted
2.00 to 4.00	Very poorly sorted
>4.00	Extremely poorly sorted

Ski: Graphic skewness standard values

Calculatedskewness	**Verbal skewness (Fig.)**
> +0.30	Strongly fine skewed
+0.30 to +0.10	Positively skewed
+0.10 to –0.10	Near symmetrical
–0.10 to –0.30	Negatively skewed
< −0.30	Strongly coarse skewed

K_G: Graphic kurtosis standard values

CalculatedKurtosis	**Verbal Kurtosis**
<0.67	very platykurtic
0.67– 0.90	platykurtic

0.90–1.11	mesokurtic
1.11-1.50	leptokurtic
1.50 -3.00	very leptokurtic

3.4.2 Paleocurrent Analysis

The azimuthal readings of the dip directions of all types of cross-stratification generated by the flow within the limits of preservation were measured in the field. This is because a paleocurrent system cannot be fully specified in terms of its directional and dynamic aspects by reference to a single type of bedform or its internal structure (Allen, 1965). The practice of measuring one foreset in each cross-stratified layer, as advocated by Potter and Olsen (1954), was adopted in this study because the variability at an outcrop is usually greater between than within cross-bedded units. Furthermore, this approach yields the best estimate of foreset dip directions for a given number of measurements (Potter and Pettijohn, 1963). Foreset dip directions of cross-strata were measured both in plan view and the bisectrix directions.

A total of 45 readings of cross-strata azimuthal dip directions were taken from beds of the Ajali Sandstone while 80 readings from the sandstone beds of the Mamu Formation. For this study a "location" is taken to include all readings taken from the sand body within a radius of 100 m. Generally, a location contains 1-5 outcrops ranging in thickness from 3 to more than 100 m. The recorded maximum number of readings per location is 45. Correction for tectonic dip was not made because the dip values of the Ajali Sandstone and sandstone beds of Mamu Formation are generally less than 8°. This is because Selley (1976) suggests that tectonic dip corrections for such low values does not significantly affect the interpretation.

Current roses were plotted and standard deviations computed ((Table 4.4 and 4.5)). Each arrow on the paleocurrent map represents the arithmetic mean of readings from a location. According to (Potter and Pettijohn, 1977) this method is preferable when most measurements fall within a few quadrants as is the case in this study.

3.4.3 Data Processing and Compilation of Report

This is the final stage. This is done through the collection of all datasets obtained from individual methods adopted together, process and then report writing.

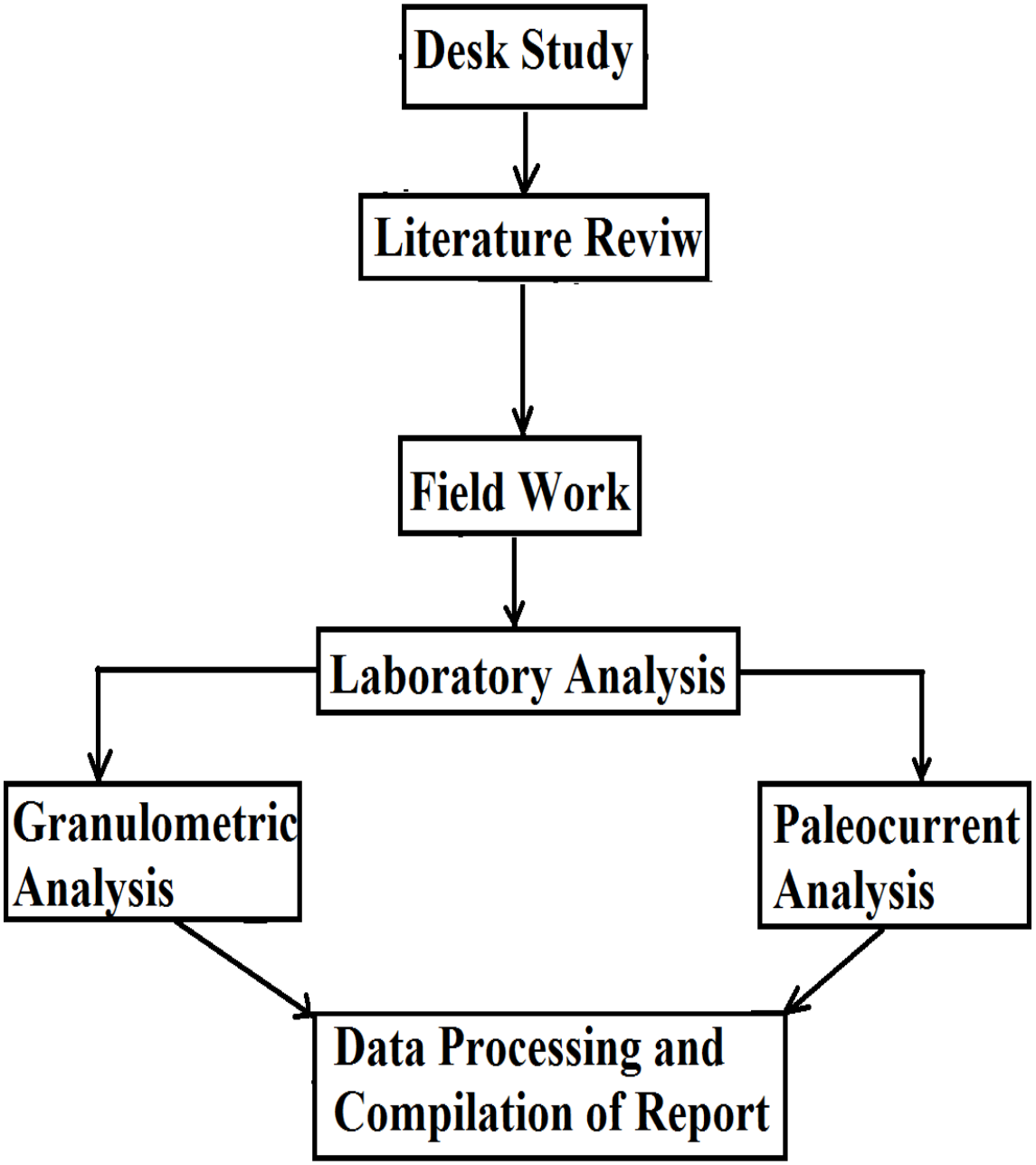


Figure 3.1: Work flow of the activities carried out in the research.

CHAPTER FOUR

RESULTS

4.1 INTRODUCTION

Sediments from each sedimentary environment exhibit uniquely different characteristics and properties that distinguished them from sediments of different environment.

Stratigraphy is defined by Whittaker *et al.* (1991) as the description, defining and naming of rock units. Hedberg (1976), defined lithostratigraphy as a tool of stratigraphy that deals with the lithology of strata and with their organization into units based on lithological characteristics.

4.2 Lithostratigraphic sections

In the study area, three formations which are the Nkporo Shale, Mamu Formation and the continental Ajali Sandstone were studied (Figure 4.1).

4.2.1 The Nkporo Shale

This formation is the oldest marine deposit in the area. Reyment (1965) estimated a maximum thickness of 100 m and Zaborski (1983) described this marginal marine sediments that made up the Nkporo Shale to cosists of dark grey fissile shales, sandy shales and mudstones. Two sections of the Nkporo Shale were studied and logged. Plates I and II and Figures 4.2 and 4.3 show exposures of this formation encountered along a road cut near Achago village and along a road cut north of Ukunube town with thickness of 3.62 m and 5.0 m respectively.

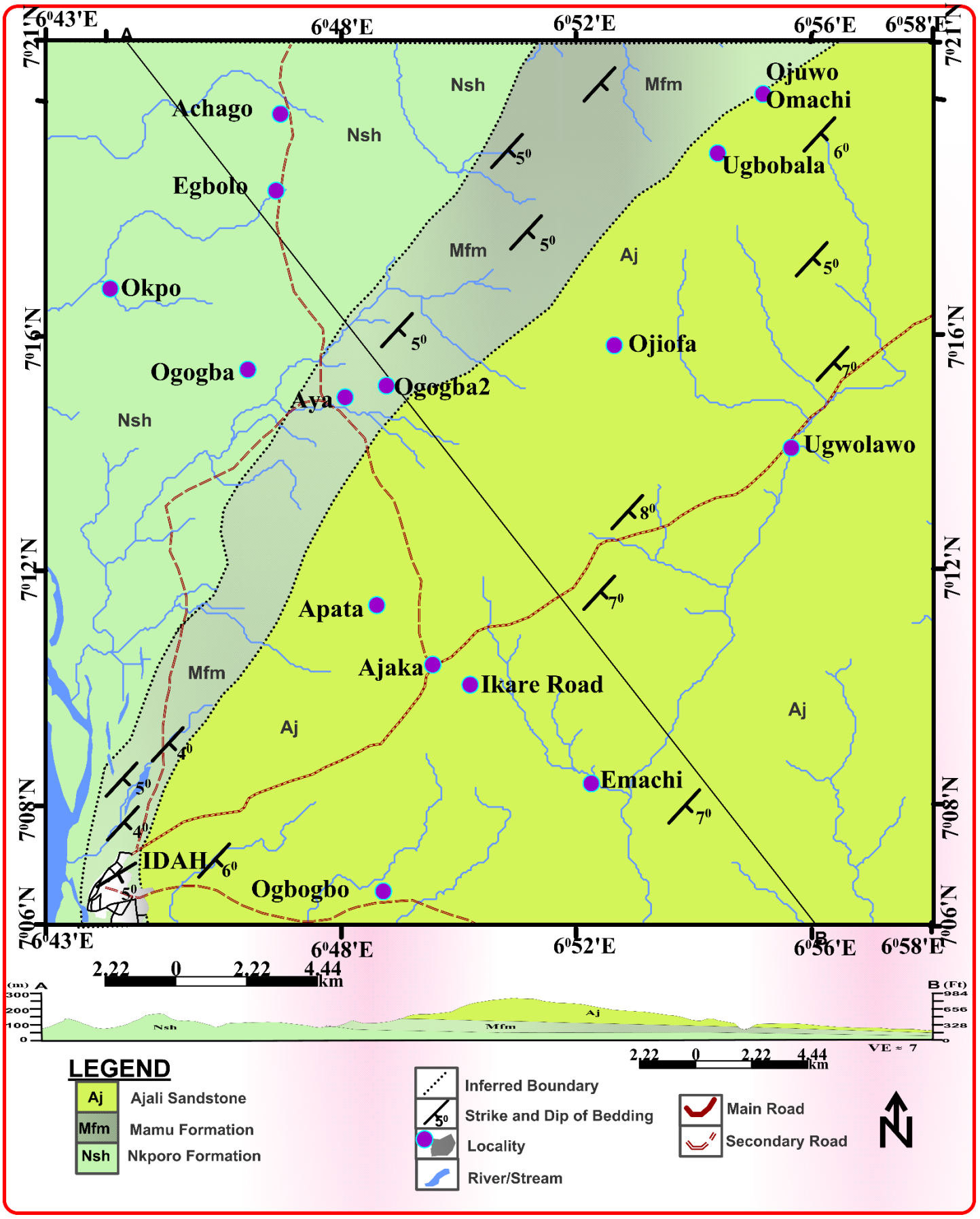


Figure 4.1: Geological map and cross section A-B of the study area with V.E of 7.

Lithologic descriptions of Nkporo Shale section exposed in the northern part of Achago town, is hereby presented from base to top. It comprise of a (i) 0.4 m thick dirty white to dark orange laminated bioturbated siltstone overlain by (ii) 0.8 m thick milky white to dirty red silty clay which passes upward into (iii) 1.5 m thick bed of ferruginized amber to dark grey weakly stratified siltstone with erosional base underlying (iv) 0.8 m thick bed of dirty red siltstone with rings of iron stain which is overlain by (v) 0.12 m thick bed of lateratized siltstone at the top (Plate I and Figure 4.2).

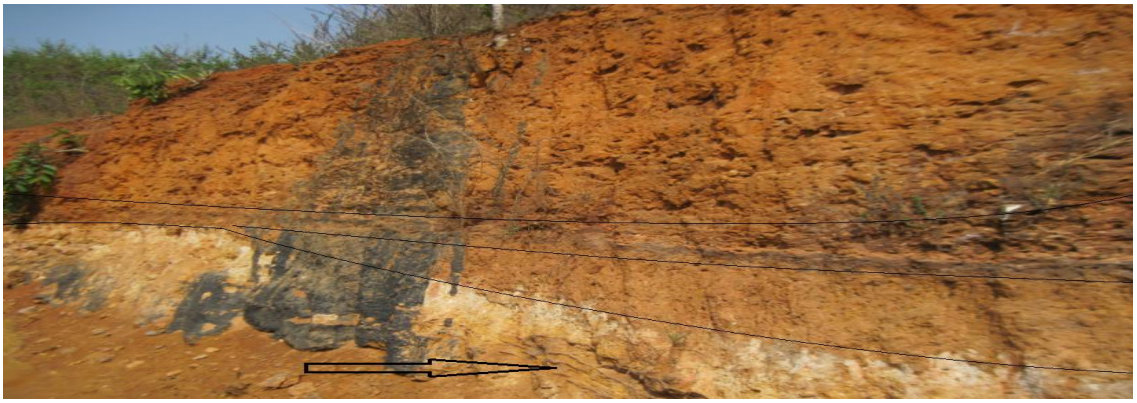


Plate I: Nkporo Shale exposed near Achago village. Photograph showing whitish to dark orange laminated bioturbated (the arrow) siltstone bed overlain by milky white to reddish silty clay which passes upward into a bed of ferruginized amber to dark grey, weakly stratified siltstone with erosional base underlying a bed of reddish siltstone which is overlain by a lateratized Siltstone (**7° 19' 48.1"N, 6° 47' 02.8"E).**

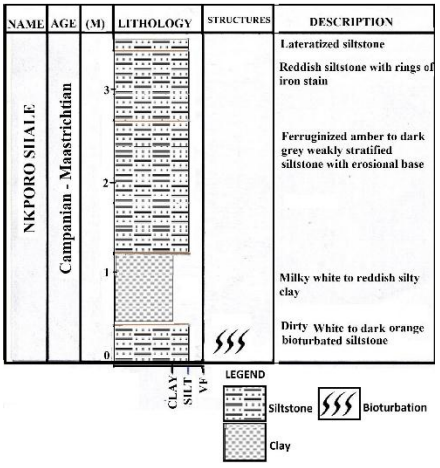


Figure 4.2: Lithostratigraphic section of Nkporo Shale exposed near Achago village (7° 19' 48.1"N, 6° 47' 02.8"E).

Lithologic descriptions of Nkporo Shale section exposed in the northern part of Ukunube town, comprising of a (i) 2.8 m thick of light grey to milky white siltstone which pass upward into a (ii) 0.8 m thick of grey to dirty blue mudstone intercalated with sandy shale overlained by a (iii) 1.4 m thick light grey to milky white siltstone terminating the section (Plate II and Figure 4.3).

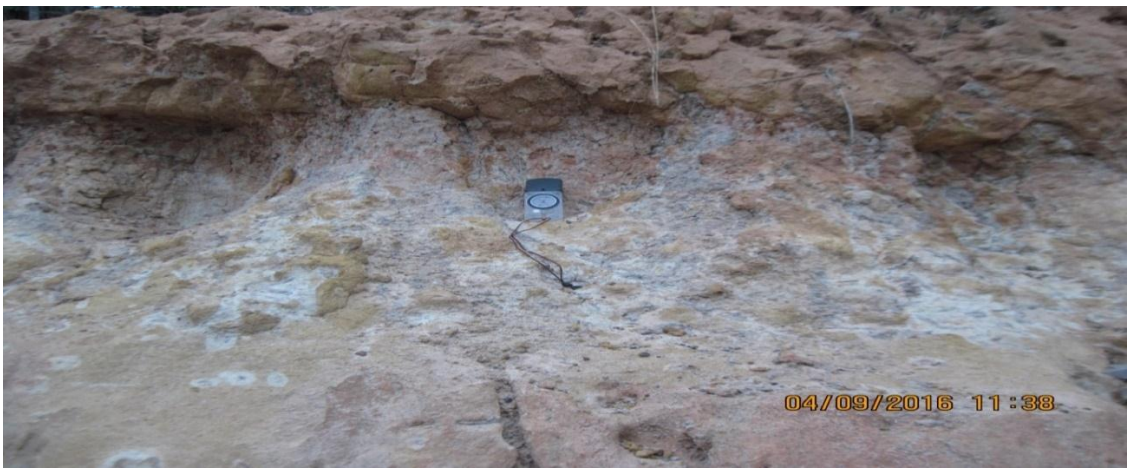


Plate II: Nkporo Shale exposed north of Ukunube town. Photograph showing fine-grained sandstone which passes upward into a intercalation of grey to bluesh mud and siltstone overlain by a fine grained sandstone (**070 21' 15.1"N, 06^0 47' 06.2"E).**

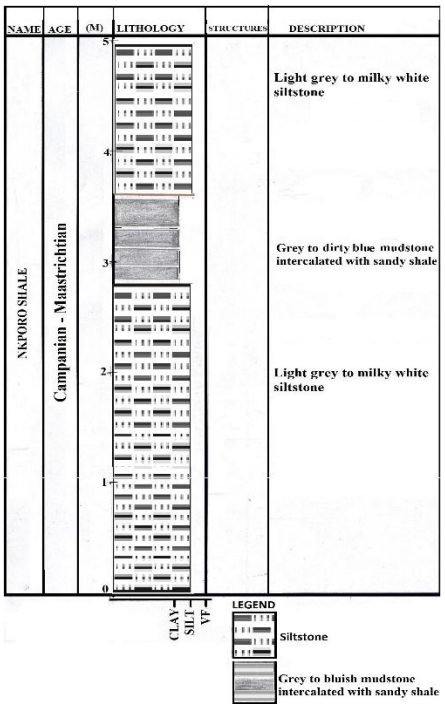


Figure 4.3: Lithostratigraphic section of the Nkporo Shale exposed north of Ukunube town (**07^0 21' 15.1"N, 06^0 47' 06.2"E).**

4.2.2 The Mamu Formation

The formation is transitional between marine Nkporo Shale of the Nkporo Group and continental Ajali Sandstone. Seven sections of the Mamu Formation were studied and logged, and they comprise an alternation of red to whitish medium to coarse-grained planar laminated sandstone overlain by white coarse to medium-grained cross – bedded sandstone with cross bedding striking northwest. With sedimentary structures such as trough, herringbone and tabular cross bedding with erosive base. The beds dips 5^{o} in the direction of northwest. This transit into an intercalation of white and red tabular cross bedded moderately sorted fine to medium-grained sandstone with cross bedding striking in northeast direction, reddish to milky white siltstone, ferruginized siltstone, evenly laminated milky white sandy shale with thin band of claystone no trace fossil observed.

Below are the descriptions of sections of the Mamu Formation in the study area.

A 27 m thick exposure studied in the northeastern part of the study area (southwestern part of Ojodu town) and consists of a bed of (i) 8 m thick of evenly laminated dark grey fissile shale, thinly intercalated with milky white clay and light grey mudstone overlain by a (ii) 9 m thick evenly laminated dark grey fissile shale, thinly intercalated with light grey mudstone overlain by a (iii) 6 m thick intercalation of thick grey mudstone and thin lens of dark grey fissile shale and a (iv) 4 m thick intercalation of light grey to milky white clay and sandy shale (Plate III and Figure 4.4). No trace fossil was observed.

Lithologic descriptions of Mamu Formation section exposed in the western part of Ojuwo Olijo town, comprises a 16 m thick intercalation of grey fissile shale and thin lens of mudstone with no trace fossil observed (Plate IV and Figure 4.5).



Plate III: Mamu Formation exposed southwest of Ojodu town. Photograph showing intercalation of grey mudstone and dark grey fissile shale overlying a evenly laminated dark grey fissile shale thinly intercalated with grey shaly mudstone which is inturn overlain by intercalation of light grey to milky white sandy shale and silt (**07^0 20' 44.9"N, 06^0 55' 09.2"E).**

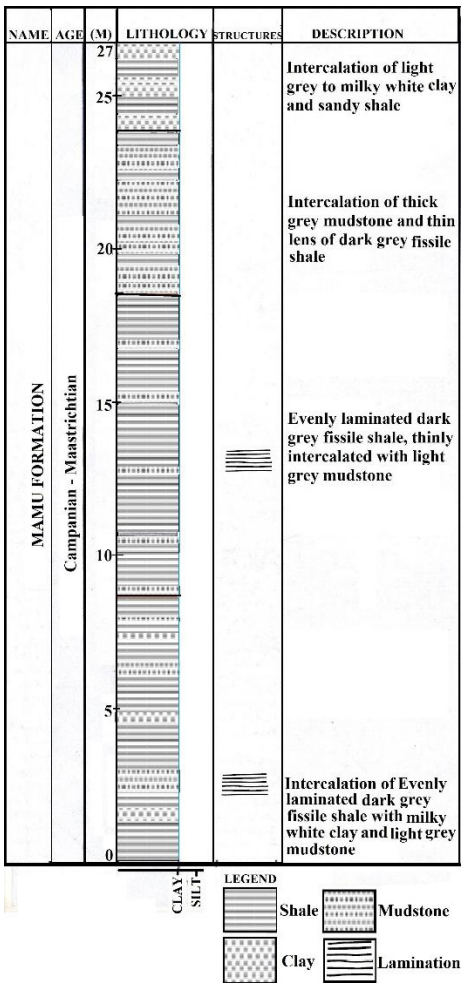


Figure 4.4: Lithostratigraphic section of the Mamu Formation exposed southwest of Ojodu town (**07^0 20' 44.9"N, 06^0 55' 09.2"E).**



Plate IV: Mamu Formation exposed west of Ojuwo Olijo town. Photograph showing intercalation of grey fissile shale and thin lens of mudstone (**07^0 20' 59.1"N, 06^0 53' 58.2"E).**

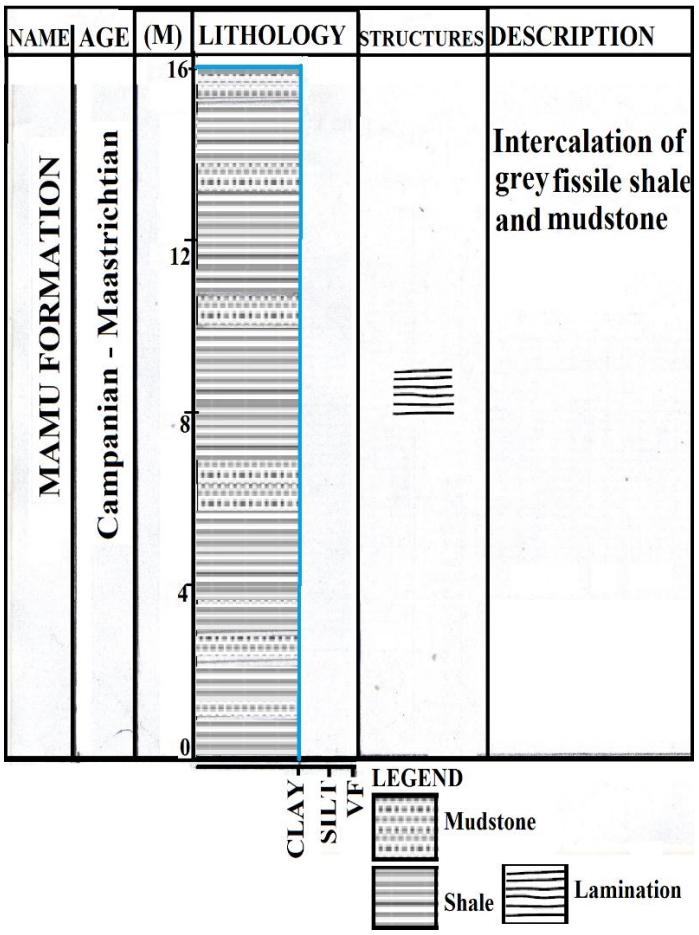


Figure 4.5: Lithostratigraphic section of the Mamu Formation exposed west of Ojuwo Olijo town (**07^0 20' 59.1"N, 06^0 53' 58.2"E).**

Lithostratigraphic descriptions of Mamu Formation section exposed in the western part of Ajegwu town, comprising of a (i) 14 m thick dark grey fissile shale with thin lens of grey mudstone overlain by a (ii) 8 m thick bed of light to milky white fissile shale overlain by a (iii) 6 m thick intercalation of light grey sandy shale with milky white claystone (Plate V and Figure 4.6).



Plate V: Mamu Formation exposed west of Ajegwu town. Photograph showing dark grey fissile shale with thin lens of grey mudstone, light to milky white fissile shale overlain by intercalation of light grey sandy shale with milky white claystone (**07^0 20' 47.7"N, 06^0 55' 16.9 "E).**

Lithologic descriptions of Mamu Formation section exposed in the western part of Ojodu town, comprising a 4 m thick intercalation of grey fissile shale, mudstone and clay, and no trace fossil was observed (Plate VI and Figure 4.7).

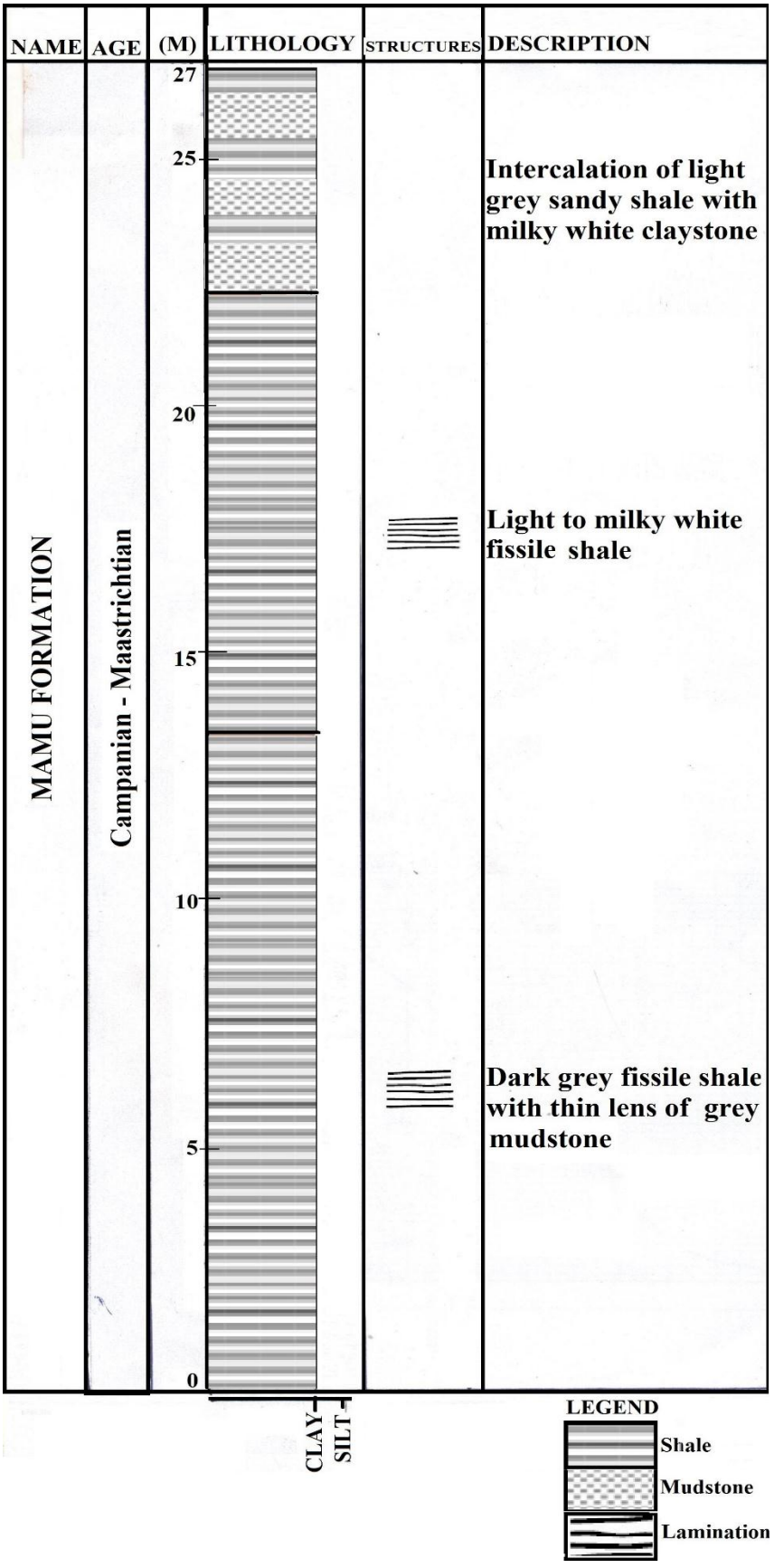


Figure 4.6: Lithostratigraphic section of the Mamu Formation exposed west of Ajegwu town (**07^0 20' 47.7"N, 06^0 55' 16.9 "E).**



Plate VI: Mamu Formation exposed west of Ojodu town. Photograph showing intercalation of grey fissile shale and shaly mudstone (**07^0 20' 49.9"N, 06^0 56' 00.3 "E).**

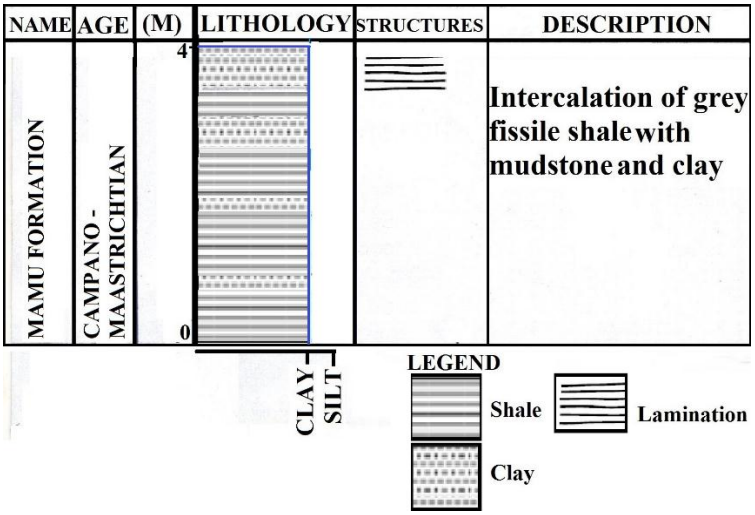


Figure 4.7: Lithostratigraphic section of grey fissle shale, mudstone and clay of Mamu Formation exposed west of Ojodu town (**07^0 20' 49.9"N, 06^0 56' 00.3 "E).**

Lithologic description of section of Mamu Formation exposed near Aya village comprises a bed of (i) 0.8 m thick dirty white to yellow siltstone overlain by a (ii) 0.3 m thick brown to amber red ferruginized siltstone which passes upward to a bed of (iii) 1.3 m thick brown to milky white weakly stratified ferruginized siltstone with convolute bedding structure (Plate VIIb) overlained by a (iv) 1.0 m thick dirty red to yellow siltstone bed which is caped by a (v) 0.4 m thick brown, dirty red to yellow lateratized siltstone bed (Plate VII and Figure 4.8).

(a)



(b)



Plate VII: Mamu Formation exposed near Aya village. (a) Photograph showing yellowish siltstone overlain by a ferruginized siltstone with convolute structure, a brownish to milky white weakly stratified ferruginized siltstone overlain by a bed of reddish to yellowish siltstone passing upward to a brown, reddish to yellowish lateratized siltstone (b) convolute bedding structure within siltstone (**07° 14' 59.4"N, 06° 48' 02.7"E)**.

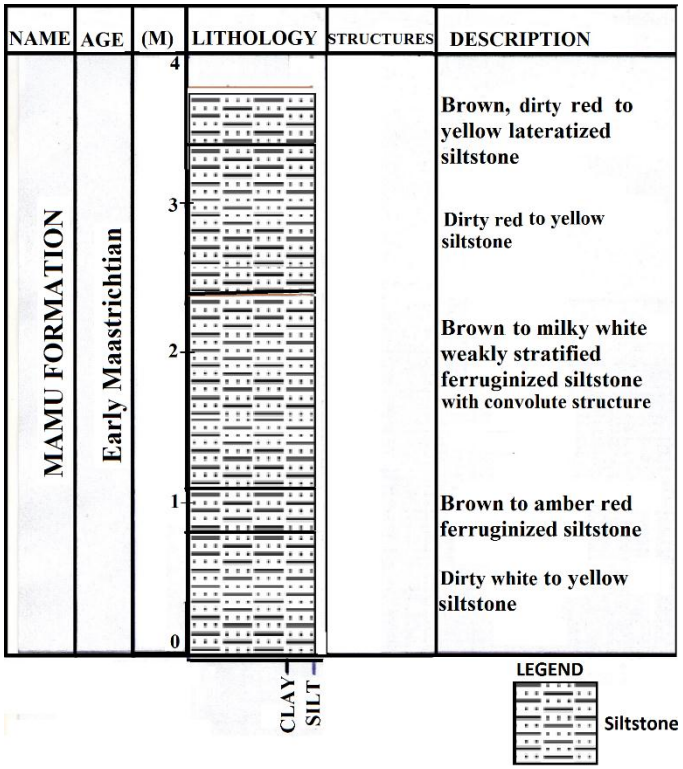


Figure 4.8: Lithostratigraphic section of Mamu Formation exposed near Aya village (**7° 14' 59.4"N, 6° 48' 02.7"E**).

Lithologic description of section of Mamu Formation exposed close to Ocheche River near Idah shows that the formation comprises a 2.0 m thick alternation of red to dirty white medium to coarse grained massive sandstone, a 3.0 m thick white, medium to coarse-grained, tabular cross-bedded sandstone with reactivation surfaces, a 5.0 m thick white, fine to medium grained, trough, herringbone and tabular cross-bedded sandstone with lens of reworked clay and sinuous crested dunes, a 6.0 m thick intercalation of dirty white to grey, medium to coarse-grained, moderately sorted, bioturbated, tabular cross-bedded sandstone with erosional surfaces and clear imprints of trace fossils burrows belonging to *ophiomorpha* genera, a 5.0 m thick medium grained, tabular cross-bedded sandstone with bedding planes, a 2.0 m thick coarse-grained, cross-bedded sandstone with wave ripple and reactivation surface, a 4.3 m thick intercalation of white and red tabular cross-bedded moderately to poorly sorted medium grained sandstone with reactivation surfaces, a 2.0 m thick fine to medium grained tabular cross-bedded sandstone, a 1.1 m

thick milky white to light grey, parallel laminated clayey siltstone with lens of clay, a 0.4 m thick red, weakly stratified ferruginized siltstone and a 0.5 m thick of lateratized siltstone overburden (Plate VIII – XIV and Figure 4.9).



Plate VIII: Mamu Formation exposed along Ocheche River near Idah. Photograph showing the milky white to light grey, parallel laminated clayey siltstone with lens of clay overlained by the red, weakly stratified ferruginized siltstone caped by the lateratized siltstone overburden.



Plate IX: Mamu Formation exposed along Ocheche River near Idah. Photograph showing the medium to coarse grained tabular cross bedded sandstone with arrows pointing at reactivation surfaces.



Plate X: Mamu Formation exposed along Ocheche River near Idah. Photograph showing medium to coarse grained cross – bedded sandstone with wave ripples (**07° 07' 27"N, 06° 44' 20.6"E).**



Plate XI: Mamu Formation exposed along Ocheche River near Idah. Photograph showing medium grained tabular cross bedded sandstone with bedding planes.



Plate XII: Mamu Formation exposed along Ocheche River near Idah. Photograph showing vertical section of intercalation of white and grey, medium to coarse grained, moderately sorted, bioturbated, tabular cross – bedded sandstone with erosional surfaces (**07° 07' 27"N, 06° 44' 20.6"E).**



Plate XIII: Mamu Formation exposed along Ocheche River near Idah. The arrows showing vertical (*Ophiomorpha*) burrows identified by red and blue arrows (**07° 07' 27"N, 06° 44' 20.6"E).**



Plate XIV: Mamu Formation exposed along Ocheche River near Idah. Photograph showing fine to medium grained trough (TrB), tabular (TB) and herringbone cross – bedded (HB) sandstone with lens of reworked clay (RC) and sinuous crested dunes.

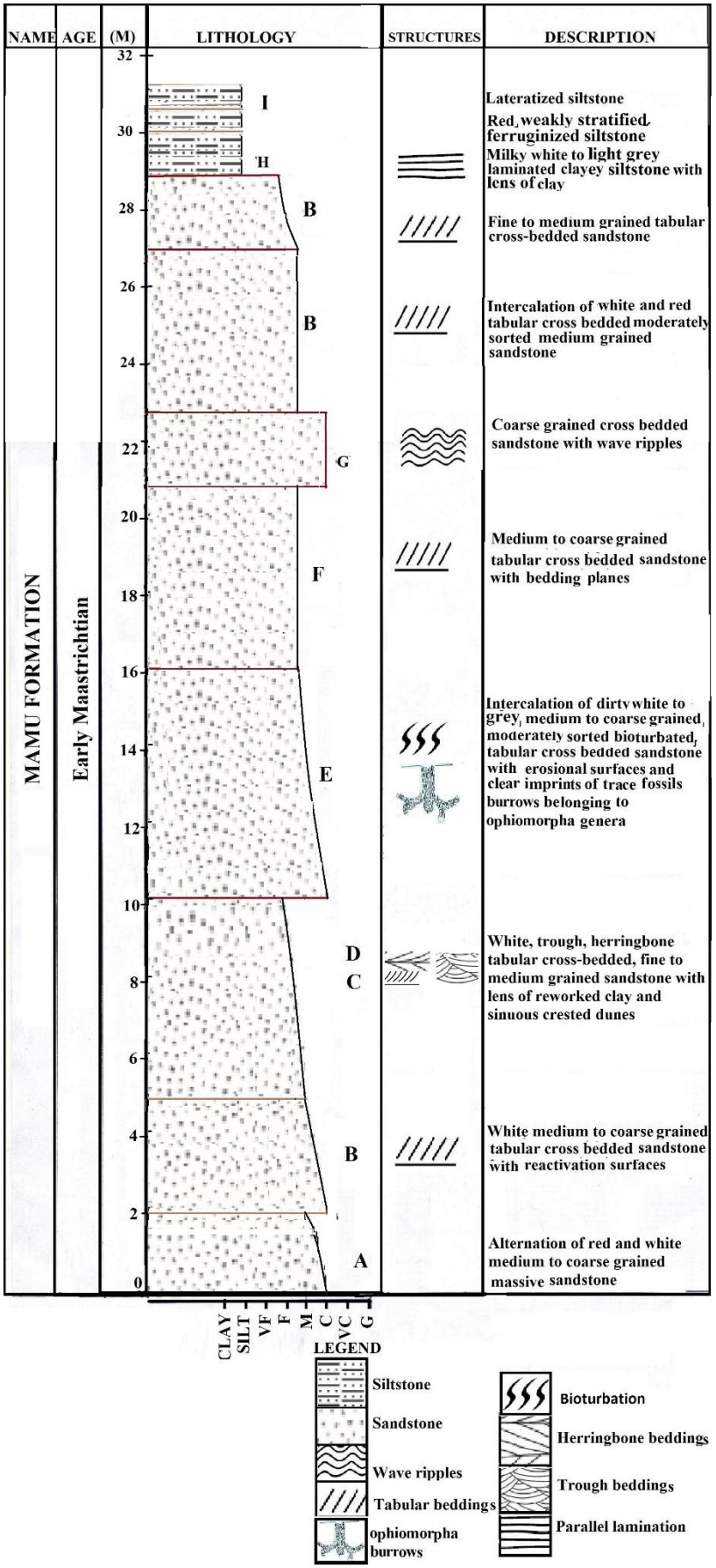
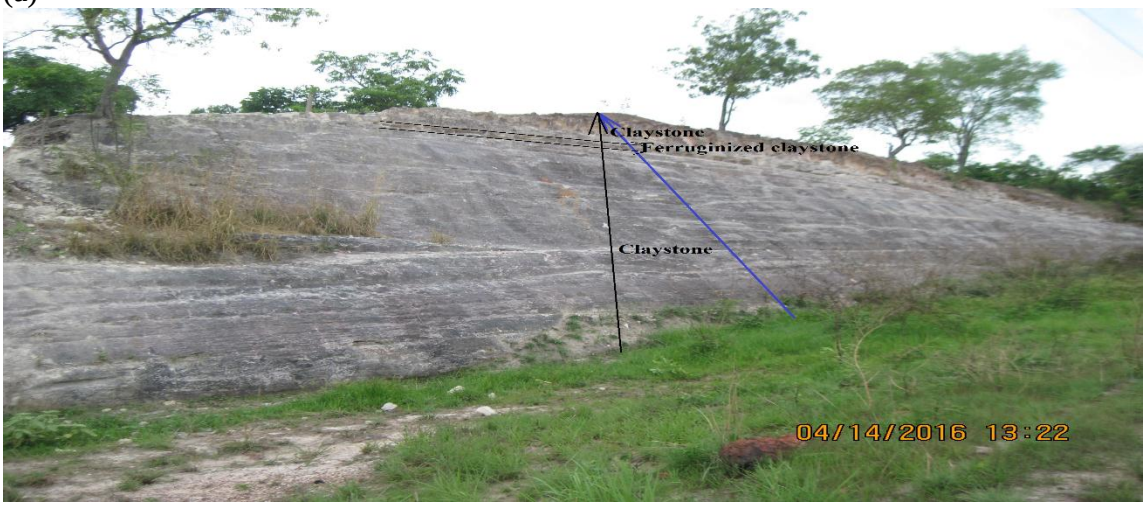


Figure 4.9: Lithostratigraphic section of sandstones of Mamu Formation exposed near Ocheche River at Idah (**07° 07' 27"N, 06° 44' 20.6"E)**.

Lithologic description of section of Mamu Formation exposed northwest of Ojuwo Omachi town comprises of a 15 m thick evenly laminated white to milky white clay with bedding planes and low angle discondant and a thin (0.2 m) band of brown ferruginized claystone towards the top of the section due to subareal exposure overlain by another 2 m thick evenly laminated white to milky white clay (Plate XV and Figure 4.10).

(a)



(b)



Plate XV: Mamu Formation exposed northwest of Ojuwo Omachi town. (a) The complete exposure of the section (b) evenly laminated claystone (**07^0 20' 35.0"N, 06^0 56' 14.8 "E).**

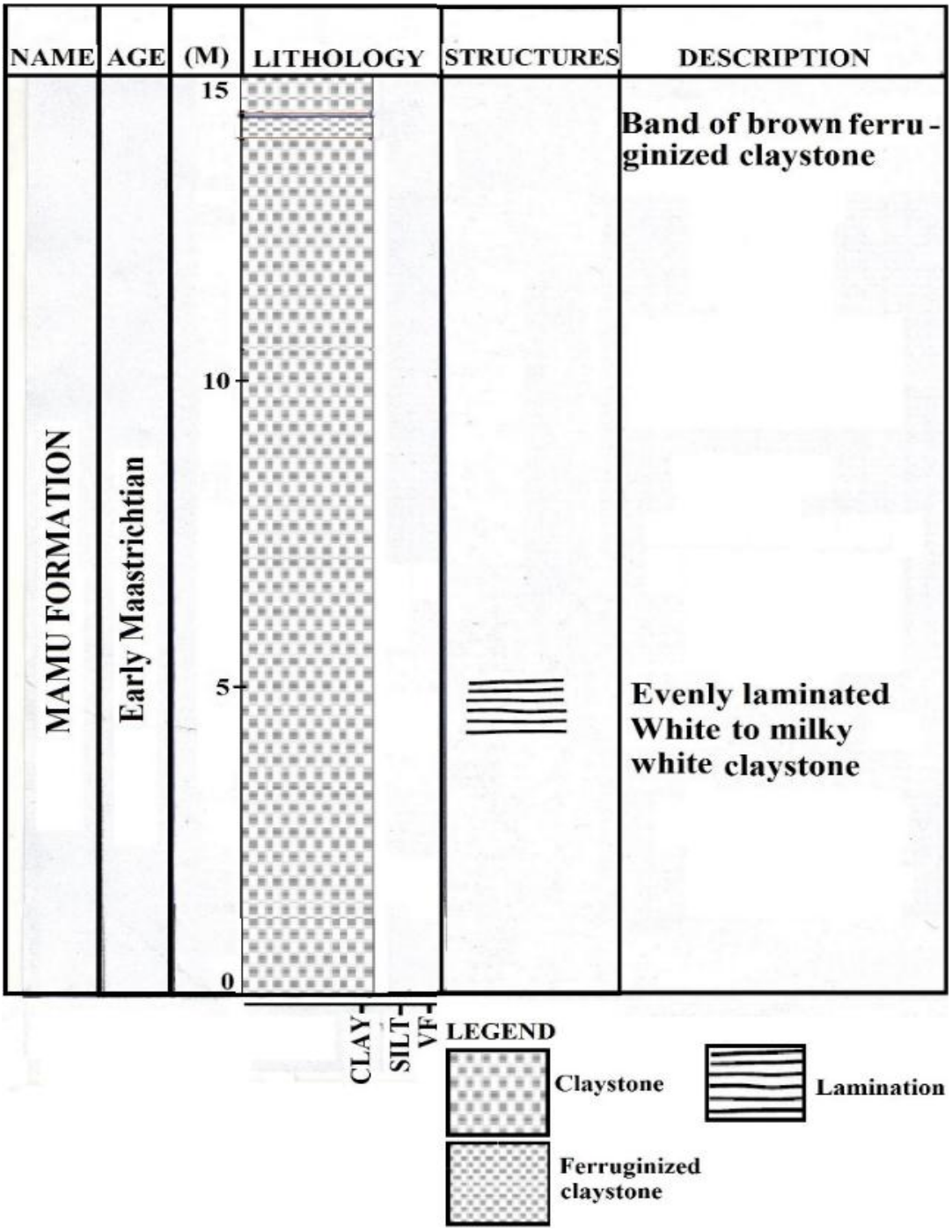


Figure 4.10: Lithostratigraphic section of Mamu Formation exposed northwest of Ojuwo Omachi town **07^0 20' 35.0"N, 06^0 56' 14.8 "E.**

4.2.3. The Ajali Sandstone

Outcrops of Ajali Sandstone were studied in the southern to western part of the study area towards Ikare from Ajaka main town (Figure 4.11). They occurred as lateratized shale with thin beds of very fine-grained sandstone and siltstone (Plate XVI). A section was studied at Ogbogba, west of Ajaka town and found to comprise a 8.0 m

thick white, coarse grained, friable moderately sorted sandstone with a thin lens of clay, alternation of red and white friable moderately sorted sandstone, white coarse grained, poorly sorted sandstone with clasts ranging from angular to subangular, white coarse grained poorly sorted ferruginized sandstone and coarse grained friable dirty red sandstone, alternation of milky white, yellow, grey and brown parallel laminated sandstone (Plate XVI, XVII, XIX and Figure 4.12). Sedimentary structures in the Ajali Sandstone are flaser cross-bedding, tabular cross-bedding and reactivation surfaces occur (Plate XVI, XVII, XIX, Figure 4.11 and 4.12).

Lithologic description of Ajali Sandstone exposed at Ikare Road, south of Ajaka town, comprises of a 8.0 m thick intercalation of dark yellow to grey lateratized fissile shale and dirty red very thin lens of very fine sandstone and siltstone (Plate XVI and Figure 4.11).



Plate XVI: Ajali Sandstone exposed at Ikare Road, south of Ajaka town. Photograph showing intercalation of dark yellow to light grey lateratized fissile shales and dirty red very thin lens of very fine sandstone and siltstone (**7° 10' 02.2"N and 6° 50' 12.8"E)**.

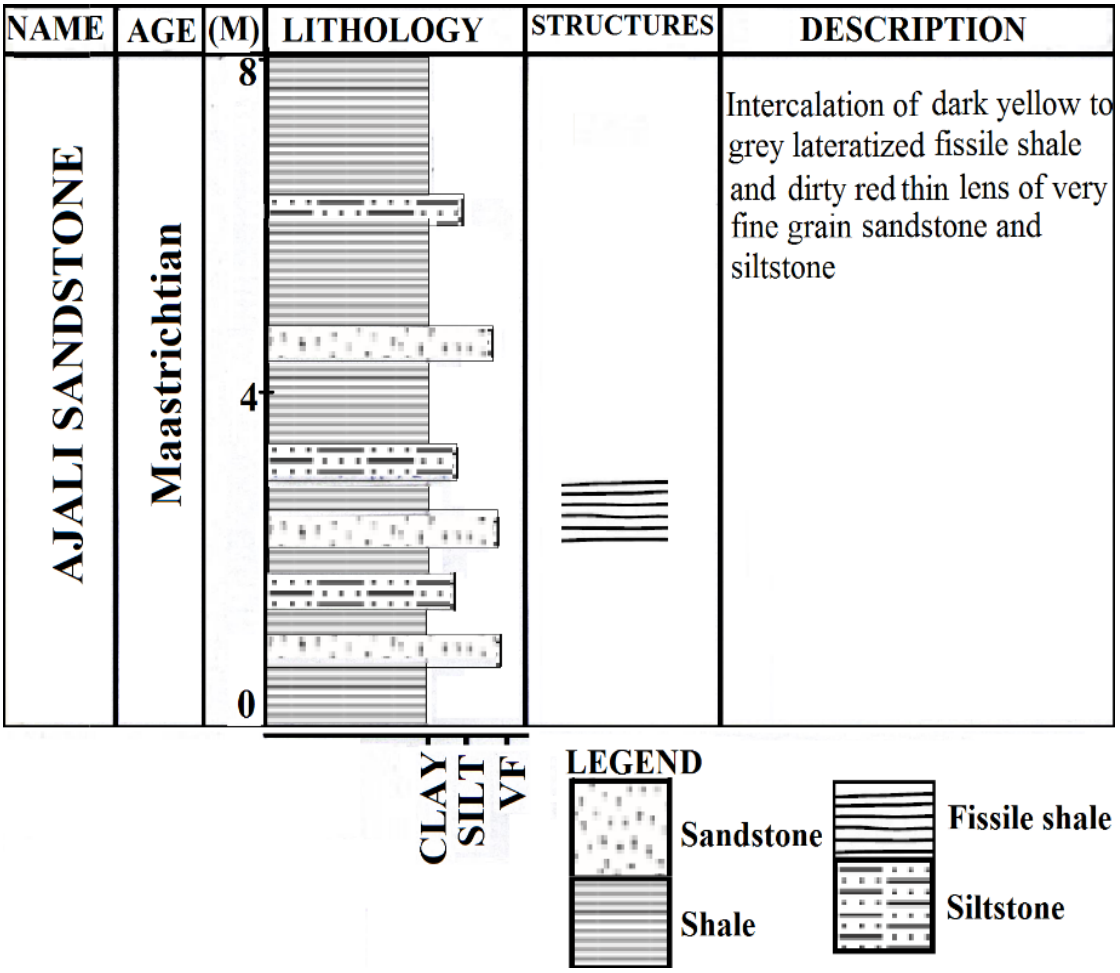


Figure 4.11: Lithostratigraphic section of lateratized shales of Ajali Sandstone exposed at Ikare Road, south of Ajaka town **07° 10' 02.2"N and 06° 50' 12.8"E**.

Lithologic description of Ajali Sandstone exposed northwest of Ogbogba town comprises of (i) a 3 m thick of white coarse grained, friable, moderately sorted, tabular cross-bedded sandstone with clast ranging from angular to well rounded towards the base and reactivation surfaces (Plate XVII) overlain by (ii) a 0.7 m thick alternation of red and white, friable, poorly sorted, negatively skewed, mesokurtic, flaser cross – bedded coarse grained sandstone which passes upward into (iii) a bed of a 1.8 m thick poorly sorted, coarse to gravel grained, near symmetrical, mesokurtic, herringbone cross-bedded sandstone with wave ripples and clasts ranging from angular to subangular. The bed shows a change in clast, that is pebbly coarse grain highlighting the base of the bedset and lens of clay towards the top of the bed showing a fining upward sequence respectively (Plate

XIVb and Figure 4.12) and in turn overlain by (iv) a 0.7 m thick bed of white, coarse grained, poorly sorted, ferruginized, flaser cross-bedded sandstone. The ferruginied, flaser cross-bedded sandstone overlie a 1m thick coarse grained, friable, moderately sorted, negatively skewed, platykurtic, dirty red sandstone which is overlain by (v) a 0.5 m thick medium grained, poorly sorted, near symmetrical, very platykurtic, tabular cross-bedded sandstone which transit into (vi) a 0.5 m thick, medium grained, poorly sorted, near symmetrical, very platykurtic, tabular cross-bedded sandstone underlying a (vii) 0.8 m thick bed of intercalation of dark yellow to grey, lateritized fissile shale and dirty red thin lens of very fine sandstone and siltstone terminating the section (Plate XVI, XVII, XIX and Figure 4.12).



Plate XVII: Ajali Sandstone exposed at Ogbogba Hill northwest Ogbogba town. Photograph showing tabular cross-bedded sandstone (**7° 12' 31.5"N, 6° 52' 22.2"E).**



Plate XVIII: Ajali Sandstone exposed at Ogbogba Hill northwest Ogbogba town. Photograph showing tabular cross bedding and herringbone cross bedding **(7° 12' 31.5"N, 6° 52' 22.2"E).**



Plate XIX: Ajali Sandstone exposed at Ogbogba Hill northwest Ogbogba town. Photograph showing the complete section **(7° 12' 31.5"N, 6° 52' 22.2"E).**

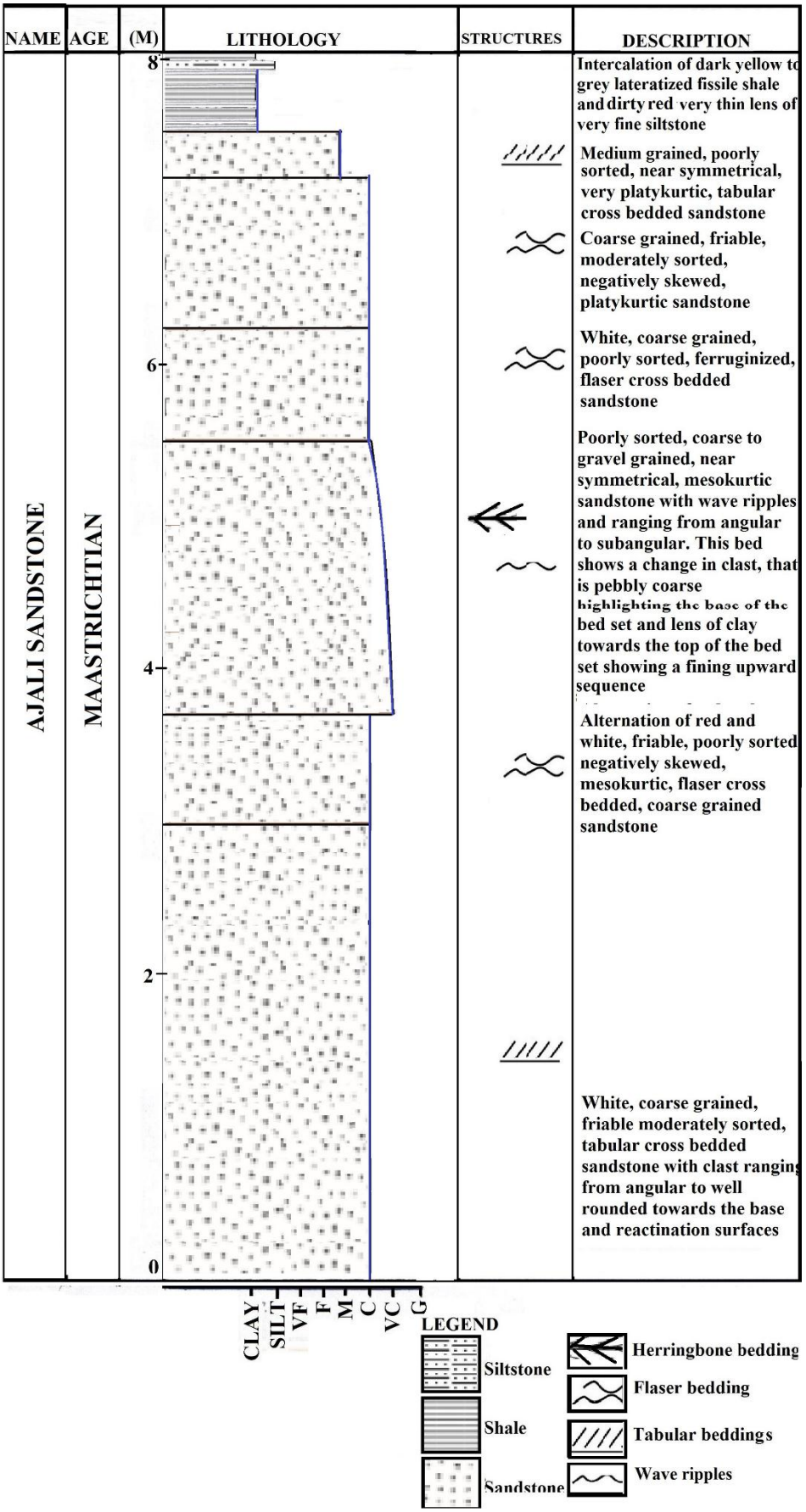


Figure 4.12: Lithostratigraphic section of Ajali Sandstone exposed at Ogbogba Hill northwest Ogbogba town (**07° 12' 31.5"N and 06° 52' 22.2"E).**

4.3 Granulometric Studies

4.3.1 Grain size and statistical parameters

The mean grain size in a deposit is generally a function of the energy of the processes controlling transport and deposition, that is particles are segregated according to their hydrodynamic behaviour which depends on the size, specific gravity and shape. In contrast, the degree of sorting of grains in a deposit is a function of the persistence and stability of the energy condition except by availability of grains that can be deposited in the environment.

Quantitative graphical values of percentile from various sample obtained from the cumulative frequency curve in (Appendix I) are presented in (Table 4.1).

Table 4.1: Percentile value from cumulative curve plots of sandstones samples in the study area.

Sample ID	ϕ5	ϕ16	ϕ25	ϕ50	ϕ75	ϕ84	ϕ95	Formation
ID1-1	-0.70	0.20	0.75	1.45	1.90	2.20	2.80	Mamu Formation
ID1-1b	-0.65	-0.35	-0.10	0.55	1.20	1.50	1.90	Mamu Formation
ID1-2	-0.90	-0.50	-0.20	0.60	1.40	1.60	2.10	Mamu Formation
ID1-3	-1.90	0.30	0.60	1.30	1.97	3.30	3.80	Mamu Formation
ID1-4	-1.80	0.40	0.70	1.40	2.30	2.80	4.30	Mamu Formation
OCH-1a	-0.70	-0.10	0.30	1.30	2.80	2.40	3.20	Mamu Formation
OCH-1b	0.20	0.50	0.80	1.30	1.80	2.00	2.50	Mamu Formation
OCH-2a	1.75	1.98	2.12	2.42	2.84	3.14	3.62	Mamu Formation
OCH-2b	-1.80	0.30	0.60	1.30	2.00	2.40	2.80	Mamu Formation
OCH-3a	-0.69	0.15	0.27	2.10	3.40	4.20	4.90	Mamu Formation
OCH-3b	0.90	1.30	1.50	2.00	2.50	2.80	3.20	Mamu Formation
OCH-4a	-0.60	-0.11	0.30	1.80	3.39	4.19	4.90	Mamu Formation
OCH-4b	0.00	0.00	0.00	0.00	0.40	0.94	2.80	Mamu Formation
OCH-5	0.20	0.82	1.18	1.80	2.60	2.98	4.20	Mamu Formation
AY-1	-1.50	-0.60	-0.15	1.15	1.80	2.20	2.90	Ajali Sandstone
OG1	-0.80	-0.35	0.00	0.95	1.60	1.80	2.20	Ajali Sandstone
OG2	-0.00	-0.20	0.20	1.20	1.70	1.95	2.80	Ajali Sandstone
OG3	-1.70	-1.00	-0.80	-0.05	0.60	1.00	1.70	Ajali Sandstone
OG5	-0.90	-0.20	-0.05	0.95	1.60	1.80	2.40	Ajali Sandstone
OJF1	-1.20	-1.80	0.10	0.60	1.30	1.80	3.00	Ajali Sandstone
OJU1	-2.80	-1.20	-1.60	0.90	2.00	2.80	3.60	Ajali Sandstone
UG1	-0.70	-0.10	0.30	1.30	2.80	2.40	3.20	Ajali Sandstone
UGB1	-0.90	-0.20	-0.05	0.95	1.60	1.80	2.40	Ajali Sandstone

Twenty three samples were sieved and statistical parameters of each of the sandstone samples were determined as presented in (Table 4.2a and b). The cumulative curves plotted for various sample were presented in (Appendix I).

Table 4.2a: Grain size distribution and quantitative parameters of samples of the sandstone facies of Ajali Sandstone in the study area.

S/N	Sample ID	Mean (mm)	Sorting (ϕ)	Skewness (ϕ)	Kurtosis (ϕ)	Formation
1	AY-1	0.920 Coarse sand	1.370 Poorly sorted	-0.230 Negatively skewed	0.920 Mesokurtic	Ajali Sandstone
2	OG1	0.800 Coarse sand	0.990 Moderately sorted	-0.190 Negatively skewed	0.770 Platykurtic	Ajali Sandstone
3	OG2	0.980 Coarse sand	1.110 Poorly sorted	-0.230 Negatively skewed	1.040 Mesokurtic	Ajali Sandstone
4	OG3	-0.020 Gravel	1.020 Poorly sorted	0.040 Near symmetrical	1.000 Mesokurtic	Ajali Sandstone
5	OG5	0.850 Coarse sand	1.000 Moderately sorted	-0.140 Negatively skewed	0.820 Platykurtic	Ajali Sandstone
6	OJF1	0.200 Coarse sand	1.520 Poorly sorted	-0.095 Negatively skewed	1.430 Leptokurtic	Ajali Sandstone
7	OJU1	0.800 Coarse sand	1.970 Poorly sorted	-0.100 Negatively skewed	0.730 Platykurtic	Ajali Sandstone
8	UG1	1.200 Medium sand	1.220 Poorly sorted	0.070 Near symmetrical	0.640 Very platykurtic	Ajali Sandstone
9	UGB1	0.850 Coarse sand	1.000 Moderately sorted	-0.140 Negatively skewed	0.820 Platykurtic	Ajali Sandstone

Table 4.2b: Grain size distribution and quantitative parameters of samples of the sandstone facies of Mamu Formation in the study area.

S/N	Sample ID	Mean (mm)	Sorting (Φ)	Skewness (Φ)	Kurtosis (Φ)	Formation
1	ID1-1	1.280 Medium sand	1.030 Poorly sorted	-0.240 Negatively skewed	1.250 Leptokurtic	Mamu Formation
2	ID1-1b	0.570 Coarse sand	0.85 Moderately sorted	0.04 Near symmetrical	0.800 Platykurtic	Mamu Formation
3	ID1-2	0.570 Coarse sand	0.980 Moderately sorted	-0.020 Near symmetrical	0.770 Platykurtic	Mamu Formation
4	ID1-3	1.600 Medium sand	1.610 Poorly sorted	0.100 Positively skewed	1.710 Very leptokurtic	Mamu Formation
5	ID1-4	1.500 Medium sand	1.520 Poorly sorted	0.060 Near symmetrical	1.560 Very leptokurtic	Mamu Formation
6	OCH-1a	1.200 Medium sand	1.220 Poorly sorted	0.070 Near symmetrical	0.640 Very leptokurtic	Mamu Formation
7	OCH-1b	1.700 Medium sand	0.720 Moderately well sorted	0.0083 Near symmetrical	0.940 Mesokurtic	Mamu Formation
8	OCH-2a	2.513 Fine sand	0.578 Moderately well sorted	0.2523 Positively skewed	1.082 Mesokurtic	Mamu Formation
9	OCH-2b	1.681 Medium sand	1.050 Poorly sorted	-0.170 Negatively skewed	1.220 Leptokurtic	Mamu Formation
10	OCH-3a	2.050 Fine sand	1.985 Poorly sorted	0.0588 Near symmetrical	0.7319 Platykurtic	Mamu Formation
11	OCH-3b	2.000 Medium sand	0.720 Moderately sorted	0.09 Near symmetrical	0.94 Mesokurtic	Mamu Formation
12	OCH-4a	1.960 Medium sand	1.908 Poorly sorted	0.1195 Positively skewed	0.7295 Platykurtic	Mamu Formation
13	OCH-4b	0.310 Coarse sand	0.660 Moderately well sorted	0.990 Stronly fine skewed	2.870 Very leptokurtic	Mamu Formation
14	OCH-5	1.870 Medium sand	1.150 Poorly sorted	0.250 Positively skewed	1.15 Leptokurtic	Mamu Formation

The histogram plots of the cumulative weight percentage against phi scale show that the sandstone facies of Ajali Sandstone and the sandstone facies of Mamu Formation in the study area are unimodal (Appendix II). These indicates samples support mixing of populations as indicated by kurtosis values (Table 4.2 a and b).

4.3.2 Univariate grain size parameters

The samples display a wide variety of grain sizes, that is, they range from medium to coarse grained sizes. Most of the samples have their peaks between 0.20φ and 1.60φ which is the equivalent of coarse to medium-grained classes of the Wenthworth (1922) scale (Figure 4.13).

a) Median

The median grain is the grain size that separate 50% of the sample (by weight) from other 50%. It thus corresponds to φ_{50} (that is, the φ value for the 50^{th} percentile). It corresponds to certain grain size in mm.

The true mean would be the average size of all the grains present. We cannot possibly do such a calculation so the graphic mean is conventionally quoted. It too corresponds to certain grain size. The average size is generally controlled by the strength of the depositing current, the initial grain size and source of the material (Folk and Ward, 1957; Pettijohn 1975). The graphic mean values for the analyzed samples are as shown in Table 4.1a and b.

Ajali Sandstone ranges from coarse to medium grained sand (AY-1, OG1, OG2 to OG3, OJF1, OJU1, UG1 and UGB1) (Table 4.1), while samples from Mamu Formation range from fine (OCH-2a and OCH-3a) though medium (ID1-1, ID1-3, ID1-4, OCH-1a, OCH-1b, OCH-2a, OCH-3b, OCH-4a and OCH-5) to coarse grained (ID1-1b, ID1-2 and OCH-4b (Table 4.2).

b) Inclusive Graphic Standard Deviation (Sorting)

The degree of sorting in sandstones generally depends on the sediment source, grain size and the depositional regime. It is indicative of hydrodynamic condition (i.e. range of velocities and degree of turbidity) operating within the transporting medium and to some extent it is suggestive of the distance travelled (Krumbein and Sloss, 1963).

The value of the standard deviation show that most of the samples are poorly sorted with few moderately sorted (Table 4.1). Samples from Ajali Sandstone are pooly sorted (AY-1, OG2, OG3, OJU1, OJF1 and UG1) to moderately sorted (OG1, OG5 and UGB1) while samples from Mamu Formation ranges from poorly sorted (ID1-1, ID1-3, ID1-4, OCH-1a, OCH-2b, OCH-3a, OCH-4a and OCH-5) through moderately sorted (ID1-1b, ID1-2 and OCH-3b) to moderately well sorted (OCH-1b, OCH-2b and OCH-4b) (Table 4.1).

Generally, the poorly to moderately sorted nature of the sandstone imply that the transporting medium responsible for the deposition was rapid or the sedimentation was fast or is suggesting a short distance of transportation and the nearness of sediment source. This is in conformity with Friedman (1979).

However, diagenesis may introduce secondary clay to sandstone thereby disrupting the degree of sorting that would be obtained from the sieve analysis. Therefore, it is the measure of scatter of grain size about the mean and corresponds with the standard deviation.

c) The (graphic) Skewness.

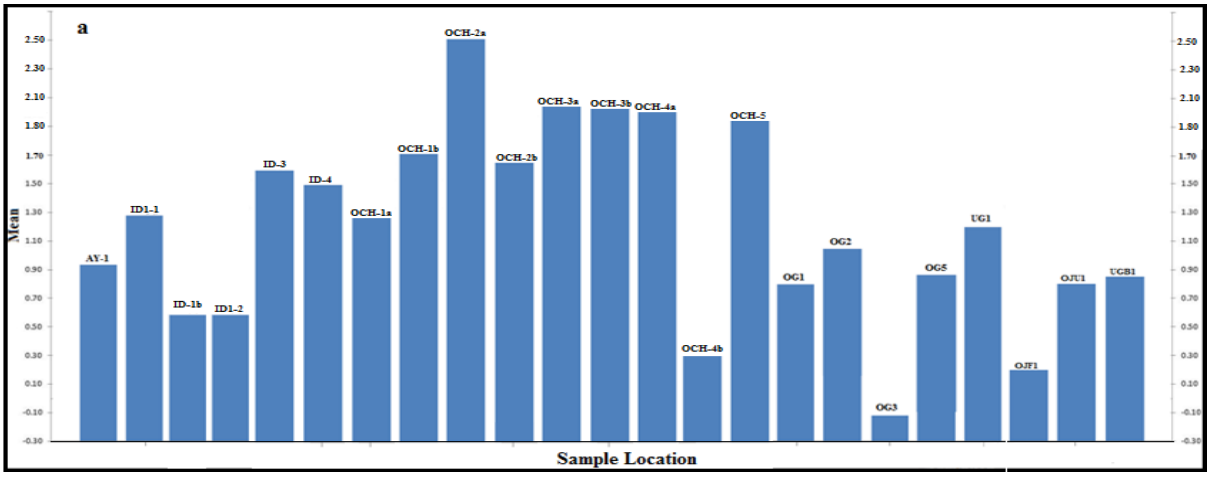
It is the measure of the symmetry or bias in the grain size distribution towards the coarser or finer-grained end of the size range and it is a very useful descriptive term for the depositional processes of the sediments. Positively skewed samples have an excess of fine grains, but negatively skewed samples consist of excess coarse grain. The samples analyzed have skewness values ranging from -0.02 to 0.10 from negatively skewed to nearly symmetrical (Table 4.1). The result shows that Ajali Sandstone range from negatively

skewed (AY-1, OG1, OG2, OG5, OJF1, OJU1, and UGB1), to nearly symmetrical (OG3 and UG1) and samples from Mamu Formation in the study area range from negatively skewed (ID1-1 and OCH-2b), positively skewed (ID1-3, OCH-2a, OCH-4a and OCH-5), near symmetrical (ID1-1b, ID1-2, ID1-4, OCH-1a, OCH-1b, OCH-3a and OCH-3b) to strongly fine skewed (OCH-4b) (Table 4.2a and b).

d) The (graphic) Kurtosis

Kurtosis is the measure of the flatness of grain size distribution as it will appear on the simple frequency curve. Flat distributions are platykurtic and peaked distributions are leptokurtic.

The various samples analyzed from (Table 4.1) shows that samples from Ajali Sandstone are very leptokurtic (OJF1) to platykurtic (OG1, OG5, OJU1, UGB1) to mesokurtic (AY-1, OG2 and OG3) to very platykurtic (UG1). While samples from the Mamu Formation are very leptokurtic (ID1-3, ID1-4, OCH-1a and OCH-4b), leptokurtic (ID1-1, OCH-2b and OCH-5), platykurtic (ID1-1b, ID1-2, OCH-3a and OCH-4a) to mesokurtic (OCH-1b, OCH-2a and OCH-3b). Little geological information can be derived from the value of kurtosis (Pettijohn 1975).



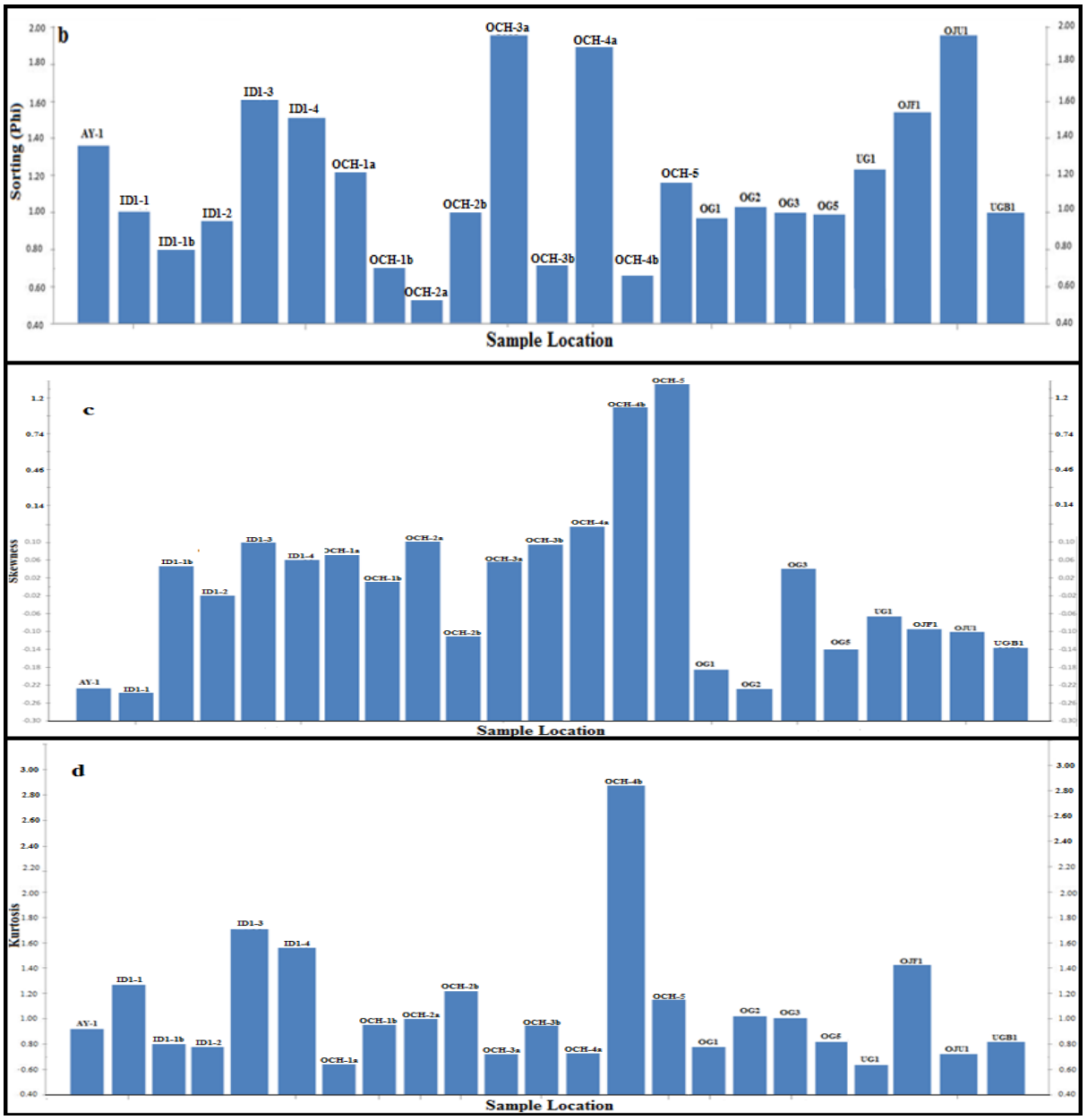


Figure 4.13: Average values of grain size statistical parameters of the study area: (a) mean; (b) sorting; (c) skewness and (d) kurtosis

4.3.3 Linear Discriminate Function

According to Sahu (1964), the statistical method of analysis of the sediments to interpret the variations in the energy and fluidity factors seems to have excellent correlation with the different processes and the environment of deposition. Linear discriminate function (LDF) analysis of the sediment samples was carried out using the following equations shown. (i). For the discrimination between Aeolian process and Littoral (intertidal zone) environment, the following equation was used:

$Y_{1(A:B)} = -3.5688\ M + 3.7016\sigma I^2 - 2.0766\ SK + 3.1135\ KG$

If Y is >-2.7411, Beach is suggested but if Y is <-2.7411, Aeolian deposition is indicated.

(ii). For the discrimination between Beach (back shore) and Shallow agitated marine environment (sub – tidal environment), the following equation was used:

$Y_{2(B:SM)} = 15.6534\ M + 65.7091\ \sigma I^2 + 18.1071\ SK + 18.5043\ KG$

If Y is <63.3650, the environment is 'Beach (backshore)' but if Y is >63.3650, the environment is 'Shallow agitated marine' (sub – tidal environment).

(iii). For the discrimination between Shallow agitated marine environment (sub – tidal environment) and the fluvial deltaic environment, the following equation was used:

$Y_{3(SM:F)} = 0.2852\ M - 8.7604\sigma I^2 - 4.8932 SK + 0.0482 KG$

If Y is >-7.4190, the environment is 'Shallow marine' (sub – tidal) but if Y is <-7.4190, the environment is 'Fluvial deltaic'.

Where M is the mean grain size, $\boldsymbol{\sigma}$I is the inclusive graphic standard deviation (sorting), SK is the skewness and KG is the graphic kurtosis.

Table 4.3: Linear discriminate function (After Sahu, 1964 as adopted by Rajganapathi *et al*, 2012) of sandstone facies of Mamu Formation and Ajali Sandstone in the study area.

S/N	Sample ID	Y1	Remark	Y2	Remark	Y3	Remark
1	ID1-1	3.749	Beach	108.532	Sh. Agitated Marine (Subtidal)	-7.69	Fluvial deltaic
2	ID1-1b	3.048	Beach	71.925	Sh. Agitated Marine (Subtidal)	-6.324	Sha. Marine
3	ID1-2	3.96	Beach	85.916	Sh. Agitated Marine (Subtidal)	-8.12	Fluvial deltaic
4	ID1-3	9.001	Beach	228.832	Sh. Agitated Marine (Subtidal)	-22.66	Fluvial deltaic
5	ID1-4	7.931	Beach	205.248	Sh. Agitated Marine (Subtidal)	-20.03	Fluvial deltaic
6	OCH-1a	3.365	Beach	127.161	Sh. Agitated Marine (Subtidal)	-12.32	Fluvial deltaic
7	OCH-1b	-1.239	Beach	78.218	Sh. Agitated Marine (Subtidal)	-4.052	Sha. Marine
8	OCH-2a	-6.847	Aeolian	74.225	Sh. Agitated Marine (Subtidal)	3.421	Fluvial deltaic
9	OCH-2b	2.233	Beach	118.255	Sh. Agitated Marine (Subtidal)	-8.288	Fluvial deltaic
10	OCH-3a	9.418	Beach	306.058	Sh. Agitated Marine (Subtidal)	-34.168	Fluvial deltaic
11	OCH-3b	-2.471	Beach	84.394	Sh. Agitated Marine (Subtidal)	-4.366	Sha. Marine
12	OCH-4a	6.238	Beach	285.63	Sh. Agitated Marine (Subtidal)	-32.87	Fluvial deltaic
13	OCH-4b	7.386	Beach	104.509	Sh. Agitated Marine (Subtidal)	-8.434	Fluvial deltaic
14	OCH-5	1.283	Beach	141.979	Sh. Agitated Marine (Subtidal)	-12.22	Fluvial deltaic
15	AY-1	7.006	Beach	150.589	Sh. Agitated Marine (Subtidal)	-15.01	Fluvial deltaic
16	OG1	3.565	Beach	87.732	Sh. Agitated Marine (Subtidal)	-7.39	Sha. Marine
17	OG2	4.779	Beach	111.38	Sh. Agitated Marine (Subtidal)	-9.34	Fluvial deltaic
18	OG3	6.953	Beach	87.279	Sh. Agitated Marine (Subtidal)	-9.27	Fluvial deltaic
19	OG5	3.512	Beach	91.653	Sh. Agitated Marine (Subtidal)	-7.79	Fluvial deltaic
20	OJF1	13.978	Beach	180.056	Sh. Agitated Marine (Subtidal)	-19.65	Fluvial deltaic
21	OJU1	21.778	Beach	261.123	Sh. Agitated Marine (Subtidal)	-28.35	Fluvial deltaic
22	UG1	3.365	Beach	127.161	Sh. Agitated Marine (Subtidal)	-12.32	Fluvial deltaic
23	UGB1	5.589	Beach	73.546	Sh. Agitated Marine (Subtidal)	-2.9	Fluvial deltaic
			B=95.65% A=4.35%		100%		FD=82.61% Sh.=17.39%

The three discriminate functions (Y1, Y2 and Y3) were plotted as bivariate scatter plots and used to improve the success rate and refinement of the discrimination of the depositional environment. Figure 4.13a shows the scatter plot of Y1 and Y2. Based on the classification of depositional environments using Y2 Vs Y1 graph (Sahu, 1964), 97.83% of the analysed sandstone samples in this study are plotted within the field of beach/shallow marine environment while 2.17% are plotted within the field of Aeolian shallow agitated. These graphs are divided into three fields (1) the eolian processes/beach environment, (2) beach and littoral environment and (3) beach environment/shallow marine agitated deposition (Sahu, 1964). A similar plot of Y3 Vs Y2 (Sahu, 1964) to distinguished fluvial

deltaic and beach deposits shows that 91.30% of the samples were plotted in the fluvial deltaic field while 8.70% were plotted within turbidity field (Table 4.3 and Figure 4.14a and b).

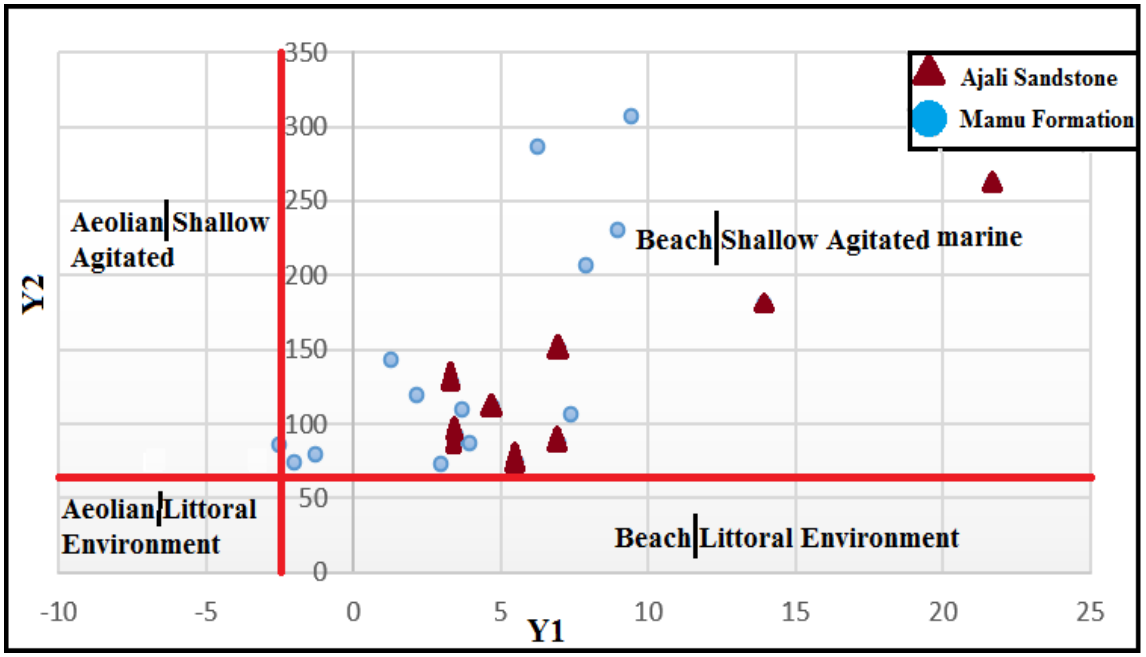


Figure 4.14a: Linear Discriminate Function (LDF) Y1 Vs Y2 scatter plot for the sandstone facies of Mamu Formation and Ajali Sandstone in the study area.

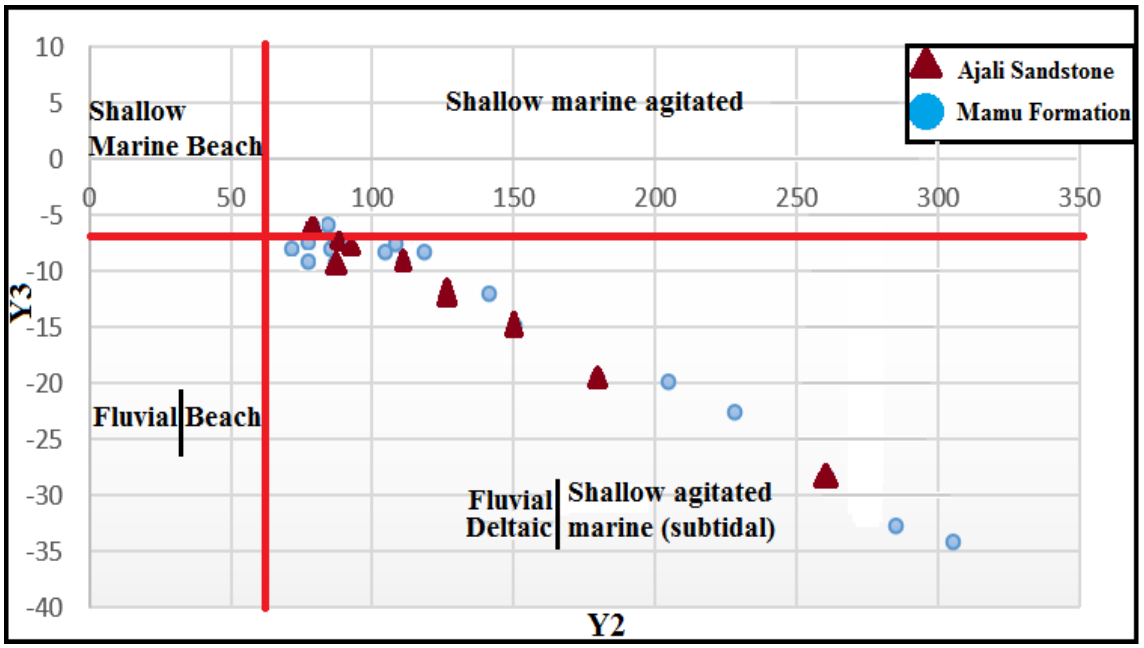


Figure 4.14b: Linear Discriminate Function (LDF) Y2 Vs Y3 scatter plot for the sandstone facies of Mamu Formation and Ajali Sandstone in the study area.

4.3.4 CM Pattern

Grain size parameters and the plots of CM patterns help to distinguish between the sediments of different environments of fluvial and deltaic deposits (Passega, 1964; Visher, 1969). In the present study, an attempt has been made to identify the modes of deposition of sediments of the area northeast of Idah by CM pattern. Parameter C (one percentile of the grain size distribution) and M (the median) were plotted with phi values of the C and M obtained from cumulative curves in microns (Figure 4.14). The relation between C and M is the effect of sorting by bottom turbulence. CM pattern is subdivided into three segments namely, NO (rolling), OPQ (bottom suspension and rolling), QR (graded suspension no rolling), RS (uniform suspension), S (pelagic suspension). The plotted results of northeast of Idah sediments shows that 65.2% of the samples fall in rolling while 35.8% fall in bottom suspension and rolling condition (Figure 4.15).

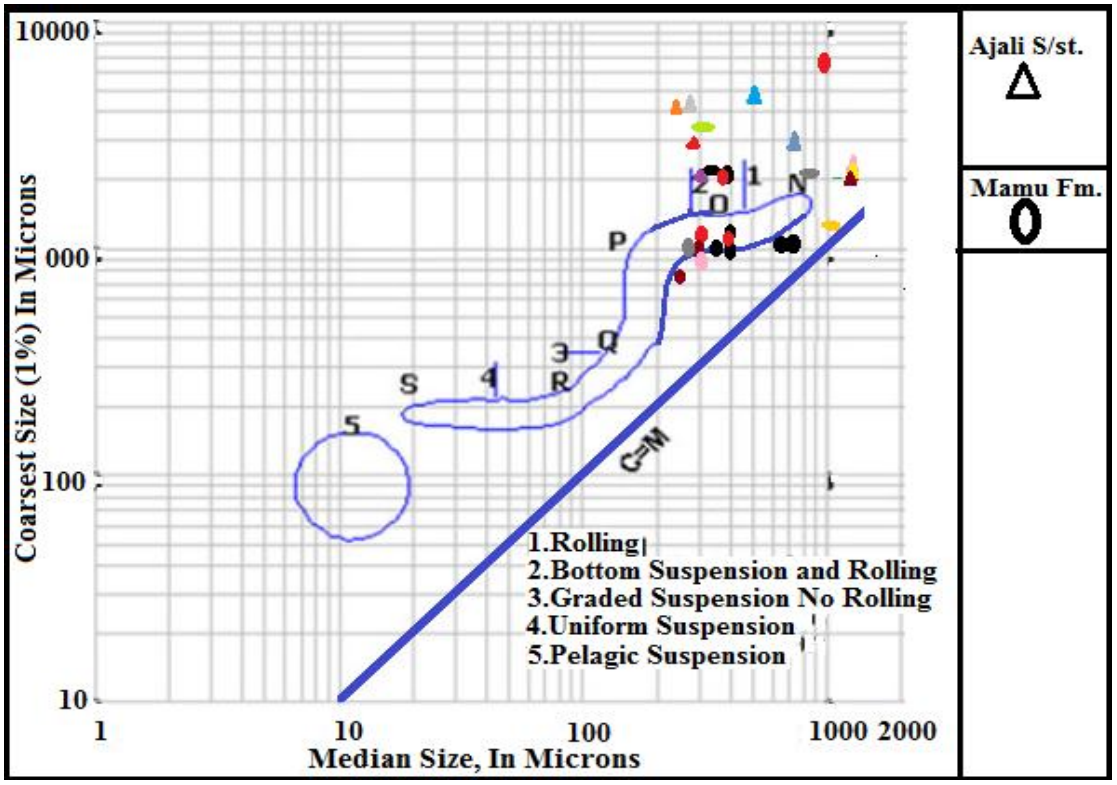


Figure 4.15: CM diagram (Passega 1957, 1964) for sandstone facies samples in the study area showing sedimentary processes in the Mamu Formation and Ajali Sandstone to include rolling, bottom suspension and rolling.

4.4 Paleocurrent Studies

Cross-stratification is ubiquitous in the sandstone facies of the Mamu Formation and Ajali Sandstone in the study area. The cross-beds range from large-scale tabular, wedge-shaped and trough to small-scale ripple and herringbone cross-strata (Hoque, 1976, 1977; Banerjee, 1979; Ladipo, 1985; Amajor, 1986). The average length of a cross-stratum is about 90 cm. Foreset contacts vary from scoured through curved to sharp parallel plane surfaces. In some beds the cross-strata are graded, with coarse sand at the base and fine sand at top. In others, suspension deposits drape foreset strata whereas others show a pronounced alternation of coarse and fine cross-strata (Tables 4.4, 4.5 and Figures 4.16, 4.17 and 4.18).

Table 4.4: Azimuthal readings and statistical values for the sandstone facies of Ajali Sandstone in the study area.

S/N	Azimuthal Reading (x)	F	$F(x)$	$x-\bar{x}$	$(x-\bar{x})^2$	$F(x-\bar{x})^2$	%	Foreset dip
1	30	1	30	-230	53268.64	53268.64	2.2	21
2	47	1	47	-213.8	45710.44	45710.44	2.2	24
3	249	1	249	-11.8	139.24	139.24	2.2	18
4	254	3	762	-6.8	46.24	138.72	6.7	22
5	255	1	255	-5.8	33.64	33.64	2.2	22
6	257	1	257	-3.8	14.44	14.44	2.2	23
7	259	2	518	-1.8	3.24	6.48	4.4	21
8	260	2	520	-0.8	0.64	1.28	4.4	23
9	261	1	261	0.2	0.04	0.04	2.2	21
10	262	1	262	1.2	1.44	1.44	2.2	20
11	265	4	1060	4.2	17.64	70.56	8.9	18
12	270	6	1620	9.2	84.64	507.84	13.3	22
13	271	1	271	10.2	104.04	104.04	2.2	22
14	274	2	548	13.2	174.24	348.48	4.4	25
15	275	5	1375	14.2	201.64	1008.2	11.1	19
16	276	1	276	15.2	231.04	231.04	2.2	18
17	280	3	840	19.2	368.64	1105.92	6.7	24
18	281	2	562	20.2	408.04	816.08	4.4	21
19	286	3	858	25.2	635.04	1905.12	6.7	25
20	288	1	288	27.2	739.84	739.84	2.2	21
21	291	2	582	30.2	912.04	1824.08	4.4	23
22	297	1	297	36.2	1310.44	1310.44	2.2	22
		$\sum F$ = 45	$\sum F(x)$ = 11738			$\sum F(x-\bar{x})^2$ = 109286		

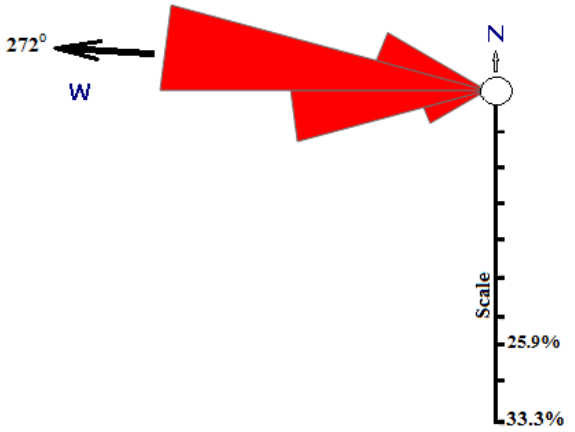


Figure 4.16: Paleocurrent pattern from cross bed azimuths in the Ajali Sandstone showing a unimodal high variability pattern in the NWW direction in fluvial environment.

Table 4.5: Azimuthal readings and statistical values for the sandstone facies of Mamu Formation in the study area.

S/N	Location Cross-bed	Number of measurements	Mean Azimuthal Reading	Standard deviation	Average Foreset dip
1	Ocheche1 **N07^{0}07'27", E06^{0}44'20.6"**	25	299.6	4.6	17
2	Ocheche2a **N07^{0}07'27.8", E06^{0}44'20.3"**	10	192.1	1.3	19
3	Ocheche2b **N07^{0}07'28.4", E06^{0}44'19.6"**	11	352.5	1.6	18
4	Ocheche3 **N07^{0}07'34", E06^{0}44'17.2"**	14	9	1.8	22
5	Ocheche4 **N07^{0}07'37", E06^{0}44'16.7"**	20	329.2	6.8	17

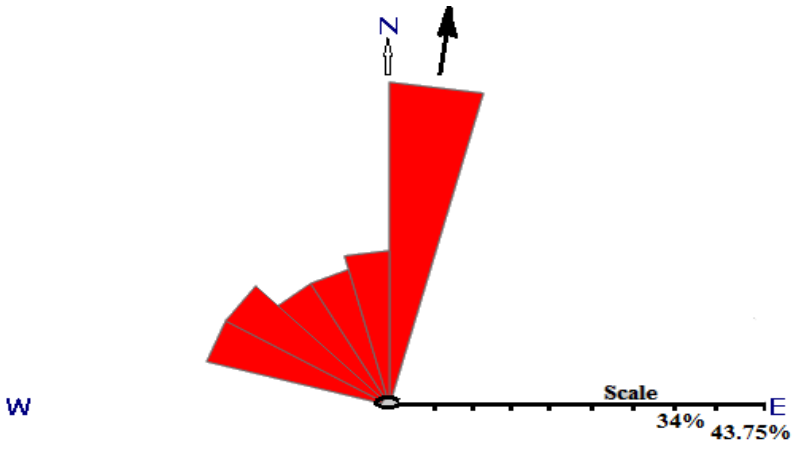


Figure 4.17: Paleocurrent pattern from cross bed azimuths in the Sandstone beds of the Mamu Formation showing a bimodal pattern in the NW and NE direction in tidal environment.

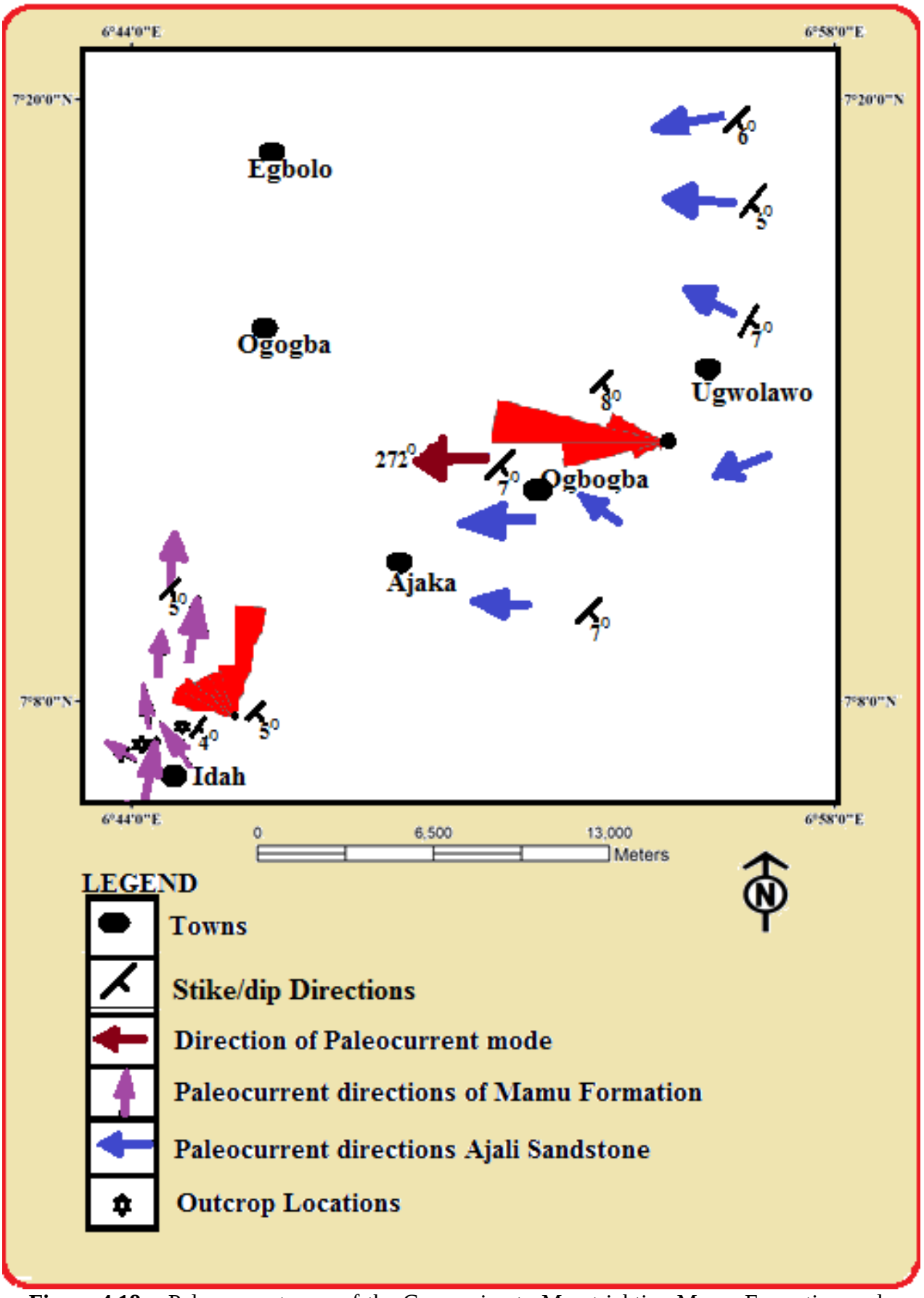


Figure 4.18: Paleocurrent map of the Campanian to Maastrichtian Mamu Formation and Ajali Sandstone in the study area.

CHAPTER FIVE

DISCUSSION

5.1 SEDIMENTOLOGY, FACIES DESCRIPTION AND DEPOSITIONAL ENVIRONMENTS OF THE CAMPANIAN – MAASTRICHTIAN SUCCESSION IN THE STUDY AREA

Detailed descriptions of the studied outcrop sections in the northern Anambra Basin indicate that the formations were deposited in a wide range of environments. Generally, the facies associations (cross-bedded sandstone, siltstone, ferruginized siltstone, mudstone, shale and claysone facies) and peculiar sedimentary features such as laminations, tabular/planar cross-bedding, cross-bedding with ripples, trough cross-bedding, herringbone cross-bedding, flaser cross-bedding, reactivation surface, fissility and bioturbations in the study area are indicative of progressive topset, foreset and bottomset sedimentary facies suggesting a deposition in fluvial, delta platform (delta-plain) which grades away from the source into the delta slope (delta-front) and passes down into the pro-delta.

5.1.1 Nkporo Shale

The Campanian sediment which overlies the Awgu Formation is the Nkporo Shale. The Nkporo Shale documents the transgressive event that followed the Santonian deformation in the Anambra Basin (Murat, 1972; Obi, 2000; Obi and Okogbue, 2004). Being predominantly shales, exposures are rare and mostly weathered. After the folding and uplift of the initial axis of subsidence in the Santonian, deltaic sedimentation and formation of coal swamps became prevalent during the final Campanian-Maastrichtian infilling of the basin (Petters, 1983). Its lithofacies characteristically form low-lying topographic forms.

In the study area, the Nkporo Shale outcrops in the northwestern part. It is made up of thin parallel beds of milky white to dirty red silty clay underlying grey, dirty white to dark orange intensely bioturbated siltstone. The section passes upward into a bed of ferruginized

amber to dark grey weakly stratified siltstone overlain by dirty red, rings of iron-stained siltstone with erosional base which pass into a lateritized siltstone terminating the section. At the north of the northwestern part, the section includes intercalation of grey mudstone and siltstone overlying milky white siltstone.

The presence of mudstone, shale, claystone and siltstone in a stratigraphic section suggest deposition in quiet water palaeoenvironment reflecting fluctuations in river sediment carried in buoyant plumes. The presence of intense bioturbation indicates low sedimentation as a result of low sediment supply. The presence of weakly to non lamination, suggests water bottom codition to be aerobic. The sediment characteristics and the sedimentary structures (silty clay, intensly bioturbation, ferruginouse surface, weakly stratified, iron-stained, mudstone, fissility and sandy shale) of the Nkporo Shale in the study area are indicative of prodelta. This conforms to what Ladipo *et al*. (1992) reported. Thus, the shale represents the prodeltaic facies of the Campanian-Maastrichtian marine incursion.

5.1.2 Mamu Formation

This unit is the Lower Coal Measures of the Geological Survey of Nigeria (Tattam, 1944; and Reyment and Barber, 1956) later renamed by Reyment (1965). The deposition of the Nkporo Group was followed by the Maastrichtian regressive event during which the Mamu Formation was deposited. The Mamu Formation by its stratigraphical position appears to have been deposited towards the end of the Maastrichtian regressive event, in a transitional environment between the predominantly marine and the fluviatile conditions.

The Anambra Basin was silted up, leading to the development of extensive thickly vegetated swamps near sea level on top of a broad delta fan. This coal forming regime (the Lower Coal Measures) was terminated by a period of fluviatile and marginal marine

sedimentation. In the study area, the Mamu Formation consists of sandstone facies, siltstone facies and mudstone facies (Figures 4.4 to 4.10).

Sandstone facies of Mamu Formation comprises;

(a) Massive sandstone subfacies **A**: They are made up of alternation of red and white, medium-grained, poorly to moderately well sorted, near symmetrical, platykurtic to very platykurtic, massive sandstone commonly seen at the base of the section (Figure 4.9). The fluctuation in values from medium to coarse sands suggests a change in energy of the deposition. Predominance of poorly to moderately sorted values reflect less reworking of the sediment during transport and indicate rapid deposition by fluvial process (Freidman, 1967). These features suggest deposition in upper flow regime. Massive sandstone associated with medium-grained sandstone may have been formed as a result of partial fluidization (Romos *et al*., 2006) and/or similar to high density turbidity flows in distal shelf (Nichols, 2009).

(b) Tabular cross – bedded sandstone with reactivation surface subfacies **B**: Consists of intercalation of white and red, medium to coarse-grained, poorly sorted, negatively skewed to positively skewed, leptokurtic to very leptokurtic sandstone with reactivation surfaces and bedding planes (Plate IX). According to (Tucker, 1996), river sands are generally poorly sorted and positively skewed, while beach sands are well sorted and negatively skewed. The fluctuation in values from coarse to medium sands suggests a change in energy of the deposition. Predominance of poorly to moderately sorted values reflects less reworking of the sediment during transport and indicate rapid deposition by fluvial process (Freidman, 1967). The fluctuation in kurtosis values may suggest change in energy of the depositional medium. The presence of reactivation surfaces suggests a tidal environment as a result of lee-face modification of the bedforms by subordinate tidal currents (Ladipo, 1986). Boggs (1995) attributed them to tidal reversal during an asymmetrical tidal cycle under which the

ripple crests can be eroded and redeposited during the next tidal cycle thereby giving rise to reactivation surfaces. The reactivation surfaces may occur in tidal sands deposits through tidal current reversals in fluvial sediments through change in river stages suggesting a moderately upper flow regime (relatively high energy), tranverse bars deposit. The presence of tabular cross-stratification is a reflection of river deposition by migrating sand waves (Harms *et al*., 1975 and Collins and Morris, 1982).

(c) Trough cross – bedded sandstone subfacies **C**: Consists of white, fine to medium-grained, moderately well sorted to poorly sorted, negatively to positively skewed, mesokurtic to leptokurtic, trough bedded sandstone with lens of reworked clay and sinuous crested dunes (Plate XIV). The presence of trough cross beddings is indicative of tidal influence, it is formed through migration of sinuous and lunate dune bedforms. In many situations there are changes of flow velocity or depth during bedform migration so that the dunes are modified and eroded. When deposition resumes an erosional surface will be formed similar to what we have here. Predominance of poorly to moderately sorted values reflects less reworking of the sediment during transport and indicates rapid deposition by fluvial process (Freidman, 1967).

(d) Herringbone Cross – bedded sandstone subfacies **D**: Consists of white fine to medium-grained, moderately to poorly sorted, near symmetrical, mesokurtic to platykurtic, trough, tabular and herringbone cross-bedded sandstone with reactivation surfaces and lens of reworked clay and sinuous crested dunes (Plate XIV). Herringbone cross-bedding indicates deposition by tidal currents that is, bipolar cross-bedding, where cross bed dips of adjacent set are oriented in opposite direction. Herringbone cross-beddeding is produced by reversals of the current, causing dunes and sand-waves to change their direction of migration. The presence of features such as herringbone cross-stratification on beds formed during the slack

water stages of tidal cycles and reactivation surfaces formed by erosion of part of a bedform when a current is reversed indicate tidal influence of transport and deposition. Th features is the typical expression of alternating tidal currents in high energy subtidal settings.

(e) Bioturbated sandstone subfacies **E**: Consists of dirty white to grey, medium to coarse-grained, poorly to moderately well sorted, positively to strongly fine skewed, very leptokurtic to platykurtic, tabular cross-bedded sandstone with reactivation surfaces, erosional surfaces and clear imprints of trace fossils burrows belonging to *Ophiomorpha* genera. The fluctuation in values from coarse to medium sands suggest change in energy of the deposition. Predominance of poorly to moderately sorted values reflects less reworking of the sediment during transport and indicates rapid deposition by fluvial process (Freidman, 1967). The presence of reactivation surfaces suggests a tidal environment as a result of lee – face modification of the bedforms by subordinate tidal currents (Ladipo, 1986). The presence of tabular cross – stratification is a reflection of river deposition by migrating sand waves (Harms *et al*., 1975 and Collins and Morris, 1982). The identified forms of trace fossils are cylindrical vertical burrow of length 7 cm and diameters between 2 and 3 cm. Some of them are identified as *Ophiomorpha* (Plate XII and XIII). *Ophiomorpha* burrows belong to the *Skolithos* ichnofacies. The interpretation of *Ophiomorpha* ichnofacies are indication of intertidal flats and marginal marine settings (Pemberton *et al.,* 1992).

(f) Tabular cross – bedded sandstone with bedding planes subfacies **F**: Consists of intercalation of white and red, medium-grained, poorly sorted, positively skewed, leptokurtic sandstone with bedding planes (Plate XI). According to Tucker (1996) river sands are generally poorly sorted and positively skewed. Predominance of poorly sorted values reflects less reworking of the sediment during transport and indicates rapid deposition by fluvial process (Freidman, 1967). The presence of tabular cross – stratification is a reflection of river deposition by migrating sand waves (Harms *et al*., 1975 and Collins and Morris, 1982).

(g) Cross – bedded sandstone with wave ripples subfacies **G**: Consist of white medium to coarse-grained, moderately sorted (Table 4.1), cross-bedded sandstone wave ripple and reactivation surfaces which passes upward into intercalation of white and red, high angled tabular cross-bedded fine to medium grained, moderately sorted sandstone overlain by a tabular cross-bedded, fine to medium-grained sandstone terminating the whole sandstone section. The fluctuation in values from coarse to medium sands suggest change in energy of the deposition. Predominance of moderately sorted values reflects less reworking of the sediment during transport and indicates rapid deposition by fluvial process (Freidman, 1967). The fluctuation in kurtosis values may suggest change in energy of the depositional medium. The presence of reactivation surfaces (Plate X) suggests a tidal influence. The facies features suggest a transverse bars, upper flow regime.

Siltstone facies of the Mamu Formation comprises;

(h) Laminated Siltstone/clay subfacies **H**: Consists of milky white to light grey, parallel laminated clayey siltstone with lens of clay. This facies is interpreted as a floodplain deposits resulting from deposition out of suspension in overbank subenvironment during upper flow regime. The floodplain environment is indicated by the unfossiliferous clay and siltstone (Plate VIII).

(i) Ferruginized siltstone subfacies **I**: This consists of white to dirty yellow siltstone which passes upward into brown to amber red ferruginized siltstone overlained by brown to milky white weakly stratified concretional siltstone with convolute structure and graded into dirty red to yellow siltstone overlained by brown, red to dirty yellow lateritized siltstone terminating the section (Plate VII and VIII). The presence of convolute bedding indicates seismicity taking place at a time when the deposited sediment has not been fully lithified

(Selley, 1969). The facies features suggest a floodplain deposits resulting from deposition out of suspension in overbank subenvironment.

Mudstone facies of the Mamu Formation; consists of;

(a) Shale subfacies **J**: Consists of evenly laminated dark grey fissile shale thinly intercalated with light grey mudstone overlain by intercalation of thick grey mudstone and a thin lens of dark grey fissile shale which is in turn overlain by intercalation of light grey to milky white silt and sandy shale (Plate III – VI). The presence of mudstones and shales in a stratigraphic section suggests deposition in quiet water palaeoenvironment. The presence of mudstone suggest marine relatively low energy conditions. Where shales show fissility it indicates that burrowing organisms were absent in the depositional environment (Friedman, 1979). The variation of colour ranging from dark grey at the bottom to light grey at the top exhibited by the outcrops (Figure 4.4 to 4.7) suggest a quantitative variation in organic matter content that may have been caused by a change from a relatively anoxic to oxic palaeoenvironmental conditions. No fossils encountered. This could be as a result of the rapid changes in salinity, temperature, nutrient supply to environmental extremes appear to have occurred occasionally, in isolated localities, and resulting in the massive migration of organisms. The absence of marine fossils suggest prevalence of freshwater in this low-energy environment. These features suggest deposition unaffected by wave or tidal process, that is, a stable zone where mud are deposited from suspension to form well – (evenly) laminated sediments reflecting fluctuations in river sediment carried in buoyant plumes where bottom waters are anoxic.

(b) Laminated claystone subfacies **K**: This consists of evenly laminated light grey to milky white claystone with erosional surfaces and a thin (0.2 m) thick band of light grey to brownish ferruginized claystone due to subareal exposure overlain by another thin bed of milky white

claystone terminating the section (Plate XII). The characteristics of this facies may represent low energy depositional environment. Absence of marine fossils suggests prevalence of freshwater in this low-energy environment probably a lower delta plain.

With reference to the Y1, Y2 and Y3 values from the Linear Discriminate Plots of Y2 versus Y1 indicate that all the sandstone samples of the Mamu Formation in the study area fall within Beach/Shallow marine environment (subtidal) (Sahu, 1964 as adopted by Rajganapathi *et al*, 2012), Y3 versus Y2 indicate that 100% of the sandstone samples (ID1-1, ID1-1b, ID1-2, ID1-3, ID1-4, OCH-1a, OCH-1b, OCH-2a, OCH-2b, OCH-3a, OCH-3b, OCH-4a, OCH-4b and OCH-5) fall within Shallow marine agitated with 92.86% ploted within Fluvial/deltaic field and 7.14% in Turbidity field suggesting that the sandstone of Mamu Formation in the study area was deposited under shallow marine environment (Figure 4.14a and b and Table 4.3). This conforms to the work of Sahu, (1964).

The probability curve (CM pattern) for the samples from the area northeast of Idah show that the sandstone units of Mamu Formation (ID1-1, ID1-1b, ID1-2, ID1-3, ID1-4, OCH-1a, OCH-1b, OCH-2a, OCH-2b, OCH-3a, OCH-3b, OCH-4a, OCH-4b and OCH-5) were deposited by rolling to bottom suspension and rolling condition (Figure 4.15).

Facie Association in Mamu Formation

Facies association is a group of facies that is used to define a particular sedimentary environment (Anderton, 1985; Nichols, 2009). From the description and interpretation of the facies, two facies associations were recognized; the FA-1 (subtidal) and the FA-2 (Intertidal).

(i) **FA-1** (subtidal): This facies composed of **A** (massive sandstone subfacies), **B** (Tabular cross-bedded sandstone subfacies), **C** (Trough cross-bedded sandstone), **D** (Herringbone Cross-bedded sandstone subfacies), **G** (Cross-bedded sandstone

with wave ripples subfacies), **H** (Siltstone/clay subfacies) and **I** (Ferruginized siltstone subfacies). This Association ranges in thickness between 0.5 to 3 m. Due to its fining upward sequence, presence of bedform and structures above its usually associated with moderately to high energy environment and characterized by high current velocity therefore, interpreted as subtidal environment (Boggs, 1995; Dalrymple, 2010).

(ii) **FA-2** (Intertidal): This facies is composed of **B** (Tabular cross-bedded sandstone with reactivation subfacies), **C** (Trough cross-bedded sandstone subfacies), **E** (Bioturbated sandstone subfacies), **F** (Tabular cross-bedded sandstone with bedding planes subfacies), **H** (Siltstone/clay subfacies), **I** (Ferruginized siltstone subfacies), **J** (Shale subfacies) and **K** (Laminated claystone subfacies). This facies is characterized by fining upward succession reflecting decrease in energy from the lower to the upper part of the intertidal flats as recorded by texture, sedimentary structure. These features suggest an intertidal or mixed flats environment (Weimer, 1984; Boggs, 1995).

5.1.3 Ajali Sandstone

This unit has undergone perhaps the largest number of nomenclatural changes of all the stratigraphic units in the sedimentary basins of Nigeria. Bain (1924) named it a Sandstone Series, White False-bedded sandstone and the Eagle Rock Sandstone. Tattam (1944) called it the False-bedded Sandstone and Simpson (1955) called it Basal Sandstones and Shale Group, as well as the Escarpment Sandstone Series. The latter appears to have been favoured by several Geological Survey authors (Grove, 1951; Simpson, 1955; Reyment and Barber, 1956). The present name was given by Reyment (1965). The Ajali Sandstone has been assigned to continental depositional environments (Grove, 1951), fluvio – deltaic (Hoque

and Ezepue, 1977) and tide dominated marine shelf to intertidal / subtidal bar and channel systems (Banerjee, 1979; Amajor, 1984; Ladipo, 1985). Thus depending on the locality, the Ajali Sandstone shows a considerable variability in the environment of deposition.

Being a major regressive succession, the formation is a fine to coarse-grained sandstone that also shows widespread tidal influence as is evident on the exposure around Ogbogba hill in the study area (Plate XVI, XVII, XVIII and XIX). In the study area, the Ajali Sandstone consists of sandstone facies and the shale facies;

Sandstone facies of the Ajali Sandstone: Consists of white coarse-grained, friable, moderately sorted, negatively skewed, platykurtic, tabular cross-bedded sandstone (Table 4.1) with clast ranging from angular to well rounded towards the base and reactivation surfaces overlain by alternation of red and white coarse grained, poorly sorted, negatively skewed, mesokurtic, flaser cross-bedded sandstone, which passes upward into a coarse to gravel size grained, poorly sorted, near symmetrical, mesokurtic, herringbone cross-bedded sandstone with clast ranging from angular to well rounded. This bed shows a change in clast, that is pebbly coarse highlighting the base of the bed set and lens of clay towards the top of the bed set showing a fining upward sequence respectively (Plate XVII, XVIII, XIX and Figure 4.12) and in turn overlain by white coarse grained, poorly sorted, ferruginized, flaser cross-bedded sandstone with ripples which is also overlain by another coarse-grained, friable, moderately sorted, negatively skewed, platykurtic, reddish sandstone at the top of the section. Sedimentary structures such as flaser cross-bedding, herringbone, planar, tabular cross-bedding, wavy ripples and reactivation surfaces were observed (Plate XVII and XVIII). Herringbone cross-bedding indicates deposition by tidal currents. Careful observation of the reactivation surfaces show that there are erosional surfaces within them, cutting across the cross-strata. These reactivation surfaces represent short term changes in the flow conditions

which caused modification in the shape of the bedform. They occur in tidal-sand deposit through tidal-current reversals. The variation in clast, that is from pebbly coarse highlighting the base of the bed set indicating a repetitive fining upward sequence suggest a change in energy flow from high energy to low energy. The presence of reactivation surface (Plate XVIII) within Ajali Sandstone suggests fluvial action (Reading, 1996; Tucker, 1996) suggests that the presences of flaser bedding is linked to tidal influence. Flaser bedding is where cross-laminated sandstone contains mud streaks, usually in the ripple troughs. It is common in tidal-flat and delta front sediments, where there are fluctuations in sediment supply or level of current (or wave) activities (Tucker, 1996). These features suggest a tidally influenced fluvial – and fluvial channels and deltaic depositional environment.

Shale facies of the Ajali Sandstone: This occurs towards the top of the sandstone facies and consists of intercalation of dark yellow to grey lateritized shale with dirty red very thin lens of fine sandstone and siltstone (Plate XVI and XIX). Predominance of argillaceous and fine grained strata indicate a low energy or quiet environment. The yellow to light grey colour suggests oxic palaeoenvironmental conditions.

With reference to the Y1, Y2 and Y3 values from the Linear Discriminate Plots of Y2 versus Y1 indicate that all the samples of the Ajali Sandstone in the study area fall within Beach/Shallow marine environment (Sahu, 1964), Y3 versus Y2 indicate that OG1 (11.11%) fall within Shallow marine environment while 88.89% of the samples fall within fluvial deltaic or shallow agitated marine, suggesting that the Ajali Sandstone in the study area was deposited under shallow marine environment (Figure 4.13a and b and Table 4.3). This conforms to the work of Sahu, (1964).

The probability curve (CM pattern) plot of the Ajali Sandstone in the study area shows that 77.78% of Ajali Sandstone (AY-1, OG1, OG2, OG5, OJF1, OJU1 and UGB1)

were deposited by rolling to bottom suspension and rolling condition while 22.22% (OG3 and UG1) were deposited by bottom suspension condition (Figure 4.14).

5.2 Lithostratigraphic Overview of the Study Area

The Nkporo Shale in the study area comprises whitish to dark orange, laminated bioturbated siltstone as the oldest sediments that occur at the bottom. Towards the top of the section are the milky white to dirty red silty clay which is overlain by ferruginized amber to dark grey weakly stratified siltstone with erosional base underlying a red siltstone with rings of iron stain which is overlain by lateritized siltestone followed by a bed of light grey to milky white siltstone which pass upward into a bed of grey to blue mudstone intercalated with sandy shale overlain by light grey to milky white siltstone (Figures 4.2 and 4.3). They did not occur as a single complete section due to poor outcrop exposures, therefore, having stratigraphic gaps. The Nkporo Shale is overlain by the transitional Mamu Formation which chiefly comprises medium to coarse-grained parallel laminated sandstone occurring at the bottom, cross-bedded sandstone with wave ripples overlies the trough, herringbone and tabular cross-bedded sandstone with reworked clay and sinuous crested dunes which passes upward into siltstone beds.

Overlying these are beds of evenly laminated dark grey fissile shales intercalated with light grey mudstone which is overlain by intercalation of thick grey mudstone and a thin lens of dark grey fissile shales followed by light grey to milky white siltstone intercalated with sandy shale. In the studied outcrop of the Mamu Formation occurs a thick bed of claystone with very thin lens of ferruginized claystone towards the top of the section due to subareal exposure overlain by another claystone (Plate IX and Figure 4.4 to 4.10).

The Mamu Formation is overlain by the coarsed grained, flaser, herringbone, tabular cross-bedded sandstone with wave ripples and reactivation surfaces of the Ajali Sandstone which is also underlying a bed of yellowish well laminated fissile shales intercalating with

very thin lens of fine sandstone and siltstone which is the youngest in the study area (Figure 4.11 and 4.12).

5.3 Paleocurrent Studies

The paleocurrent of the sandstone facies of Mamu Formation and Ajali Sandstone was determined using paleocurrent analysis. Current rose diagrams plotted were used and studied to identify the paleocurrent directions (Figure 4.16 to 4.18).

5.3.1 Ajali Sandstone

The paleocurrent analysis result shows that the variance value is 2,429. This value indicates that Ajali Sandstone was deposited in fluvial-deltaic environment (Tanner, 1955; Pryor, 1960 and Selley, 1966). The value of the mean vector azimuth indicates 272^{o} (Table 4.4). This value and the rose diagram (Figure 4.16) suggest that the direction of paleocurrent as at the time of deposition, acted in northwest direction and the provenance was southeast. The rose diagram reflects unimodal high variability paleocurrent pattern for the Ajali Sandstone (Figure 4.16). These paleocurrent patterns (unimodal) suggest sediments deposited in an environment where fluvial currents was prevalent with net long – shore marine transport (Selley, 1966). The direction of provenance indicated that the sediments of the Ajali Sandstone in the study area were sourced from the Basement Complex of Nigeria probably the Cameroun Mountains in southeastern part of the country and or the adjacent northeast trending Okigwe-Abakaliki anticlinorium of Santonian age. This conforms to the measurements made by Hoque and Ezepu (1977), Amajor (1987), Obi (2000) and Nwajide (2014).

The radiating paleocurrent pattern is regionally significant because the trends are oriented towards the paleo-strandline and parallel to the regional structural dip (Figure 4.16). This suggests that the original depositional basin in which the Ajali sands accumulated had

a similar shape and orientation and that the paleocurrent system, paleoslope and, perhaps, the sediment dispersal pattern in the basin were all nearly parallel to one another.

These paleocurrent data suggest that the Santonian uplift shed Ajali clastics into the Anambra and western sector of the Afikpo Basin. The implication for the paleoslope is that it was generally to the west and southwest. This would place the sediment dispersal centre, i.e. the geographical location of the provenance area, to the east and northeast, which is largely the Abakaliki fold belt.

5.3.2 Mamu Formation

The rose diagram reflects bimodal high variability paleocurrent pattern for the Sandstone facies of Mamu Formation (Figure 4.17). These paleocurrent patterns (bimodal) suggest sediments deposited in an environment where tidal currents was prevalent with a net long – shore marine transport (Selley, 1966). The direction of provenance indicated that the sediments of the sandstone facies of Mamu Formation in the study area were sourced from more than one source which is similar to the observatioin made by Akaegbobi and Boboye (1999) and Adeigbe and Salufu (2009) (Table 4.5).

5.4 Depositional History

The study of the ancient environment of the sediments of the northern Anambra Basin in the area northeast of Idah has been reconstructed from the field relationships and textural analysis results. Sequel to Santonian tectonism, the study area opened up as Anambra Basin. Thus, the basin began to communicate with the Atlantic Ocean. There was a rise in the sea level during the Campanian times and the sea transgressed into the land. The incursion of the Atlantic Ocean caused the basin to become deeper and quiescent. Thus, Nkporo Shale was deposited into the basin during the Late Campanian indicating the onset of first cycle of sedimentation which marked the beginning of the marine transgression (Nwajide and Hoque, 1985).

The Santonian tectonism displaced the deposition axis into the Anambra platform, which then become the receptacle for clastics washed down from the flanks of the Abakaliki Anticlinorium (Nwajide and Hoque, 1985). As related to this, the basal part of the Nkporo Shale in the study area overly the Itobe basement as envisaged by Nwajide and Hoque, 1985, therefore, confirms the first cycle of sedimentation within the paleovally. The dark grey fissile shales, sandy shales and mudstone was observed in Egbolo village overlays the coarse-grained sandstone. This suggests submarine erosion which deposited pelagic sediment at a time when the rate of sediment supply was probably low.

Though the unexposed surface overlying this lithofacies may be coarse-grained sandstone with ophiormorpha lithofacies (Simpson, 1954; Arua, 1988; Okoro and Arua, 1989; Mode, 1991) that may has been probably weathered suggesting the end of the Late Campanian transgressive event in the study area. Gradually, the shoreline started withdrawing seaward from the land. Regression phase followed the transgression phase simultaneously and subsequently led to the withdrawal of shoreline seaward such that sediments that were transported from the land were deposited and buried the decomposed plant and tree remains in the study area as part of Mamu Formation. Thus these plant remains were transformed into carbonaceous shale that exist in the study area and coal seam towards the area northern away from my study area.

The medium-grained, poorly sorted, massive sandstone commonly seen at the base of the Acheche River section probably mark the beginning of the third cycles of sedimentation (Mamu Formation-Ajali Sandstone) and the onset of the Maastrichtian regressive event in the study area. The shoreline continued to withdraw at a rapid rate such that the basin became shallow. As a result of this shallowness of the basin at this period paved way to deposition of poorly sorted coarse sandstone of the tidally influenced fluvial- and fluvial channels origin into the basin as Ajali Sandstone.

The paleocurrent analysis suggests that the sediments were sourced from the Abakaliki Anticlinorium and Cameroun highlands and transported by rivers to the coastline where they are shaped by tidal current energy. During the regressive phases, the input from the proto-rivers dominates, leading to a gradual closing and smoothing out of the funnel shaped estuary. Sedimentation of Ajali Sandstone in the basin lasted till Late Maastrichtian times terminating the third cycle sedimentation in the study area.

CHAPTER SIX

6.1 SUMMARY AND CONCLUSION

The Anambra Basin stratigraphically is conveniently divided into two – the Nkporo Group and the Coal Measures. The Nkporo Group consists of the following lithologic formations: the older Nkporo Shale, Owelli Sandstone, and the Enugu Shale; the Coal Measures consists of the Mamu Formation, Ajali Sandstone and the youngest Nsukka Formation.

In the study area, three formations were encountered namely; the Nkporo Shale, Mamu Formation and the Ajali Sandstone. The Nkporo Shale comprises a thin parallel beds of white to reddish silty clay, grey to whitish and dark orange, intensely bioturbated siltstone, grey sandy shale, fissile shale, ferruginized amber to dark grey, weakly stratified siltstone,

rings of iron stain siltstone with erosional base and grey mudstone and siltstone intercalations. The presence of mudstone, shale, claystone and siltstone, intense bioturbation and weakly to non-lamination in the Nkporo Shale in the study area indicates deposition in a quiet water, aerobic (oxic) prodelta environment.

The Mamu Formation in the study area comprises a fine, medium to coarse-grained, poorly to moderately sorted, near symmetrical, platykurtic to very leptokurtic, parallel laminated, tabular cross-bedded, herringbone, trough cross-bedded sandstones with wave ripples, siltstone, mudstone, fissile shale and claystone and contain no fossils. Reactivation surfaces and trace fossils (*Ophiomorpha)* were observed in the sandstones. These sedimentary structures observed in the sandstone suggests subtidal to intertidal environments. Bimodal direction of the rose diagram suggests deposition in a tidal environment. The ferruginous and weakly stratified siltstone, suggest a floodplain deposits. The presence of mudstone, shales and claystone indicate deposition in quiet water palaeoenvironment. Where fissility in suggest that burrowing organisms were absent in the depositional environment.

The Ajali Sandstone of the study area consists of white to red, fine, medium, coarse to very coarse grained, friable, poorly to moderately sorted sandstone, siltstone and yellow to light grey shales. Sedimentary structures such as flaser, planar, tabular, herringbone cross – beddings and reactivation surfaces with wave ripples indicate a tidal flat and delta front environments. The variation in clast; that is from pebbly coarse grained highlighting the base of the bed set indicates a repetitive fining upward sequence, suggesting a change in energy flow from high energy to low energy. The paleocurrent studies indicate northwest direction of flow of water depositing the sediment. The rose diagram reflects unimodal high variability paleocurrent pattern suggesting a fluvial-deltaic environment for Ajali Sandstone in the study

area. The Linear Discriminate plots and Tractive current diagram of the sandstone facies of the Ajali Sandstone in the study area suggests shallow marine environment, most likely a tidal/sub-tidal shore line environment.

Comparing the results of the Linear Discriminate Function with the overall results from the sedimentary structures, sieve analysis, micropaleontological studies, CM pattern and paleocurrent analysis shows that the variations in the energy and fluidity factors have excellent correlation with the different processes and the environment of deposition. Therefore, this method of discrimination should be considered as a supporting techniques to enhance good paleoenvironmental studies.

REFERENCE

Adeigbe, O.C. and Salufu, A.E. (2009): **"**Geology and Depositional Environment of Campano- Maastrichtian sediments in the Anambra Basin, southeastern Nigeria: Evidence from field relationship and sedimentological study", *Earth Sciences Research Journal*, **13**, P. 2**.**

Adelaye, D.R. (1975): Nigerian Late Cretaceous Stratigraphy and Paleogeography. *American Association of Petroleum Geologists Bulletin*, V.**59**, P.2302-2313.

Agagu, O.K., Fayose, E.A. and Petters, S.W. (1985):**"**Stratigraphy and Sedimentation in the Senonian Anambra Basin of eastern Nigeria", *Journal of Mining and Geology*, **22**, P. 25- 36.

Agagu, O. K. and Adighije, C. I. (1983): Tectonic and sedimentation framework of the lowe Benue Trough, southeastern Nigeria. *Journal of African Earth Sciences*. **1**, P.267 – 274.

Agumanu, A. E., (1993): Sedimentology of the Owelli Sandstone (Campanian‐Maastrichtian), southern Benue Trough, Nigeria. *Journal of Mineralogy and Geology*, **29(2**): P.21-35.

Akaegbobi I.M and Boboye O.A. (1999): Textural, Structural Features and Microfossil assemblage Relationship as a Delineating criteria for the Stratigraphic boundary

between Mamu Formation and Nkporo Shale within the Anambra Basin, Nigeria. *Nigeria Association of Petroleum Exploration Bulletin*, Vol. P. 193-206.

Akande, S.O. and Erdtmann, B.D. (1998): "Burial Metamorphism (Thermal Maturation) in Cretaceous Sediments of the Southern Benue Trough and Anambra Basin, Nigeria". *American Association of Petroleum Geologists Bulletin*, **82**: P.1191-1206.

Akande, S. O., Hoffknecht, A. and Erdtmann, B. D. (1992a): Upper Cretaceous and Tertiary coals from southern Nigeria. Composition, rank, depositional environments and their technological properties. *American Association of Petroleum Geologists Bulletin,* **7**, P.26 – 38.

Akande, S. O., Hoffknecht, A. and Erdtmann, B. D. (1992b): Rank and petrographic composition of selected Upper Cretaceous and Tertiary coals of southern Nigeria. *International Journal of Coal Geologist,* **20**, P. 209 – 224.

Akande, S.O., Mucke, A., (1993): Depositional environment and diagenesis of carbonates at the Mamu/Nkporo Formation, Anambra Basin, Southern Nigeria. *Journal of African Earth Sciences* **17**, P. 445–456.

Akande, S.O. (2003): "Minerals and Fossil Fuel Discovery: The Adventures of Exploration."University of Ilorin 67th Inaugural lecture: *Unilorin Press*. P. 55.

Allen, J.R.L., (1965): On bedforms and paleocurrents. *Sedimentology*, 6: 153-189.

Allen, G. P., (1993): An introduction to estuarine lithosomes and their controls. In: Wright, V. P., (ed). Sedimentology Review. Oxford: *Blackwell Scientific Publications*, 1: 123-138.

Allix, P. (1987): Le basin d' Anambra: essai de characterisation de I' evolution tectono – sedimentaire au Cretace superieur. *Bull. Centr. Rech. Explor. –Prod. Elf – Aquitaine* **11**, P. 158 – 159.

Allix, P., Legoux, O. and Robert, P. (1984): Essai d' interpretation geodynamique de I' evolution mesozoique de sous – bassins du Fosse de la Benoue (Nigeria). *Bulletin Society of Geologist France,* (7) **26**, P. 1061 – 1068.

Amajor, L.C., (1984): Sedimentary facie analysis of the Ajali Sandstone (Upper Cretaceous) southern Benue Trough. *Journal of Mineralogy and Geology*, vol. **21**. P.171-176.

Amajor, L.C., (1986): Sedimentary facies analysis of the Campano-Maestrichtian Ajali Sandstone, southeastern Nigeria. *Bulletin Nigeria Mining and Geosciences Society,* **21**, P. 21.

Amajor, L. C. (1987): Paleocurrent, petrography and provenance analyses of the Ajalli Sandstone (Upper Cretaceous), Southeastern Benue Trough, Nigeria. *Sedimentary Geology*, **54**: P. 47-60.

Anderton, R. (1985): Clastic Facies Models and Facies Analysis. In: Brenchley, P.J. and Williams, B.P.J. (eds.) Sedimentology, Recent Developments and Applied Aspects. *Blackwell Scientific Publications.* Oxford, P. 31 – 47.

Arua, I. (1988): Episodic sedimentation: an example from the Nkporo Shale (Campano‐Maastrichtian), Nigeria. *Journal of African Earth Sciences*, **7**, P. 759-726.

Avbovbo and Ayoola, (1981): Petroleum Prospects of Southern Nigeria's Anambra Basin, *Oil and Gas Journal,* P. 334-347.

Ayoola, E, O. (1981): Paleocurrent and sedimentological studies in the Benue Trough, Nigeria. *Sedimentary Geology*, **28**, 153 – 162.

Bain, A.D.N. (1924): The Nigerian Coalfield: Section 1. Enugu Area. With Appendices by R.B. Newton and A.C. Seward. *Geological Survey of Nigeria Bulletin,* No. **6**, P. 1-62.

Banerjee, I. (1979): Analysis of cross-bedded sequences: An example from the Ajali Sandstone (Maestrichtian) of Nigeria. *Q. J. Geol. Min. Metall. Soc. India*, **51**, P. 69-8.

Baudin, P. (1991): La magmatisme mésozoïque à cénozoïque du fossé de la Bénoué (Nigeria). Géochronologie, petrogenése, cadre géodynamique. *Thése doctorat, Université d'Aix-Marseille, France.*

Benkhelil, J. (1989): The origin and evolution of the Cretaceous Benue Trough, Nigeria. *Journal of African Earth Sciences*, **8**, P.251 – 282.

Benkhelil, J. (1982): "Benue Trough and Benue Chain", *Geology magazine* **119**, P. 155- 168.

Benkhelil, J., Dainelli, P., Ponsard, J. F., Popoff, M. and Saugy, L. (1988) : The Benue Trough :wrench – fault related basin on the border of the equatorial Atlantic. In : Triassic – Jurassic rifting, continental breakup and the origin of the Atlantic Ocean and passive margins, part B (Edited by Manspeizer, W.), P. 787 – 819. *Elsevier, Amsterdam.*

Benkhelil, J. and Robineau, B. (1983) : La fosse de la Benoue est – il un rift ? *Bull. Centr Rech. Explor – Prod. Elf – Aquitaine* **7**, P. 315 – 321.

Binks, R. M. and Fairhead, J. D. (1992): A plate tectonic setting for Mesozoic rifts of West and Central Africa. *Tectonophysics***213**, P. 141 – 151.

Boggs, S., (1995): "Principles of sedimentology and stratigraphy". *Prentice Hall, Englewood Cliffs, New Jersey*, P.79- 93.

Bowen, D. W. and Weimer, P. (2004): Reservoir geology of Nicholas and Liverpool Cemetery fields (lower Pennsylvanian), Stanton County, Kansas, and their significance to the regional interpretation of the Morrow Formation incised‐valley‐fill systems in eastern Colorado and Western Kansas. *American Association of Petroleum Geologists Bulletin*, **88**, P. 47-70.

Boersma, J.R. and Terwindt, J.H.J. (1981): Neap-spring tide sequences of intertidal shoal deposits in a mesotidal estuary. *Sedimentology* **28**, P. 151 - 170.

Burke K.C., Dessauvagie T.F.J., and Whiteman A.J. (1972): Geological history of the Benue valley and adjacent areas. In *J. African Geology* (eds. Dessauvagie T.F.J. and Whiteman A.J.) [M]. P. 187–206. *Ibadan. Uni. Ibadan.*

Burke K.C., Dessauvagie T.F.J., and Whiteman A.J. (1971): Opening of the Gulf of Guinea and geological history of the Benue depression and Niger Delta. *Nature* **233**, P. 51-55.

Collins, J.S.H. & Morris, S.F. (1975): A new crab *Costacopluma concava* from the Upper Cretaceous of Nigeria. *Palaeontology*, **18**: P. 823-829.

Collins, J. S. H. and Morris, S. F. (1982): A new crab Costacopluma concava from the Upper Cretaceous of Nigeria. *Palaeontology* **18**, P. 823 – 829.

Courel, L., Desteucq, C., Essamond, R., Izart, A., Potherat, P and Sonuga, M. S. (1991): Coal occurrence related to sedimetary dynamics : three African examples. *J. Afr. Earth Sci.***12**, P. 159 – 169.

Cratchley, C.R and Jones, G.P. (1965): An interpretation of the geology and gravity anomalies of the Benue Valley, Nigeria. *Overseas Geological Surveys Geophysical Paper* **I**, P. 1-26.

Curran, H. A., Frey, R. W. (1977): Pleistocene trace fossils from North Carolina (USA) and their Holocene analogues. In: Crimes, T. P., Harper, J. C., (eds). Trace Fossils 2. Liverpool: *Seel House Press, Geological Journal Special Issue*, **9**, P. 139-162.

Dalrymple, R. W. (1992): Tidal depositional systems. In: Walker, R. G., James, N. P., (eds). Facies Models: Response to Sea Level Change. *Geologist Association of Canada,* P. 195-218.

Dalrymple, R.W. (2010): Tidal depositional systems. In: James, N., Dalrymple, R. (Eds.), Facies Models 4. *Geologist Association of Canada, St. John's, Geotext* **6**, P. 201–231.

Davis, H. R., Byers, C. W., Pratt, L. M. (1989): Depositional mechanisms and organic matter in Mowry Shale, (Cretaceous) Wyoming. *American Association of Petroleum Geologists Bulletin*, **73**, P. 1103-1116.

De Swardt, A.M.J. and Casey, O.P. (1961): The coal resources in Nigeria. *Bulletin Geological Survey Nigeria,* **25**, P. 1-100.

Dessauvagie, T.F.J. (1975): Explanatory note to the geological map of Nigeria (scale 1:1,000,000). *Nigerian Mining, Geological and Metallurgical Society,* Ibadan, Nigeria. **9**, P. 3-28.

Du Preez, J. W. (1947): Preliminary report on the Upper Coal Measures of Onisha Province. Rep. *Bulletin Geological Survey Nigeria* **1946**, P. 27 – 28.

Edet, J. J. (1992): Palynostratigraphy of Late Cretaceous (Late Campanian - Early Maastrichtian) sections in the Anambra basin, Nigeria. *Revista Espanola de Micropaleontologia,* XXIV, **2**, P. 3-18.

Ekweozor C.M. (1982): Petroleum Geochemistry Application to Petroleum Exploration in Nigeria Lower Benue Trough. *Nigerian Association of Petroleum Explorationists (NAPE), Bulletin,* **2**, P. 75-89.

Fairhead, J.D. (1988): "Mesozoic plate tectonic reconstruction of the central south Atlantic Ocean: the role of the West and Central African Rift Systems", *Tectonophysics*, **155**, P. 181- 19.

Folk R.L., Ward W.C. (1957): Brazos River bar: a study in the significance of grain size parameters. *Journal of Sedimentary Petrology* **27**, P. 3–26.

Friedman, G.M. (1967): Dynamic processes and statistical parameters compared for sized frequency distribution of beach and river sands. *Journal of Sedimentary Petrology*, **37**, P. 327 – 354.

Friedman, G.M., (1979): Difference in size distribution of populations of particles among sands of various origins. *Sedimentology* **20**, P. 3–32.

Frey, R. W., Howard, J. D. (1985): Trace fossils from the Panther Member, Star Point Formation (Upper Cretaceous) Coal Creek Canyon, Utah. *Journal of Palaeontology*, **59**, P. 370-404.

Gebhardt, H. (1998): Benthic Foraminifera from the Maastrichtian lower Mamu Formation near Leru (southern Nigeria): paleoecology and paleogeographic significance. *Journal Foraminifera Research,* **28**, P. 76 – 89.

Grove, A.T. (1951): Land Use and soil conservation in part of Onitsha and Owerri Provinces. *Bulletin Geological Survey Nigeria.* No.**21,** P. 23.

Guiraud, R., Binks, R.M., Fairhead, J. D. and Wilson, M. (1992) : Chronology and geodynamic setting of Cretaceous – Cenozoic rifting in West and Central Africa. *Tectonophysics*, **213**, P. 227 – 234.

Harms, J.C., Southard, J.B. Spearing, D.R. and Walker, R.G., (1975): Stratification Produced by Migrating Bedforms: In Depositional Environments as Interpreted from Primary Sedimentary Structures and Stratification Sequences. S.E.P.M. Short Course No. **2.** P.120.

Hazell, J. R. T. (1958): The Enugu ironstone, Udi Division, Onisha Province. Rec. *Bulletin Geological Survey Nigeria.***1955**, P. 44 – 58.

Hedberg, H.D. (Ed.) (1976): International Stratigraphic Guide.*Wiley- Interscience, New York*, P. 200.

Hockey, R. D., Sacchi, R., de Graaff, W. P. F. H. and Muotoh, E. O. G. (1986): The geology of Lokoja – Auchi area. *Bulletin Geological Survey Nigeria,* **39**, P. 71.

Hoque M. (1976): Significance of textural and petrographic attributes of sandstones, southern Nigeria [J]. *Journal Geological Society of India,* **17**, 514–521.

Hoque, M. (1977): Petrographic differentiation of tectonically controlled Cretaceous sedimentary cycles, southeastern Nigeria. *Sedimentary Geology,* **17**, P. 235-245.

Hoque, M., Nwajide, C.S. (1984): Tectono-sedimentological evolution of an elongate Intracratonic basin (Aulacogen): the case of the Benue Trough of Nigeria. *Nigerian Journal of Mining Geology,* **21** (1 and 2), P. 19 – 26.

Hoque, M. and Ezepue, C.M. (1977): Petrology and paleogeography of the Ajali Sandstone. *Journal of Nigeria Mining and Geosciences Society,* **14**, P. 16-22.

Hossain, M.T. (1981): Geochemistry and Petrology of the minor intrusive between Efut Eso and Nko in the Ugep area of Cross River State, Nigeria. *Journal of Mining Geology*, P. 42–51.

Jones, H. A. (1958): The oolitic ironstone in the Agbaja Plateau, Kabba Provine. Rec. *Bulletin Geological Survey Nigeria.***1955**, P. 20 – 43.

Kogbe, C. A. (1981a): Attempt to correlate the stratigraphic sequene in the middle Banue Basin with those of the Anambra and Upper Banue Basins. *Earth Evolution of Science*, **2**, P. 139 – 143.

Krumbein, W.C. and Sloss, L.L. (1963): Stratigraphy and Sedimentation, Second Edition, W.H. Freeman and Company, San Francisco, P. 660.

Kumaran, K. P. N. and Rajshekhar, C. (1992): 'Foraminiferal linings' from Late Cretaceous –Palaeocene sediments of Ohafia – Ozu Abam area, Nigeria. *Curr. Sci*. **62**, P. 311 – 313.

Ladipo, K.O. (1985): Paleogeography of the Anambra Basin. *13th Colloquium of African Geology, Abstr.,* Vol. 371. CIFEG (Int. Centre for Training and Exchange in the Geosciences).

Ladipo, O.K., (1986): Tidal shelf depositional model for the Ajali Sandstone, Anambra Basin, southern Nigeria. *Journal of African Earth Sciences* **5(2)**, P. 177–185.

Ladipo, K. O. (1987a): A depositional framework for the Anambra Basin, southeastern Nigeria. *Bull. Centr. Rech. Explor. – prod. Elf – Aquitaine* **11**, P. 166 – 167.

Ladipo, K. O. (1987b): Cyclicities reflected by the tide – dominated shelf deposits of Ajali Sandstones, Anambra Basin. *Bull. Centr. Rech. Explor. – prod. Elf – Aquitaine* **11**, P. c168 – 169.

Ladipo, K. O. (1988a): Paleogeography, sedimentation and tectonics of the upper Cretaceous Anambra basin, southeastern, Nigeria. *Journal of African Earth Science.* **7** (5/6), 865–871.

Ladipo, K. O. (1988b): Example of tidal current periodicities from an Upper Cretaceous sandstone succession (Anambra Basin, S.E Nigeria) In: Tide – influenced sedimentary environments and facies (Edited by de Boer, P. L., van Gelder, A. and Nio, S. D.), P. 333 – 340. *Riedel, Dordrecht.*

Ladipo, K. O., Akande, S. O. and Mucke, J. M. (1994): Genesis of oolitic ironstones from the middle Niger sedimentary basin: evidence from sedimentological, ore microscopic and geochemical studies. *Journal of Mining Geology*, **30**, P. 161 – 168.

Ladipo, K.O., Nwajide, C.S., and Akande, S.O., (1992): Cretaceous and Paleogene sequences in the Abakaliki and Anambra basins, south eastern Nigeria: a field guide. *International Symposium on Geology of Deltas, Port Harcourt,* May **1992**.

Maluski, H., Coulon, C., Popoff, M., Baudin, P. (1995): 40Ar/39Ar chronology, petrology, and geodynamic setting of Mesozoic to early Cenozoic magmatism from the Benue Trough, Nigeria. *Journal of Geological Society of London,* **152**, P. 311-326.

Martino, R. L., Curran, H. A. (1990): Sedimentology, ichnology and palaeoenvironment of the Upper Cretaceous Wenonah and Mt. Laurel Formations, New Jersey. *Journal of Sedimentary Petrology,* **60**, P. 125-144.

Mbuk, I. N. Rao, V. R. and Kumaran, k. P. N (1985): The Upper Cretaceous – Paleocene boundary in the Ohafia – Ozu Abam area, Ima state, Nigeria. *Journal of Mining Geology,* **22**, P. 195 – 113.

McKenzie, D. P. (1978): Some remarks on the developments of sedimentary basins. *Earth Planet. Sci. Lett.***40**, P. 25 – 32.

Mebradu, S. (1990): Palynofacies of Enugu/Iva vally shales, Anambra State, Nigeria. *J. Min.Geol.* **28**, P. 13 – 20.

Miall, A. D. (1992): Alluvial deposits. In: Walker, R. G., James, N. P., (eds). Facies Models: Response to Sea Level Change. *Geological Association of Canada*, P. 119-142.

Mode, A.W. (1991): "Assemblage Zones, Age, anPaleoenvironments of the Nkporo Shale, Akamu Area, Ohafia, Southeastern Nigeria. *Journal of Mining Geology,* **27**, P. 107-114.

Mode, A.W. and Onuoha, K.M. (2001): **"**Organic matter Evaluation of the Nkporo Shale, Anambra Basin, from wireline logs", *Global Journal of Applied Sci,* **7**, P. 103- 107.

Murat, R. C. (1972): Stratigraphy and palaeogeography of the Cretaceous and Lower Tertiary in southern Nigeria. In: Dessauvagie, T. F. J., Whiteman, A. J., (eds). African Geology. Nigeria*: University of Ibadan Press*, P. 251-266.

Newton, R. B. (1924): A Preliminary opinion on some valves of a Cardita from a Nigerian deposits. *Bulletin Geological Survey Nigeria* **6** *(Appendix I),* P. 64 – 65.

Nichols, G. J., (2009): Sedimentology and Stratigraphy. *John Wiley and Sons*, Ney York, P. 452

Nwajide, C.S., Reijers, T.J.A. (1996a): Geology of the Southern Anambra Basin. In: Reijers, T.J.A. (Ed.), Selected Chapters on Geology. *SPDC, Warri*, P. 133–148.

Nwajide, C.S. and Reijers, T.J.A. (1996b): Sequence architecture in outcrops: examples from the Anambra Basin. *Nigeria Association of Petroleum Exploration Bulletin,* v.**11**, P. 23-32.

Nwajide C.S. and Reijers T.J.A. (1996c): The geology of the southern Anambra Basin. In *Selected Chapters on Geology, Sedimentary Geologyand Sequence Stratigraphy in Nigeria and Three case studies andField Guide* (ed. Reijers T.F.A.) [M]. P.133–148. SPDC Shell Petroleum Development Company of Nigeria Corporate Reprographic Services, Warri.

Nwajide, C.S. (1990): Cretaceous Sedimentation and Paleogeography of the Central Benue Though. In: Ofoegbu, C.O; (Ed.), The Benue. Tough structure and Evolution *International Monograph Series, Braunschweig*, P. 19-38.

Nwajide, C.S. (2005): Hydrocarbon Potentials of the Anambra Basin, Proceedings of the First Seminar Organised by the Petroleum Technology Development Fund (PTDF) Chair in Geology, *University of Nigeria, Nsukka*. P. 1-7.

Nwajide, C.S. (2014): Geology of Nigeria's Sedimentary Basin, *CSS Bookshops Limtd, Lagos*, P. 277 – 346.

Obaje, N.G. (2009): Geology and Mineral Resources of Nigeria. *Lecture notes in Earth Science, Springer – Verlag Berlin Heidelberg*. P. 58 – 62.

Obaje, N.G., Ulu, O.K. and Petters, S.W. (1999): Biostratigraphic and geochemical controls of hydrocarbon prospects in the Benue Trough and the Anambra Basin, Nigeria. *Nigeria Association of Petroleum Exploration Bulletin*, V.**14**, P. 18-54.

Obi, G.C. (2000): Depositional Model for the Companian–Maastrichtian Anambra Basin, Southern Nigeria. *Ph.D. Thesis, University of Nigeria, Nsukka, Nigeria*, P. 291.

Obi, G. C., Okogbue, C. O., Nwajide, C. S. (2001): Evolution of the Enugu Cuesta: A tectonically driven erosional process. *Global Journal Pure Applied Sciences,* **7**(2): P. 321-330.

Obi, G. C., Okogbue, C. O. (2004): Sedimentary response to tectonism in the Campanian‐Maastrichtian succession, Anambra Basin, South‐eastern Nigeria. *Journal of African Earth Sciences,* **38**, P. 99-108.

Oboh-Ikuenobe F.E., Obi C. G. and Jaramillo C.A. (2005): Lithofacies, palynofacies, and sequence stratigraphy of Palaeogene strata in Southeastern Nigeria. *Journal of African Earth Sciences,* **41**, P. 79–102.

Offodile E.M. (1976): The geology of the Middle Benue Trough, Nigeria. *Cretaceous Research*. **1, P.** 101–124.

Ojo, O.J. (1992): Petroleum Geology and Sedimentology of Patti Formation, Bida Basin ,Nigeria. M. Sc. Thesis, University of Ibadan Nigeria. P. 190.

Ojo, O.J., Hameed, O.A., Alade, B. (2010): The Sedimentary Lithofacies, Paleoenvironments and Hydrocarbon Source Rock Facies of the Eze – Aku Formation, Lower Benue Trough, Nigeria. *The IUP Journal of Earth Sciences,* **4, 1**, P. 7 – 22.

Ojoh, K.A. (1990): Cretaceous geodynamic evolution of the southern part of the Benue Trough (Nigeria) in the equatorial domain of the South Atlantic. Stratigraphy, basin analysis and paleo-oceanography. *Bulletin Centres Recherches Exploration – Production Elf-Aquintance* **14**, P. 419-442.

Okoro, A. O. and Arua, I. (1989): Reconstruction of paleowave and paleodepth regimes of the Nkporo sea (Campano – Maastrichtian) using wave – formed ripple marks. *Journal of Mining Geology*, **25**, P. 75 – 79.

Olade, M.A., (1975): Evolution of Nigeria's Benue Trough (aulacogens): a tectonic model. *Geology Magazine*, **112**, P. 575-583.

Onuoha, K. M., (1986): Basin subsidence, sediment decompaction and burial history modelling techniques: Applicability to the Anambra Basin. *Proceedings Nigeria Association of Petroleum Exploration,* **2**: P. 6 – 17.

Passega, R. (1957): Texture and characteristic of clastic deposition. *American Association of Petroleum Geologists Bulletin*. 41: P. 1952–1984.

Passega, R. (1964): Grain size representation by CM patterns as a geological tool. *Journal of Sedimentary Petrology,* 34(4): P. 830–847.

Pemberton, S. G., MacEachern, J. A., and Frey, R. W., (1992): Trace fossil facies models: environmental and allostratigraphic significance, in: Facies Models: Response to Sea Level Change (R. G. Walker and N. James, eds.), St. John's, Newfoundland, *Geological Association of Canada,* pp. 47–72.

Peters, S. W., (1978): Stratigraphic evolution of the Benue Trough and its implication for the upper Cretaceous paleogeography of West Africa. *Journal of Geology,* **86**; p.311 – 322.

Petters, S.W., (1976): Upper Cretaceous subsurface stratigraphy of Atlantic Coastal Plain of New Jersey: *American Association of Petroleum Geologists Bulletin,* v. **60**, no. 1, P. 87-107

Petters, S.W. (1980): Biostratigraphy of Upper Cretaceous foraminifera of the Benue Trough, Nigeria. *Journal of Foraminiferal Research*, **10**, P. 191–204.

Petters, S.W. (1982): Central West African Cretaceou – Tertiary benthic foraminifera and stratigraphy. *Palaeontographica* (A) **179**, P. 1-104.

Petters, S. W. and Ekweozor, C. M. (1982): Petroleum geology of the Benue Trough and southeastern Chad Basin, Nigeria. *Bulletin American Association of Petroleum Geologists* **66**, P. 1141- 1149.

Petters, S.W., (1983): Gulf of Guinea planktonic foraminiferal biochronology and geological history of the South Atlantic. *Journal of Foraminiferal Research,* 13: 32-59.

Pettijohn, F. J., (1975): Sedimentary rocks, 3rd ed; New York, *Harper and Row*, P. 628.

Popoff, M., (1990): Deformation intracontinental gondwanienne Rifting mesozoique en Afrique (Evolution meso-cenozoique dufosse de la Benue, Nigeria)—Relations de lı´ocean Atlantique sud.*These de Etat, University Aix-Marseillea III*.

Popoff, M., Doucet, J.F and Latil-Brun, M. V. (1988): Analysé de la subsidence au Crétacé supériéur-Paléocene dans le basin d'Anambra, SW du fossé de la Bénoué. Apports à la géodynamique de la plaque Afrique. *Comptes Rendus Académie Sciences Paris (II)* **307**, P. 1271-1276.

Potter, P.E. and Pettijohn, F.J., (1963): Palaeocurrents and Basin Analysis. Springer, Berlin. P. 296.

Potter, P.E. and Olsen, J.S., (1954): Variance components of cross-bedding direction in some basal Pennsylvanian sandstones of the Eastern Interior Basin: Geological application. *Jounal of Geology*, **62**: P. 50-73.

Potter, P.E. and Pettijohn, F.J., (1977): Paleocurrents and Basin Analysis. *Springer, New York, N.Y.*, 2nded., P. 425.

Prothero, D. R., Schwab, F. (1996): Sedimentary Geology. New York*: W. H. Freeman and Company*, P. 575.

Pryor, W. A. (1960): Cretaceous sedimentation in Upper Mississippi Embayment. *American Association of Petroleum Geologists Bulletin*. 44, P. 1473-1504.

Reading, H.G. (1996): Sedimentary Environment Processes, Facies and Stratigraphy. *Blackwell Scientific Publications, Oxford*. P. 671.

Reineck, H. E., Singh, I. B. (1980): Depositional Sedimentary Environments, 2nd Edition. New York: *Springer‑Verlag*, P. 551.

Reyment, R.A. (1955a): The Cretaceous Ammonoidea of southern Nigeria and the southern Cameroons. *Bulletin Geological Survey Nigeria*, **25**, P. 1-112.

Reyment, R.A. (1955b): Upper Cretaceous Mullusca (Lamellibranchia and Gastropoda) from Nigeria. *Colon Geol. Miner. Resour*. **5**, P. 127-155.

Reyment, R.A. (1957a): The Cretaceous – Tertiary boundary of Nigeria. *Report Geological. Survey Nigeria*, P. 68 -86.

Reyment, R.A. (1964): Review of Nigerian Cretaceous Cenozoic stratigraphy. *Journal Nigerian Mining Geological Metallurgical Society* **1**, P. 61-80.

Reyment R.A. (1965): Aspects of the geology of Nigeria. *Ibadan University Press*, Ibadan, Nigeria. P. 143.

Reyment, R.A. and Barber, W.M. (1956): "Nigeria and Cameroons". In : *Lexique Stratigraphique International: Afrique*. **4**, P. 35-39.

Romos, E., Margo M. De Gibert J., Tawengi K.S. Khoja A. A., Bolatti N. D. (2006): Stratigraphy and Sedimentology of the Middle Ordovician Hawaz Formation (Murzuq Basin, Libya). *American Association of Petroleum Geologists Bulletin*, V. No.**9**, P. 1309-1336.

Sahu, B.K., (1964): "Depositional mechanisms from the size analysis of clastic sediments". *Journal of Sedimentary Petrology*, **34**(1), P. 73- 83.

Salami, M. B. (1990): Palynomorph taxa from the "Lower Coal Measures" deposits (? Campanian – Maastrichtian) of Anambra Trough, southeastern Nigeria. *Jounal of African. Earth Science.***11**, P. 135 – 150.

Selley, R.C. (1966): Paleocurent and sediment Transport in near Shore Sediment of Sincte Basin. *Libya Journal of Geology*. Vol. 75, No. **2**, P. 215-222.

Selley, R. C. (1969): Torridonian alluvium and quicksands. *Scottland Journal of Geology*. 5, 328-346.

Selley, R.C. (1976): An Introduction to Sedimentology. *Academic Press, New York, N.Y.*, P. 408.

Seward, A. L. (1924): On a collection of fossil plants from southeast Nigeria. *Bulletin Geological Survey Nigeria* **6** (Appendix II), P. 66 – 78.

Shirley O. O. and Gordian C. O. (2013): Sedimentology and Sequence Stratigraphy of the Nkporo Group (Campanian – Maastrichtian), Anambra Basin, Nigeria. *Journal of Palaeogeography*. **2**(2), P. 192 – 208.

Simpson, A. (1954): The Nigerian coalfields, the geology of parts of Onitsha, Owerri and Benue Provinces. *Bulletin Geological Survey Nigeria*, **24**, P. 85.

Simpson, A. (1955): The Nigerian coal field: the geology of parts of Owerri and Benue provinces. *Bulletin Geological Survey Nigeria*, No. **24**, P. 85, 5.

Smith, D. G. (1988): Tidal bundles and mud couplets in the McMurray Formation, Northern Alberta, Canada. *Bulletin of Canadian Petroleum Geology*, **36**, P. 216-219.

Slopes, M. C. (1914): A new Cretaceous plant from Nigeria. *Geology Magazine.***1**, P. 433 – 435.

Tanner, W. F. (1955): Paleogeographic reconstructions from cross-bedding studies. *American Association of Petroleum Geologists Bulletin*. **39**, P. 247-248.

Tattam CM (1944): A Review of the Nigerian Stratigraphy. *Report of Geological Survey of Nigeria*, **1943**, P. 27-46.

Tucker, M.E. (1996): Sedimentary Rocks in the Field. *John Weley and Sons, Chichester, New York*, P. 150.

Van Wagoner J.C., Mitchum R.M., Campion KM, RahmaniaV.D. (1990): Siliciclastic Sequence Stratigraphy in Well Logs, Cores and Outcrop. *s. Am. Assoc. Petrol. Geol. Methods in Exploration Series*, No.**2**, P. 55.

Visher, G. S. (1969): Grain size distribution and depositional processes. *Journal of Sedimentary Petrology* **39**, P. 1074–1106.

Walker, R.G., Plint, A.G. (1992): Wave-and storm-dominated shallow marine system. In: Walker, R.G., James, N.P. (Eds.), Facies Models: Response to Sea Level Change. *Geological Association of Canada, St. John's*, P. 219–238.

Wentworth, C.K. (1922): A scale of grade and class terms for clastic sediments: *Journal of Geology* (**30**), P.377 – 392.

Whiteman, A.J. (1982): Nigeria: Its petroleum Geology, Resources and Potential. *Graham and Trotman, London*, P. 394.

Whittaker, A., Cope, J. C. W., Cowie, J. W., Gibbons, W., Hailwood, E. A., House, M. R., Jenkins, D. G., Rawson, P. F., Rushton, A. W. A., Smith, D. B., Thomas, A. T., and Wimbledon, W. A., (1991): A guide to stratigraphical nomenclature, *Journal of the Geological Society of London* **148**: P. 813–824.

Weimer, R. J. (1984): Relations of unconformities, tectonics, and sea level changes, Cretaceous of Western Interior, In: Schlee, J., (ed). Interregional Unconformities and Hydrocarbon Accumulation. *American Association of Petroleum Geologists Memoir*,**36**, P. 7-35.

Wilson, R.C. (1925): The geology of the Eastern Railway: Section 1. Port Harcourt to Enugu. With notes by A.D.N. Basin. *Bulletin Geological Survey Nigeria*, No.**8**, P. 95.

Wright, J.B., Hastings, D.A. and Williams, H.R. (1985): Geology and Mineral Resources of West Africa. *George Allen and Unwin, London*, P. 187.

Zaborski, P. M. (1983): Campano – Maastrichtian ammonites, correlation and palaeogeography in Nigeria. *Journal of African Earth Sciences*, **1**, 59-63.

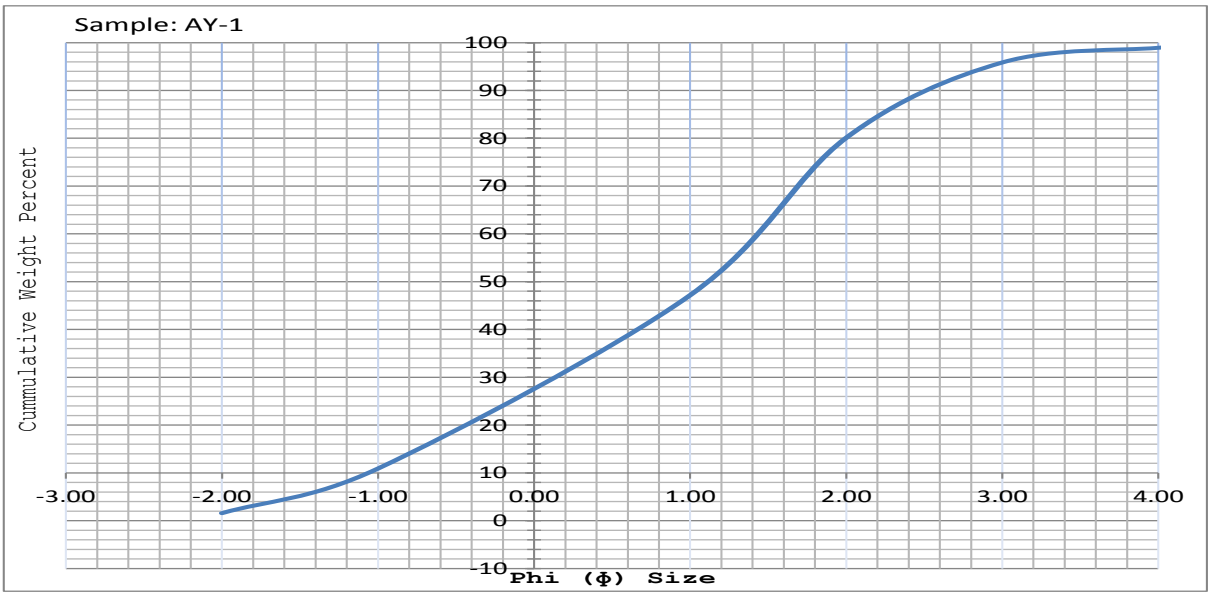
Zaborski, P.M. (1998): A review of the Cretaceous Systems in Nigeria. *Africa Geoscience Review* Vol **5**, No 4, P. 26 – 30.

APPENDICES

Appendix I: Cumulative curve plots and tables for data obtained from granulometric analysis.

Sample AY-1

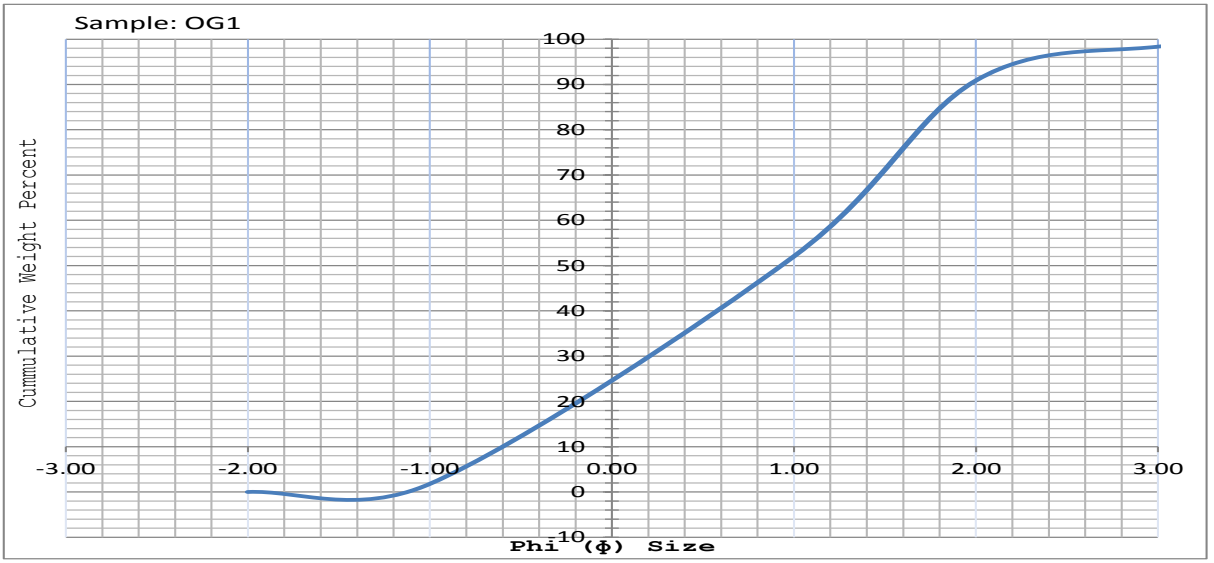
Sample: AY-1					
Sieve Size (mm)	Phi (Φ) Size	Weight retained (g)	% Weight Retained	Cumm. Weight Retained (g)	Cumm. Weight percent (%)
4.00	-2.00	1.69	1.58	1.69	1.58
1.68	-1.00	9.94	9.33	11.63	10.92
0.43	1.00	38.63	36.26	50.26	47.18
0.25	2.00	35.08	32.92	85.33	80.10
0.13	3.00	16.78	15.75	102.11	95.85
0.06	4.00	3.28	3.08	105.39	98.93
<0.06	>4.00	1.14	1.07	106.53	100.00
		106.53	100.00		



Cumulative frequency curve for sample AY-1

Sample OG1

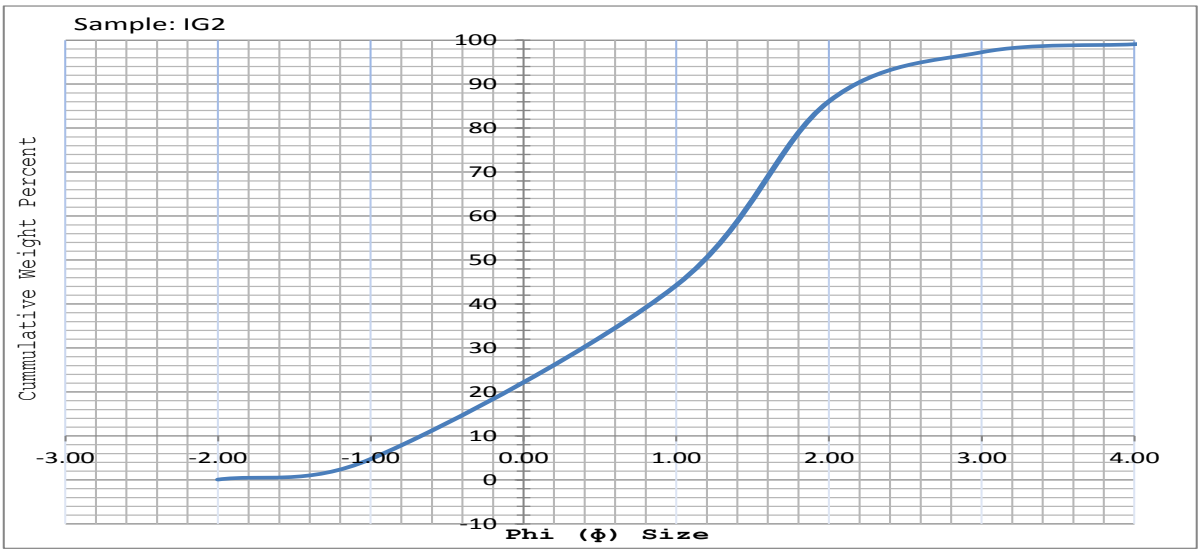
Sample: OG1					
Sieve Size (mm)	Phi (Φ) Size	Weight retained (g)	% Weight Retained	Cumm. Weight Retained (g)	Cumm. Weight percent (%)
4.00	-2.00	0.00	0.00	0.00	0.00
1.68	-1.00	1.91	1.80	1.91	1.80
0.43	1.00	53.35	50.26	55.26	52.06
0.25	2.00	41.23	38.84	96.49	90.89
0.13	3.00	7.92	7.46	104.41	98.36
0.06	4.00	1.13	1.06	105.54	99.42
<0.06	>4.00	0.61	0.57	106.15	100.00
		106.15	100.00		



Cumulative frequency curve for sample OG1

Sample OG2

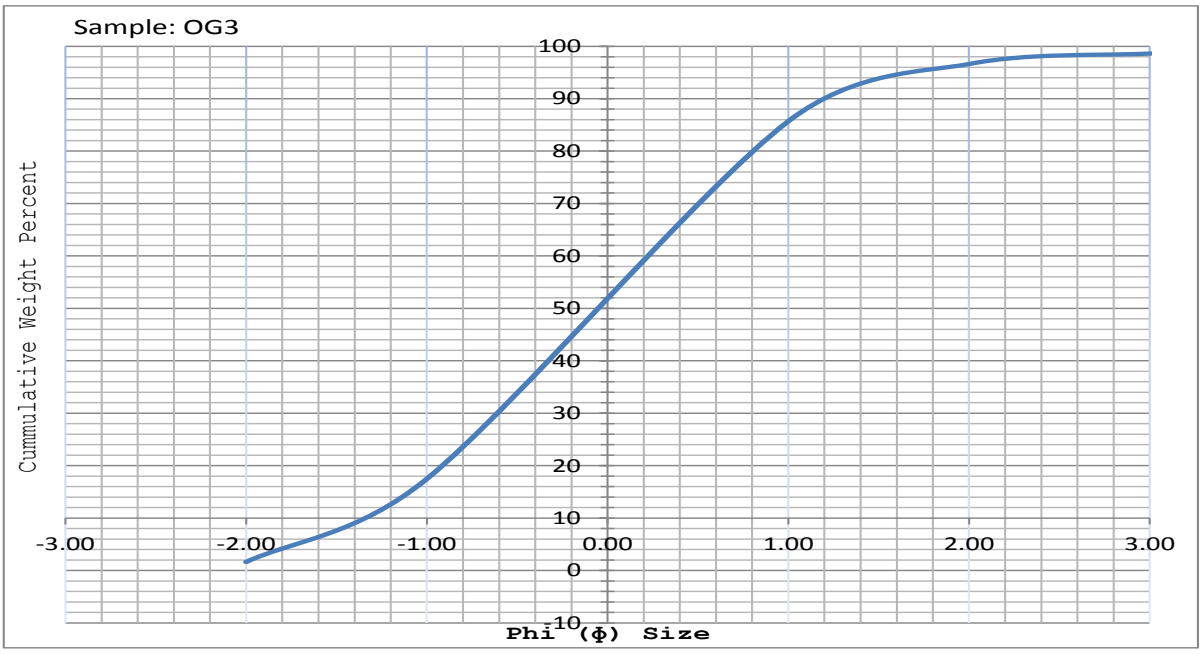
Sample: OG2					
Sieve Size (mm)	Phi (Φ) Size	Weight retained (g	% Weight Retained	Cumm. Weight Retained (g)	Cumm. Weight percent (%)
4.00	-2.00	0.09	0.08	0.09	0.08
1.68	-1.00	5.09	4.68	5.18	4.76
0.43	1.00	42.95	39.49	48.13	44.25
0.25	2.00	45.52	41.84	93.65	86.09
0.13	3.00	12.14	11.16	105.79	97.25
0.06	4.00	1.98	1.82	107.77	99.07
<0.06	>4.00	1.01	0.93	108.78	100.00
		108.78	100.00		



Cumulative frequency curve for sample OG2

Sample OG3

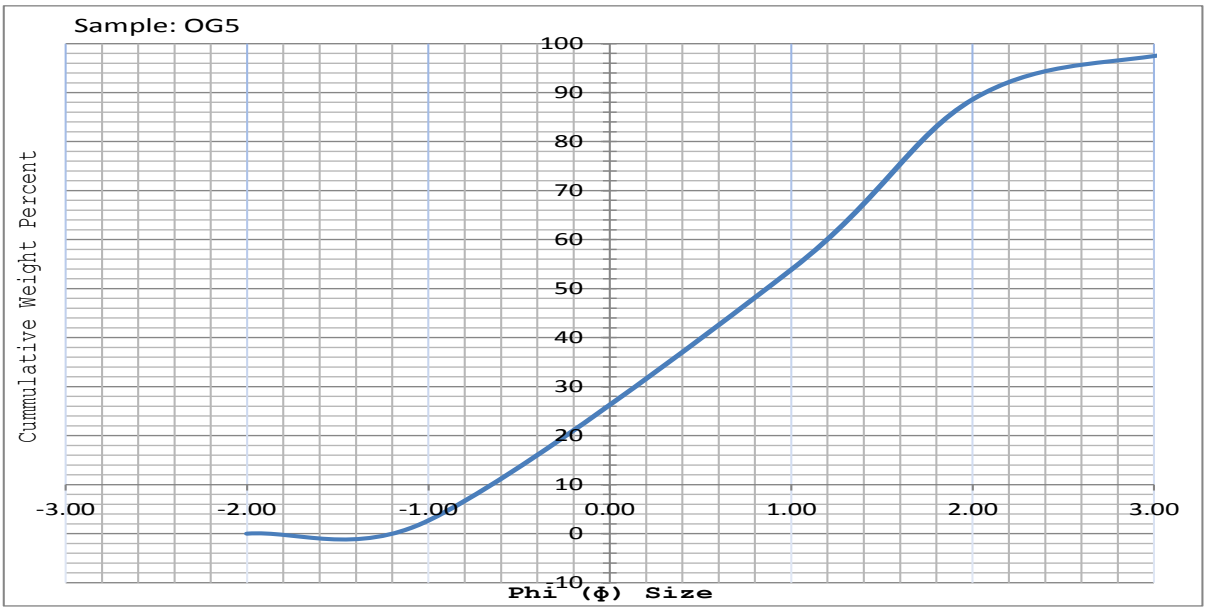
Sample: OG3					
Sieve Size (mm)	Phi (Φ) Size	Weight retained (g)	% Weight Retained	Cumm. Weight Retained (g)	Cumm. Weight percent (%)
4.00	-2.00	1.74	1.63	1.74	1.63
1.68	-1.00	17.01	15.86	18.75	17.49
0.43	1.00	73.15	68.22	91.90	85.70
0.25	2.00	11.71	10.92	103.61	96.62
0.13	3.00	2.13	1.98	105.74	98.61
0.06	4.00	0.86	0.80	106.60	99.41
<0.06	>4.00	0.63	0.59	107.23	100.00
		107.23	100.00		



Cumulative frequency curve for sample OG3

Sample OG5

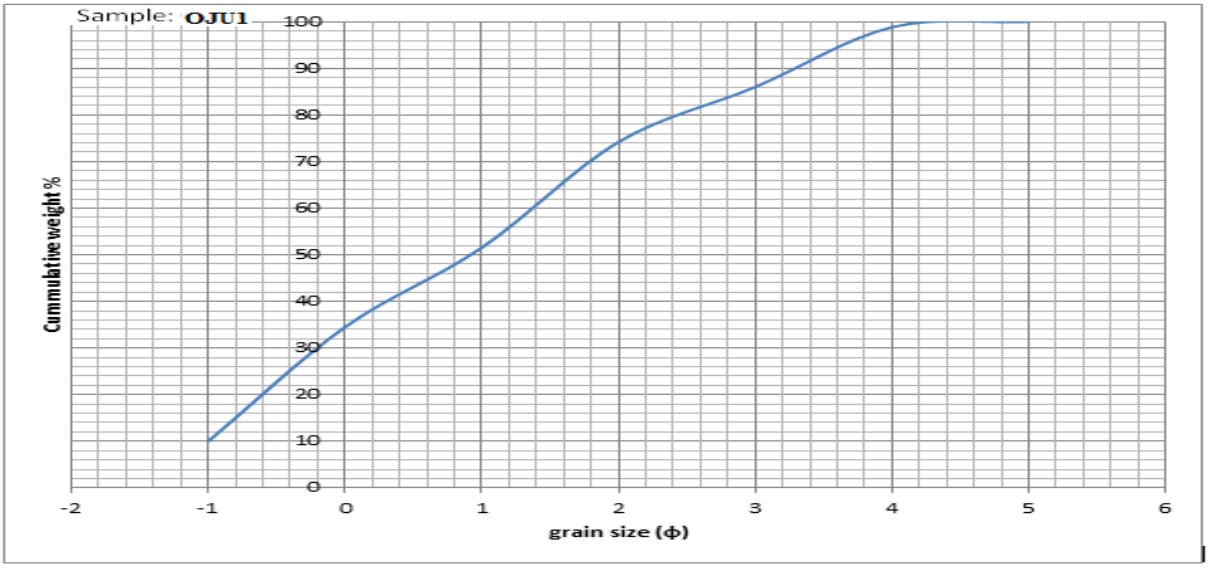
Sample: OG5					
Sieve Size (mm)	Phi (Φ) Size	Weight retained (g)	% Weight Retained	Cumm. Weight Retained (g)	Cumm. Weight percent (%)
4.00	-2.00	0.00	0.00	0.00	0.00
1.68	-1.00	2.60	2.69	2.60	2.69
0.43	1.00	49.39	51.18	51.99	53.87
0.25	2.00	33.52	34.74	85.51	88.61
0.13	3.00	8.54	8.85	94.05	97.46
0.06	4.00	1.65	1.71	95.70	99.17
<0.06	>4.00	0.80	0.83	96.50	100.00
		96.50	100.00		



Cumulative frequency curve for sample OG5

Sample OJU1

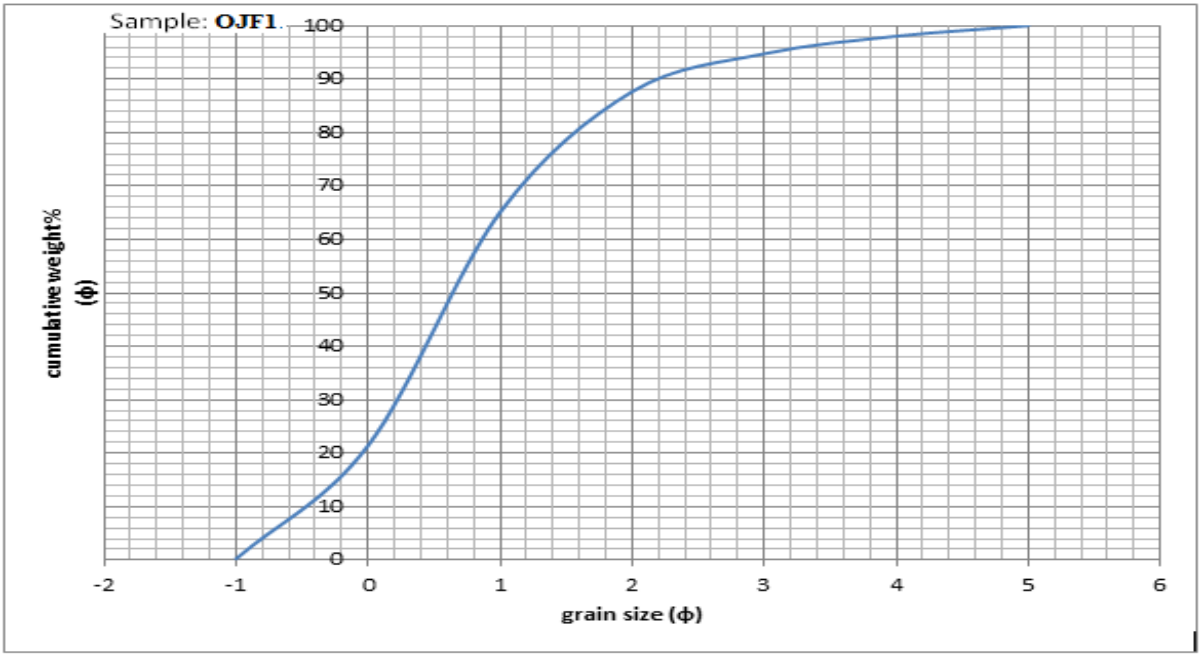
Sieve Size (mm)	Phi Scale (φ)	Weight of sieve (g)	Weight of sieve + Sample retained (g)	Weight of Sample (g)	% weight of Sample	Cum. Weight%
2mm	-1	465	475	10	10.04	10.04
1mm	0	360.61	395	24.39	24.48	34.52
500µm	1	313.57	330.53	16.96	17.02	51.54
250µm	2	317.61	340.21	22.6	22.68	74.22
125µm	3	300.93	312.7	11.77	11.81	86.03
63mic	4	268.24	281	12.76	12.81	98.84
Pan	5	272.84	274	1.16	1.16	100
				99.64	100	



Cumulative frequency curve for sample OJU1

Sample OJF1

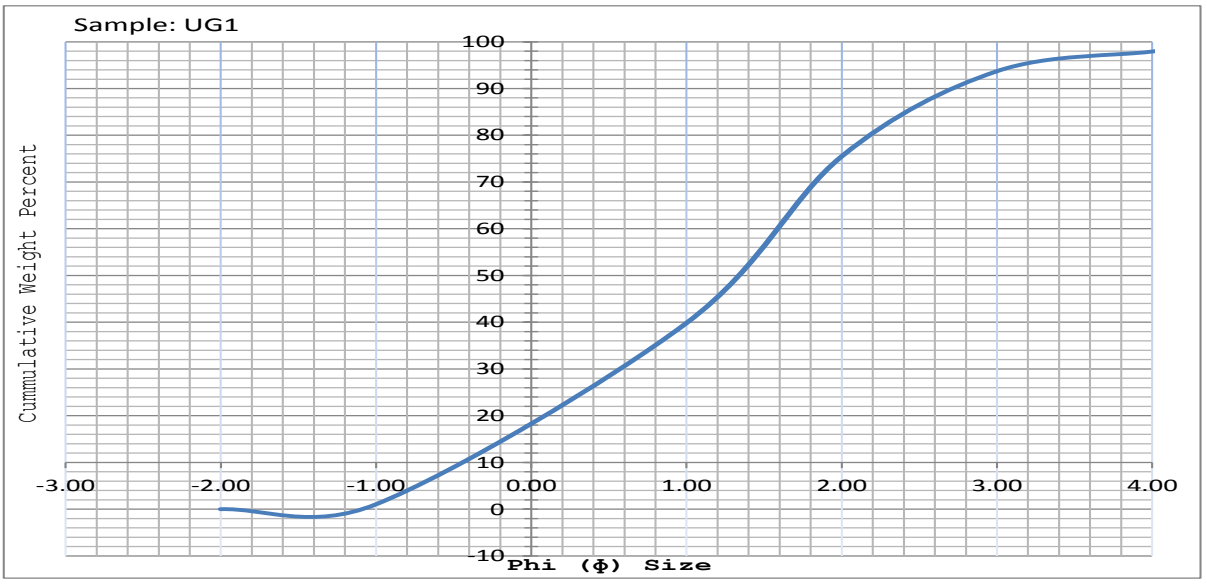
Sieve Size (mm)	Phi Scale (φ)	Weight of sieve (g)	Weight of sieve + Sample retained (g)	Weight of Sample (g)	% weight of Sample	Cum. Weight%
2mm	-1	465	465.26	0.26	0.26	0.26
1mm	0	360.61	382	21.13	21.19	21.45
500µm	1	313.57	357.12	43.54	43.66	65.11
250µm	2	317.61	340.11	22.5	22.56	87.67
125µm	3	300.93	308	7.07	7.09	94.76
63mic	4	268.24	271.52	3.28	3.29	98.05
Pan	5	272.84	274.78	1.94	1.95	100
				99.72	100	



Cumulative frequency curve for sample OJF1

Sample UG1

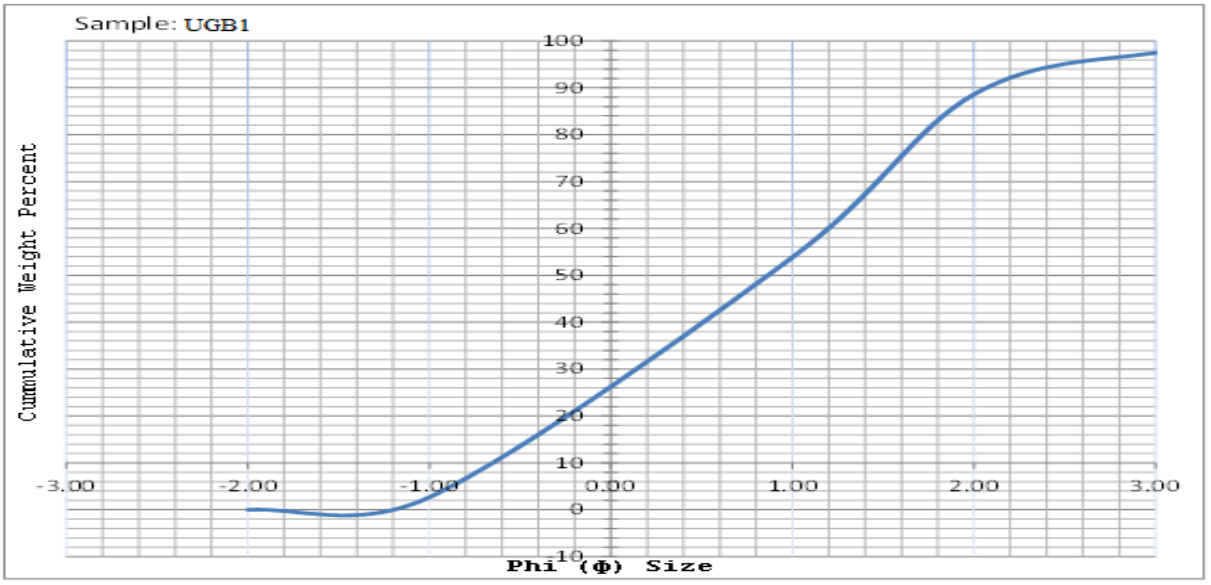
Sample: UG1					
Sieve Size (mm)	Phi (Φ) Size	Weight retained (g)	% Weight Retained	Cumm. Weight Retained (g)	Cumm. Weight percent (%)
4.00	-2.00	0.00	0.00	0.00	0.00
1.68	-1.00	1.12	1.05	1.12	1.05
0.43	1.00	41.16	38.78	42.28	39.84
0.25	2.00	37.85	35.66	80.12	75.50
0.13	3.00	19.33	18.22	99.46	93.71
0.06	4.00	4.46	4.21	103.92	97.92
<0.06	>4.00	2.21	2.08	106.13	100.00
		106.13	100.00		



Cumulative frequency curve for sample UG1

Sample UGB1

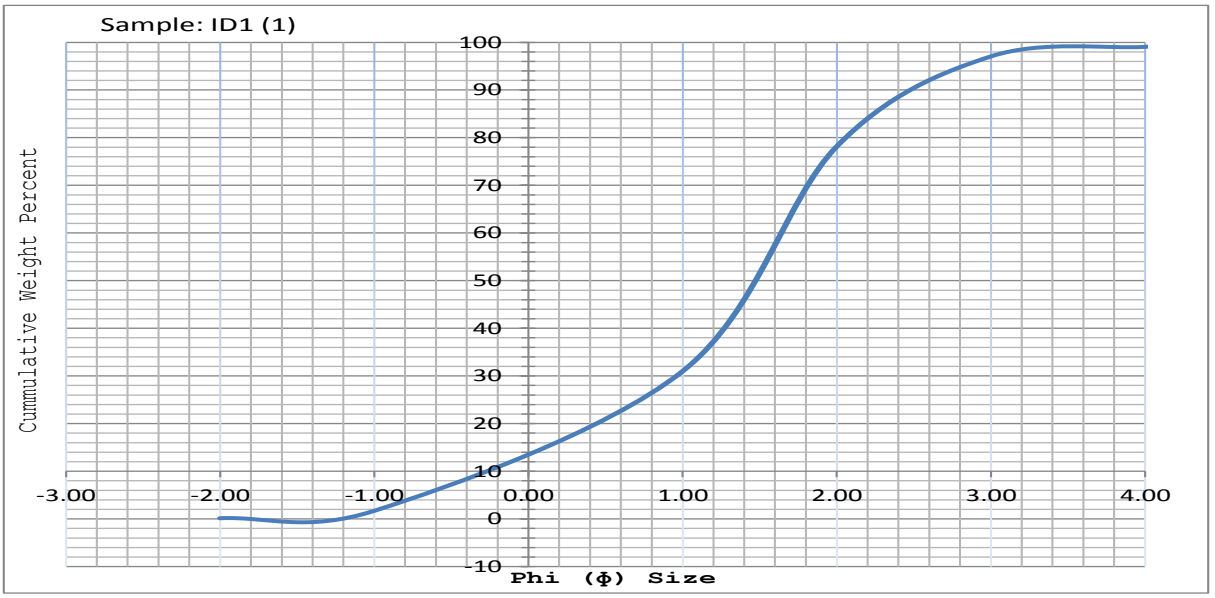
Sample:UGB1					
Sieve Size (mm)	Phi (Φ) Size	Weight retained (g)	% Weight Retained	Cumm. Weight Retained (g)	Cumm. Weight percent (%)
4.00	-2.00	0.00	0.00	0.00	0.00
1.68	-1.00	2.60	2.69	2.60	2.69
0.43	1.00	49.39	51.18	51.99	53.87
0.25	2.00	33.52	34.74	85.51	88.61
0.13	3.00	8.54	8.85	94.05	97.46
0.06	4.00	1.65	1.71	95.70	99.17
<0.06	>4.00	0.80	0.83	96.50	100.00
		96.50	100.00		



Cumulative frequency curve for sample UGB1.

Sample ID1-1

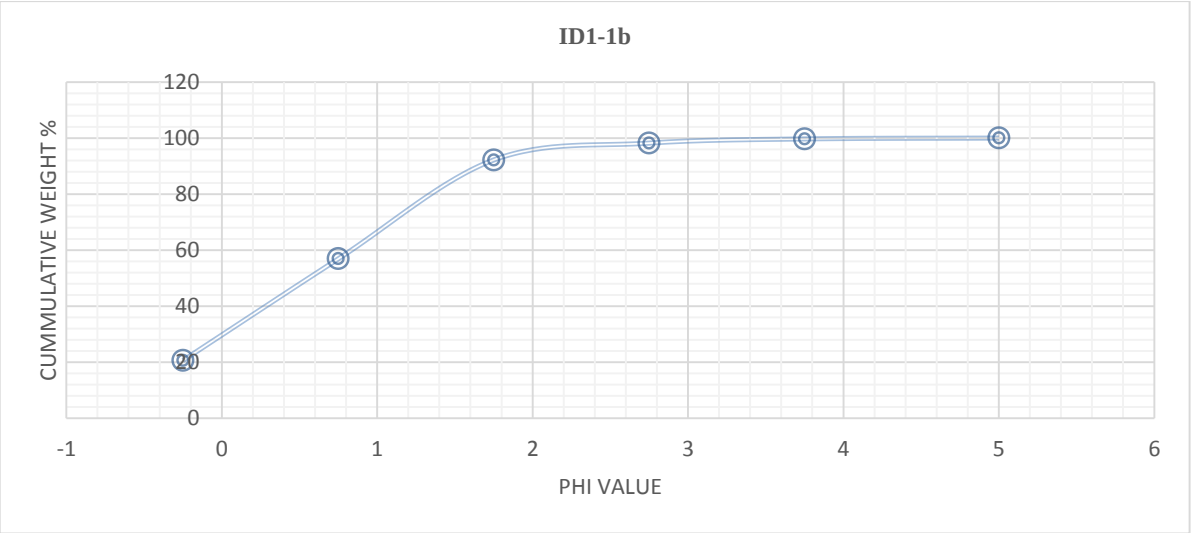
Sample: ID1 (1)					
Sieve Size (mm)	Phi (Φ) Size	Weight retained (g	% Weight Retained	Cumm. Weight Retained (g)	Cumm. Weight percent (%)
4.00	-2.00	0.14	0.14	0.14	0.14
1.68	-1.00	1.58	1.56	1.71	1.70
0.43	1.00	29.56	29.28	31.27	30.98
0.25	2.00	47.62	47.17	78.89	78.15
0.13	3.00	19.08	18.90	97.98	97.05
0.06	4.00	2.03	2.01	100.00	99.06
<0.06	>4.00	0.95	0.94	100.95	100.00
		100.95	100.00		



Cumulative frequency curve for sample ID1-1

ID1-1b

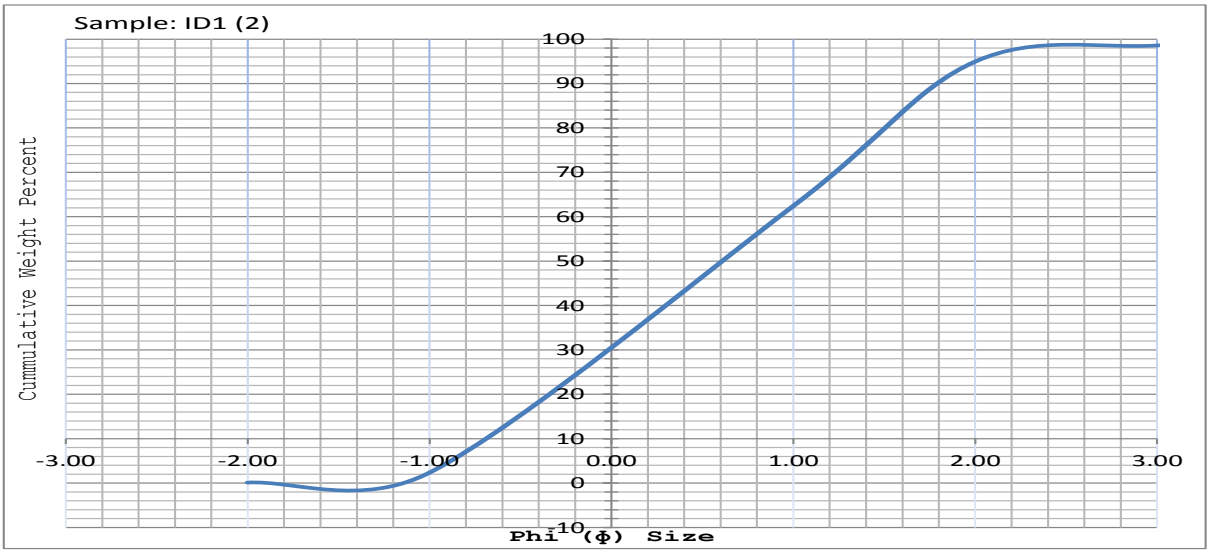
Sieve sizes	Phi scale (φ)	Weight of sieve (g)	Weight of sieve + sample (g)	Weight of sample (g)	% weight of sample	Cumulative weight percentage
1.18 mm	-0.25	347.6	368.2	20.6	20.6	20.6
600 µm	0.75	349.4	385.7	36.3	36.3	56.9
300 µm	1.75	365.9	401.2	35.3	35.3	92.2
150 µm	2.75	325.6	331.6	6.0	6.0	98.2
75 µm	3.75	313.4	314.9	1.5	1.5	99.7
Pan	5	299.9	300.2	0.3	0.3	100
				100	100	100



Cumulative frequency curve for sample ID1-1b

Sample ID1-2

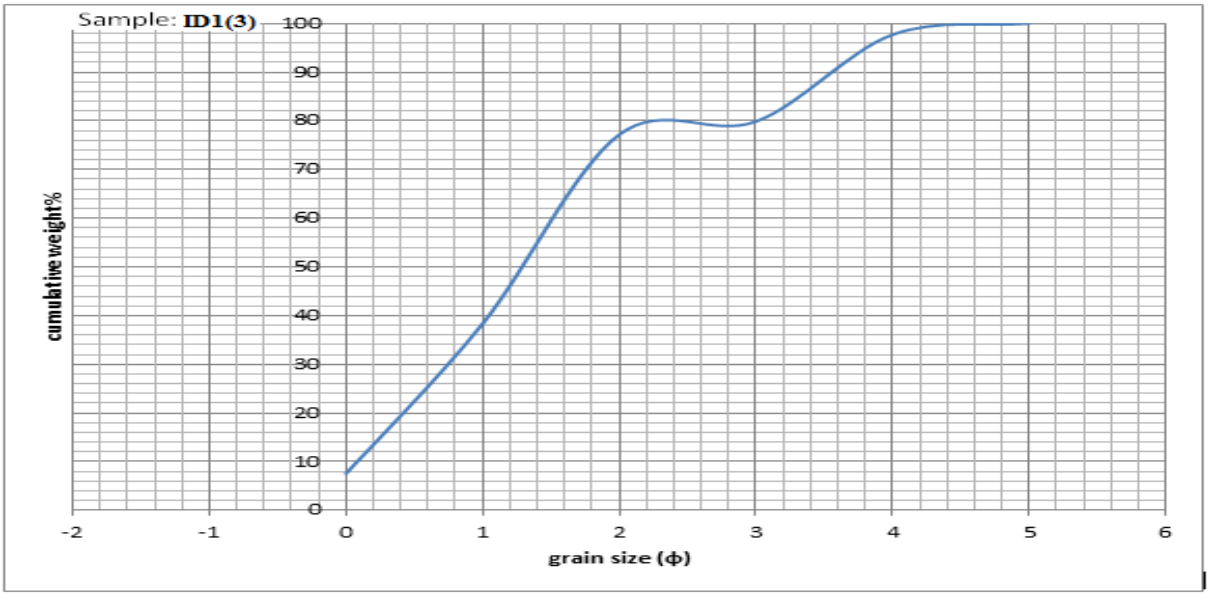
Sample: ID1(2)					
Sieve Size (mm)	Phi (Φ) Size	Weight retained (g)	% Weight Retained	Cumm. Weight Retained (g)	Cumm. Weight percent (%)
4.00	-2.00	0.11	0.11	0.11	0.11
1.68	-1.00	2.28	2.26	2.39	2.37
0.43	1.00	60.55	60.07	62.94	62.44
0.25	2.00	32.78	32.52	95.72	94.96
0.13	3.00	3.65	3.62	99.37	98.58
0.06	4.00	0.85	0.84	100.22	99.42
<0.06	>4.00	0.58	0.58	100.80	100.00
		100.80	100.00		



Cumulative frequency curve for sample ID1-2

Sample ID1-3

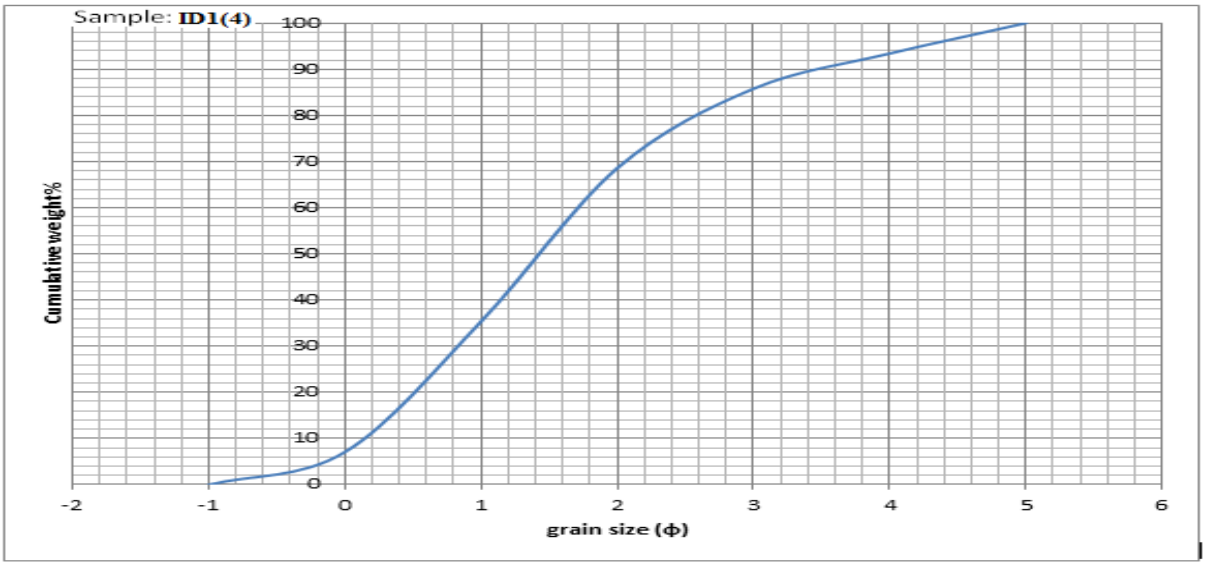
Sieve Size (mm)	Phi Scale (φ)	Weight of sieve (g)	Weight of sieve + Sample retained (g)	Weight of Sample (g)	% weight of Sample	Cum. Weight%
2mm	-1	465	468	3	3.02	3.02
1mm	0	360.61	368.13	4.52	4.56	7.58
500µm	1	313.57	344.12	30.53	30.78	38.36
250µm	2	317.61	356.11	38.5	38.81	77.17
125µm	3	300.93	303.62	2.69	2.71	79.88
63mic	4	268.24	285.92	17.68	17.82	97.7
Pan	5	272.84	275.12	2.28	2.3	100
				99.2	100	



Cumulative frequency curve for sample ID1-3

Sample ID1-4

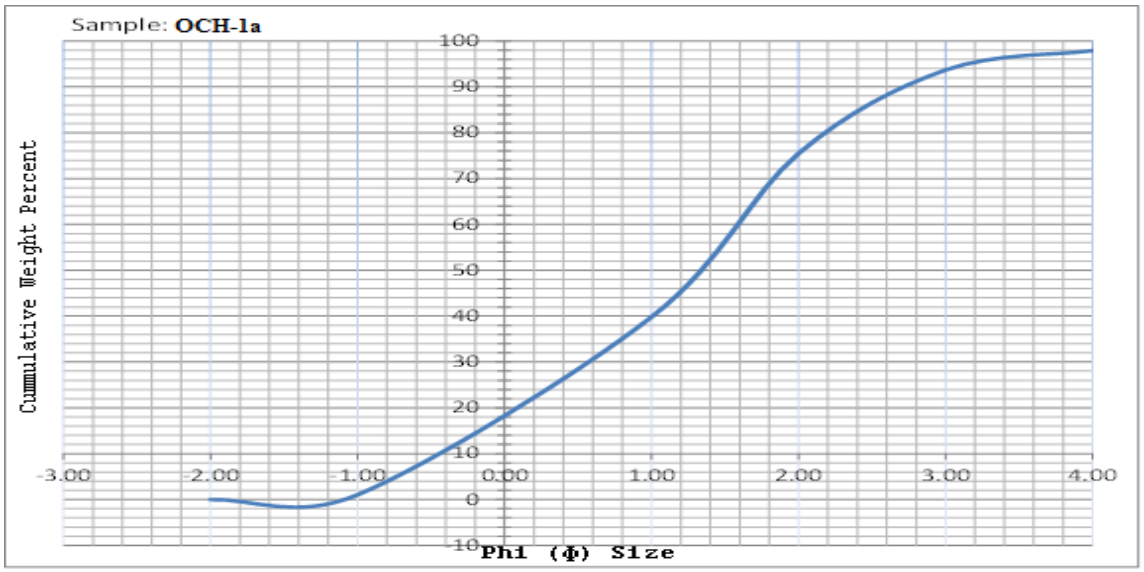
Sieve Size (mm)	Phi Scale (φ)	Weight of sieve (g)	Weight of sieve + Sample retained (g)	Weight of Sample (g)	% weight of Sample	Cum. Weight%
2mm	-1	465	465	0	0	0
1mm	0	360.61	367.64	7.03	7.09	7.09
500µm	1	313.57	341.64	28.07	28.29	35.38
250µm	2	317.61	350.56	32.95	33.21	68.59
125µm	3	300.93	318	17.07	17.21	85.8
63mic	4	268.24	275.8	7.56	7.62	93.42
Pan	5	272.84	279.37	6.53	6.58	100
				99.21	100	



Cumulative frequency curve for sample ID1-4

Sample OCH-1a

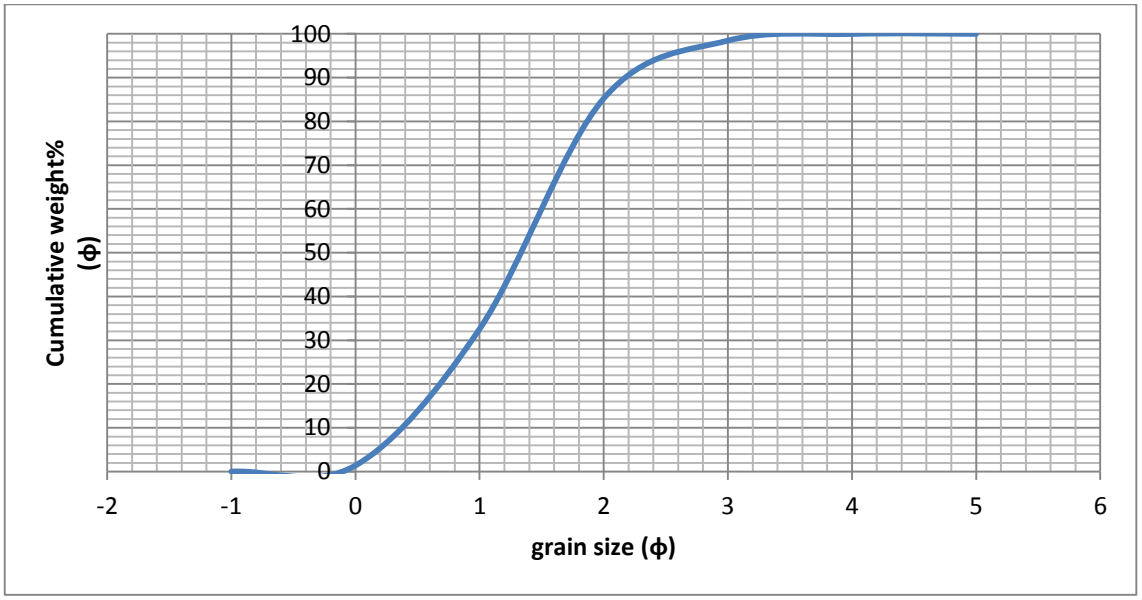
Sample: OCH-1a					
Sieve Size (mm)	Phi (Φ) Size	Weight retained (g)	% Weight Retained	Cumm. Weight Retained (g)	Cumm. Weight percent (%)
4.00	-2.00	0.00	0.00	0.00	0.00
1.68	-1.00	1.12	1.05	1.12	1.05
0.43	1.00	41.16	38.78	42.28	39.84
0.25	2.00	37.85	35.66	80.12	75.50
0.13	3.00	19.33	18.22	99.46	93.71
0.06	4.00	4.46	4.21	103.92	97.92
<0.06	>4.00	2.21	2.08	106.13	100.00
		106.13	100.00		



Cumulative frequency curve for sample OCH-1a

Table. Sample OCH-1b

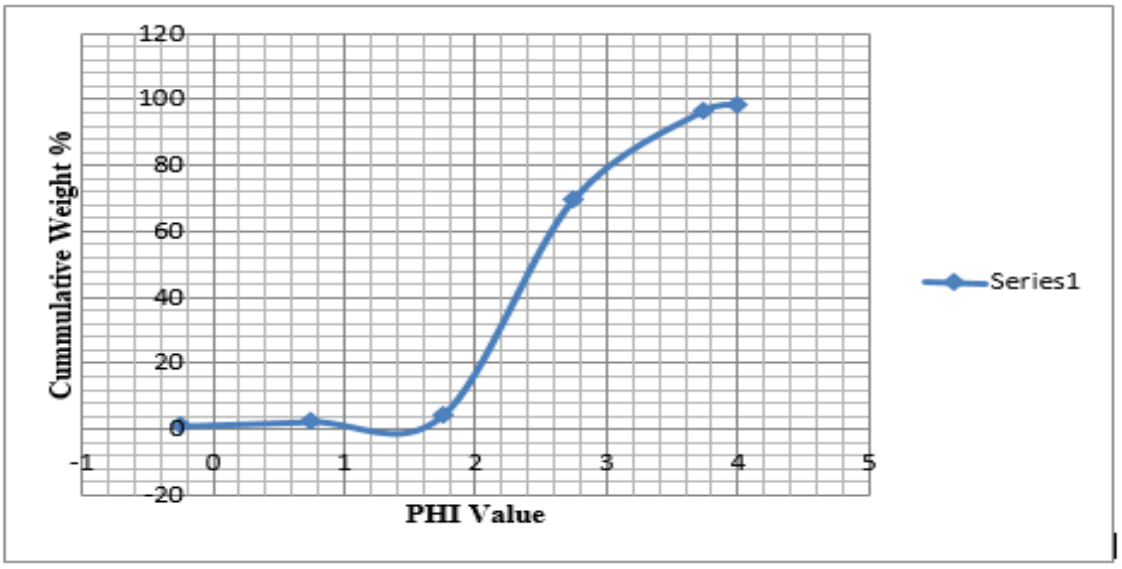
Sieve Size (mm)	Phi Scale (φ)	Weight of sieve (g)	Weight of sieve + Sample retained (g)	Weight of Sample (g)	% weight of Sample	Cumulative Weight%
2mm	-1	465	465	0	0	0
1mm	0	360.61	362	1.39	1.39	1.39
500µm	1	313.57	344.68	31.11	31.2	32.59
250µm	2	317.61	370.12	52.51	52.66	85.25
125µm	3	300.93	314.1	13.17	13.21	98.46
63mic	4	268.24	269.76	1.52	1.52	99.98
Pan	5	272.84	272.86	0.02	0.02	100
				99.72	100	



Cumulative frequency curve for sample OCH-1b

OCH-2a

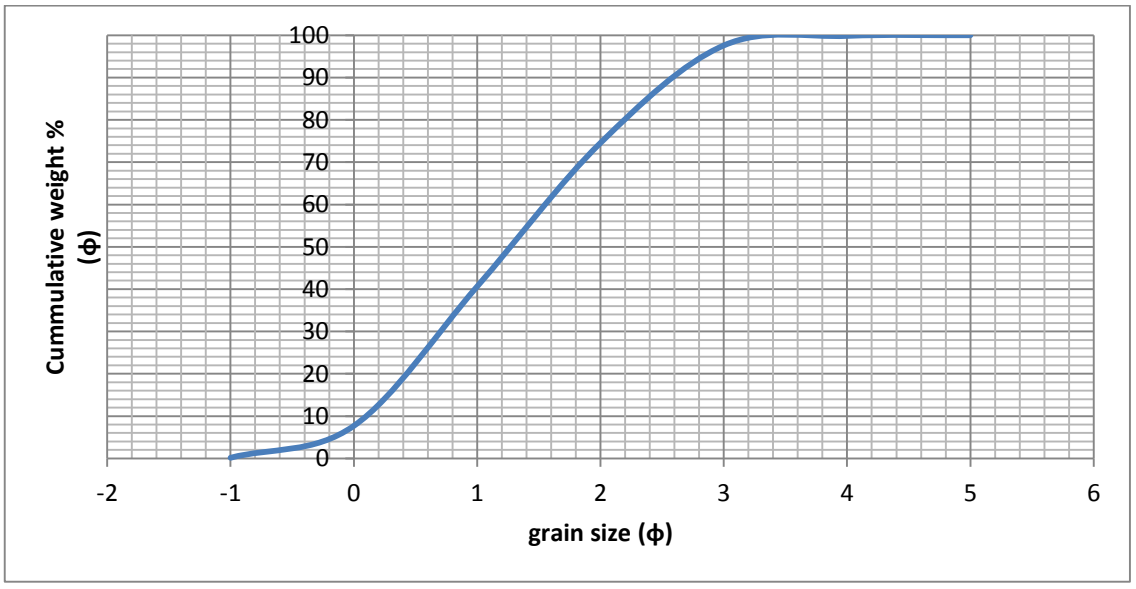
Sieve size (mm)	Phi scale (φ)	Weight retained (g)	% weight retained	Cumulative weight retained
1.18	**-0.25**	**1.14**	**1.14**	**1.14**
0.60	**0.75**	**1.32**	**1.32**	**2.46**
0.30	**1.75**	**1.81**	**1.81**	**4.27**
0.15	**2.75**	**65.48**	**65.48**	**69.75**
0.075	**3.74**	**26.91**	**26.91**	**96.66**
0.063	**4.00**	**2.00**	**2.00**	**98.66**



Cumulative frequency curve for sample OCH-2b

Table.9 Sample OCH-2b

Sieve Size (mm)	Phi Scale (φ)	Weight of sieve (g)	Weight retained (g)	% weight retained	Cumulative Weight %
2mm	-1	465	0.15	0.15	0.15
1mm	0	360.61	7.49	7.54	7.69
500µm	1	313.57	32.73	32.94	40.63
250µm	2	317.61	33.71	33.92	74.55
125µm	3	300.93	22.89	23.04	97.59
63mic	4	268.24	2.24	2.25	99.84
Pan	5	272.84	0.16	0.16	100
			99.37	100	



Cumulative frequency curve for sample OCH-2b

Table 4.Sample **OCH-3a**

Sieve Size (mm)	Phi Scale (φ)	Weight retained(g)	% weight retained	Cumulative Weight%
1.18	-0.59	6.00	6.19	6.19
600	-0.3	7.00	7.22	13.41
300	0.6	19.00	19.59	33.00
150	3.6	46.00	46.42	79.42
75	4.8	12.00	12.37	91.42
Pan	5.0	7.00	7.22	98.64
			99%	

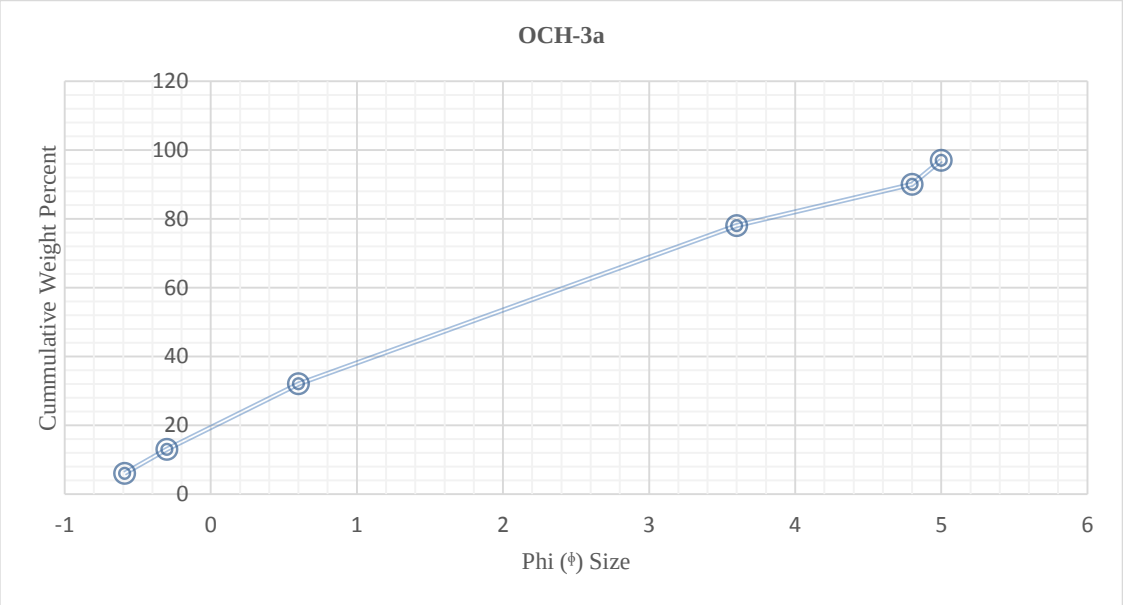
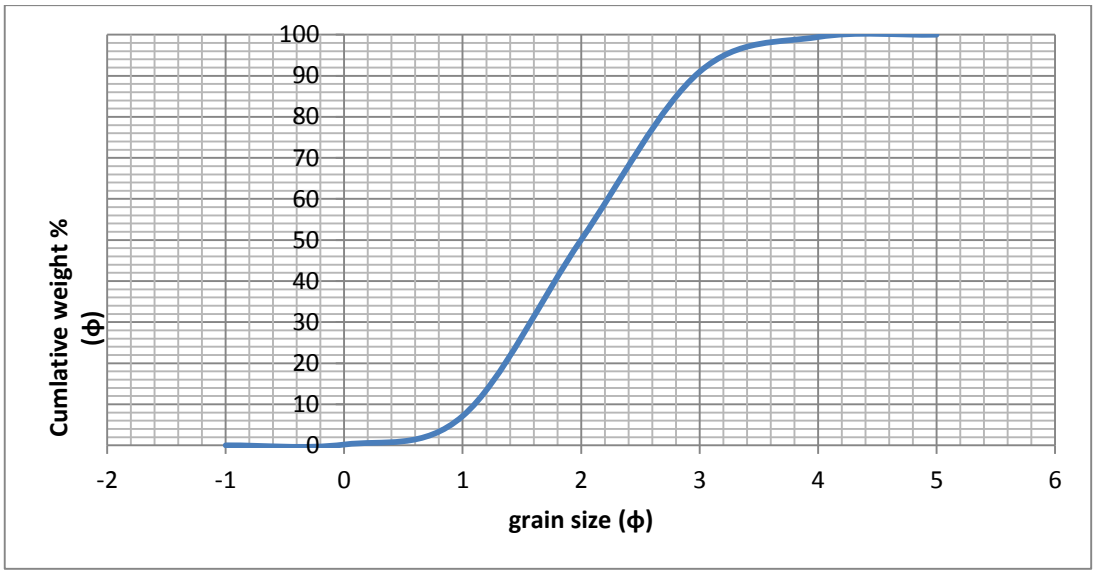


Table 4.Sample **OCH-3b**

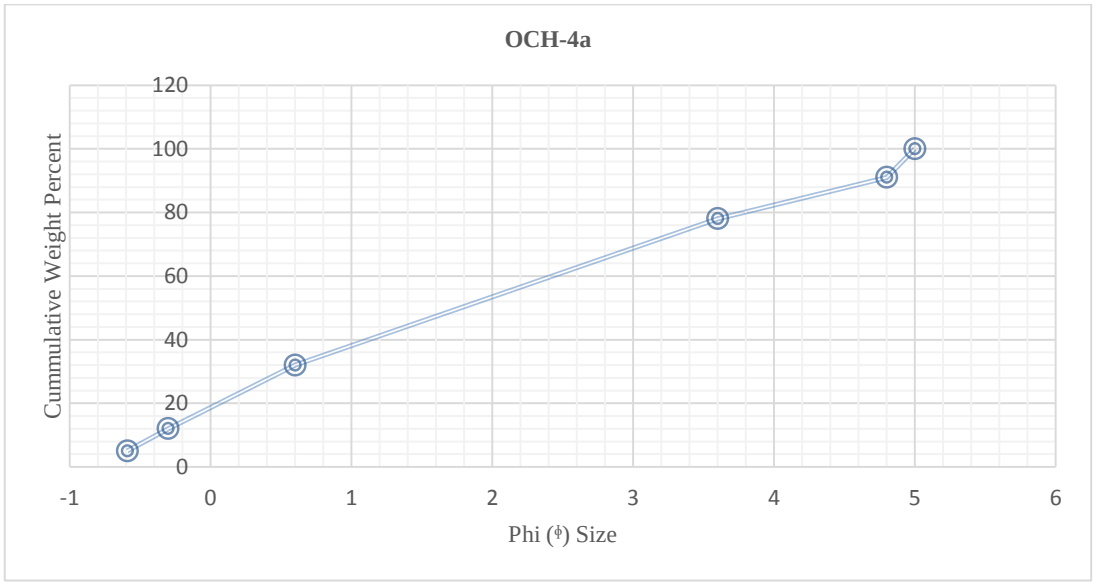
Sieve Size (mm)	Phi Scale (φ)	Weight of sieve (g)	Weight of sieve + Sample retained(g)	Weight of Sample (g)	% weight of Sample	Cumulative Weight%
2mm	-1	465	465	0	0	0
1mm	0	360.61	360.8	0.19	0.19	0.19
500µm	1	313.57	320.5	6.93	6.94	7.13
250µm	2	317.61	360.47	42.85	42.91	50.04
125µm	3	300.93	341.8	40.87	40.93	90.97
63mic	4	268.24	276.7	8.46	8.47	99.44
Pan	5	272.84	273.4	0.56	0.56	100
				99.86	100	



Cumulative frequency curve for sample **OCH-3b**

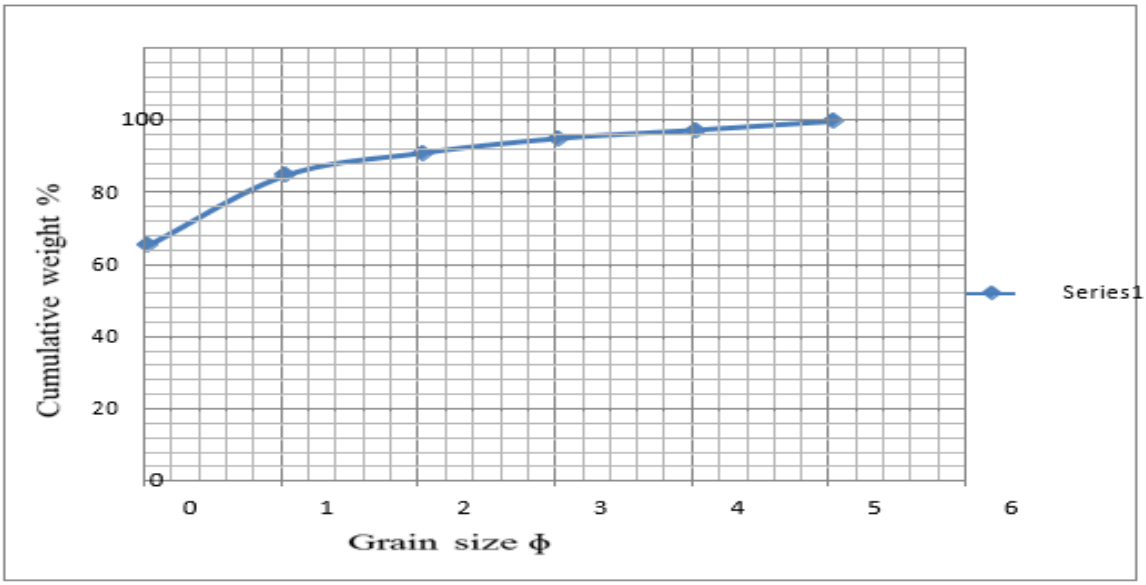
OCH-4a

Sieve size (mm)	ϕ Value	Weight retained (g)	(%) Weight retained	Cumulative weight (%)
0.18	-0.59	5.0	5.0	5.0
600	-0.3	7.0	7.0	12.0
300	0.6	22.0	22.0	34.0
150	3.6	44.0	44.0	78.0
75	4.8	13.0	13.0	91.0
Pan	5.0	9.0	9.0	100
	Total	100	100%	



Sample OCH-4b

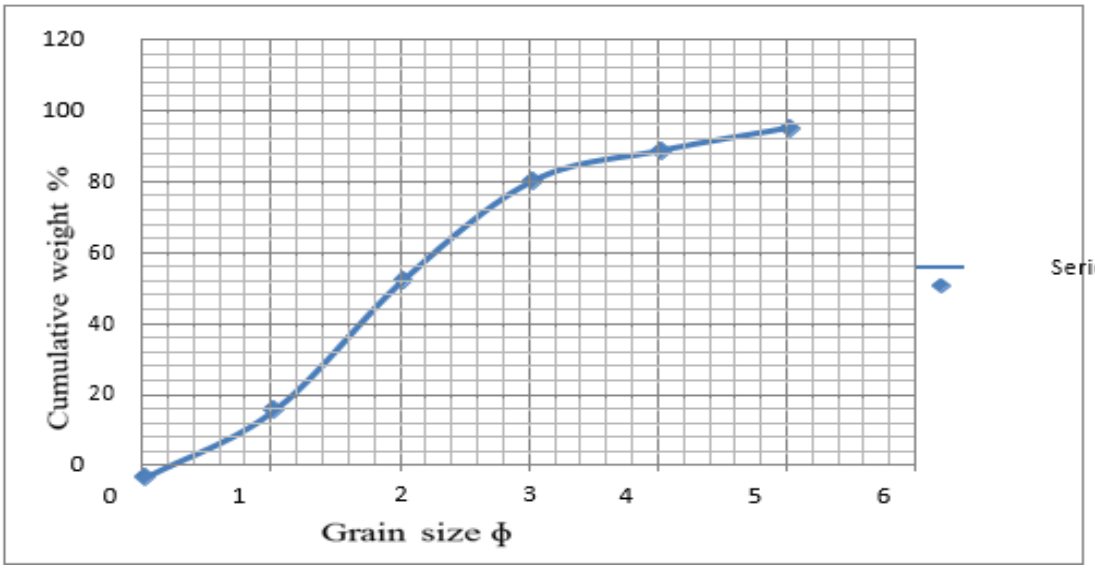
Sieve size (mm)	ϕ Value	Sieve size (mm)	Sample weight (g)	Weight (%)	Cumulative weight (%)
1mm	0	1.000	65.60	65.76	65.76
500µm	1	0.500	19.17	19.22	84.98
250µm	2	0.250	6.24	6.26	91.24
125µm	3	0.125	4.01	4.02	95.26
63mic	4	0.063	2.30	2.31	97.57
Pan	5	<0.063	2.43	2.44	100
	Total		99.75		



Cumulative frequency curve for sample OCH-4b

Sample OCH-5

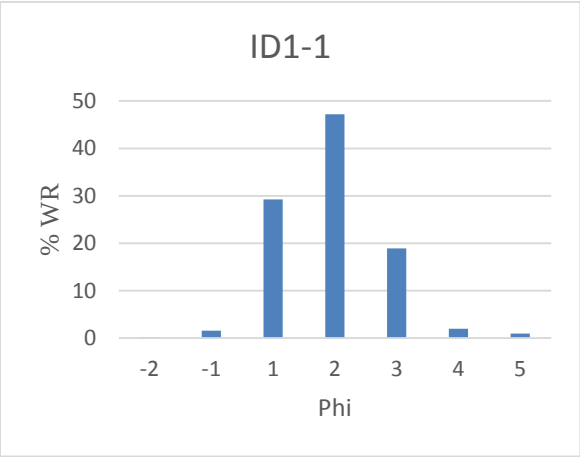
Sieve size (mm)	ϕ Value	Sieve size (mm)	Sample weight (g)	Weight (%)	Cumulative weight (%)
1mm	0	1.000	1.25	1.25	1.25
500µm	1	0.500	19.05	19.05	20.30
250µm	2	0.250	36.76	36.77	57.07
125µm	3	0.125	27.87	27.88	84.95
63mic	4	0.063	8.58	8.58	93.53
Pan	5	<0.063	6.47	6.47	100
	Total		99.98		

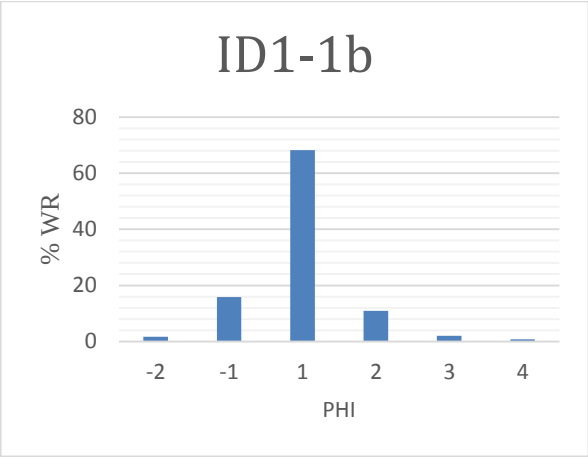


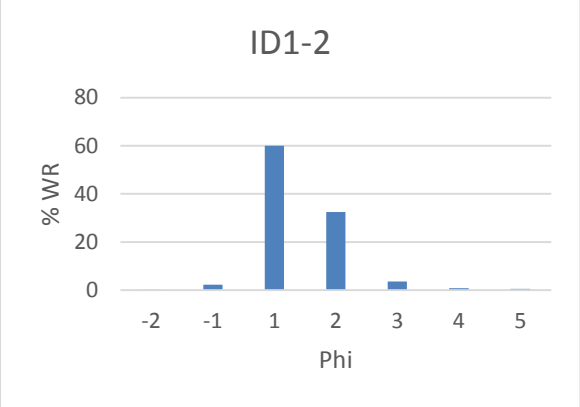
Cumulative frequency curve for sample OCH-5

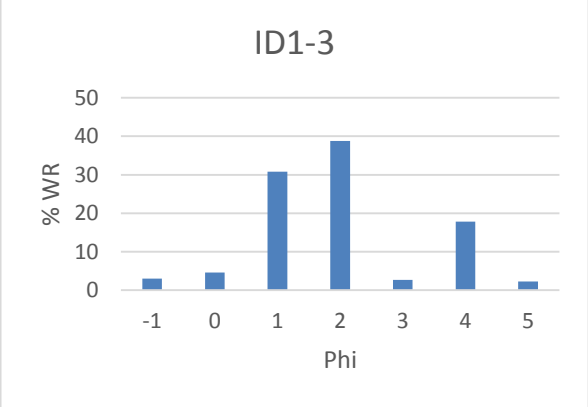
Appendix II: Histogram plots and tables of samples analysed

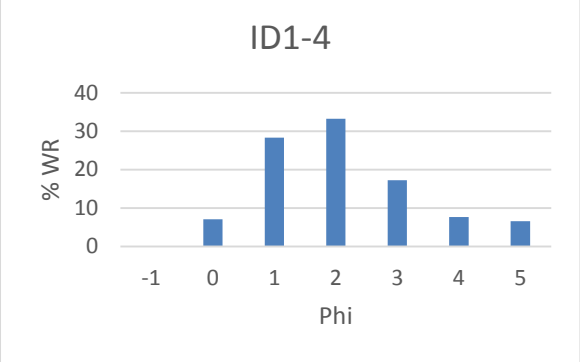
Histogram plots of the Mamu Formation and Ajali Sandstone that underlie the study area.

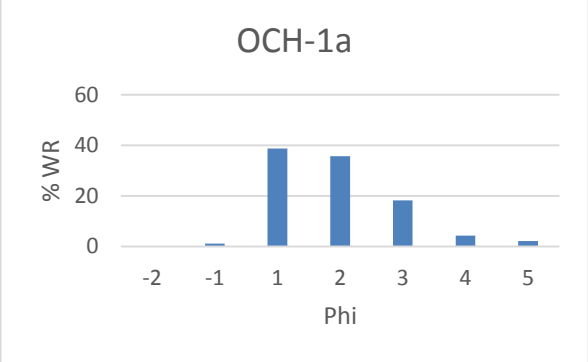


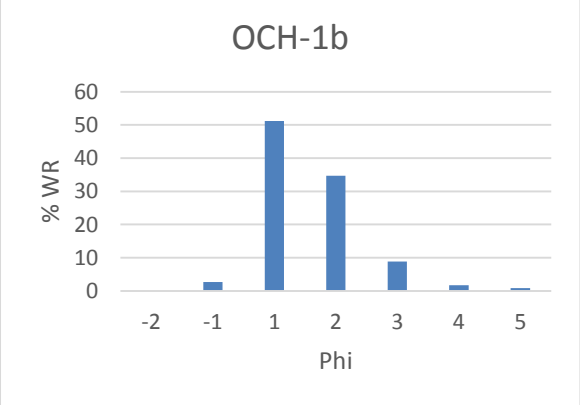


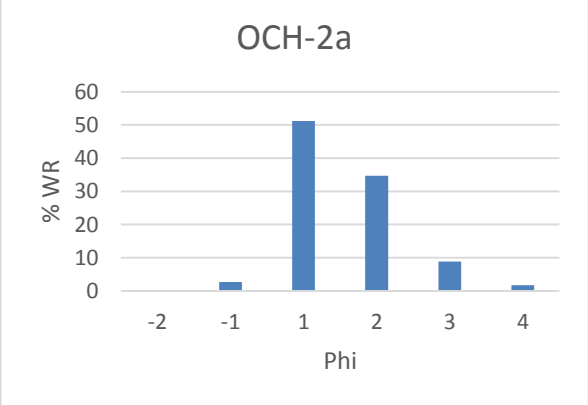


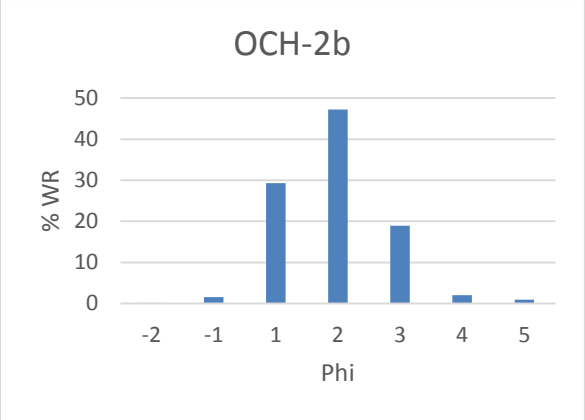


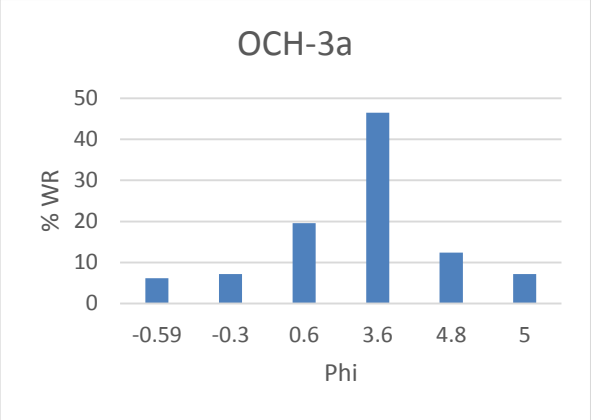


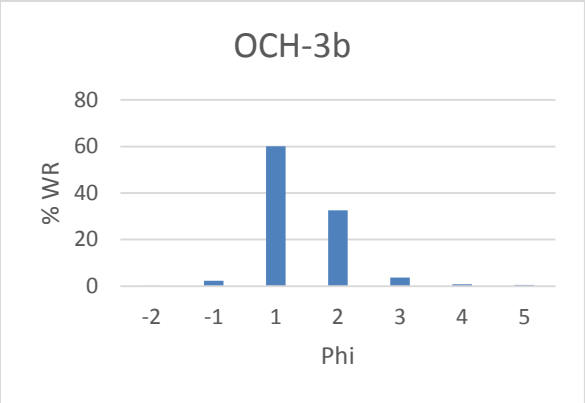


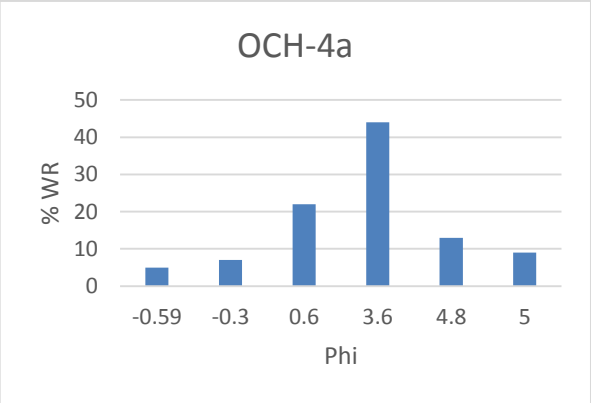


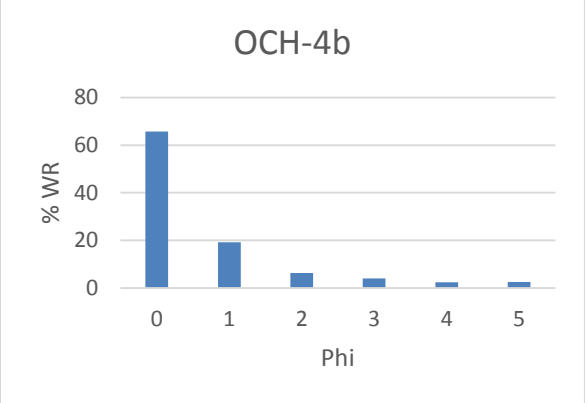


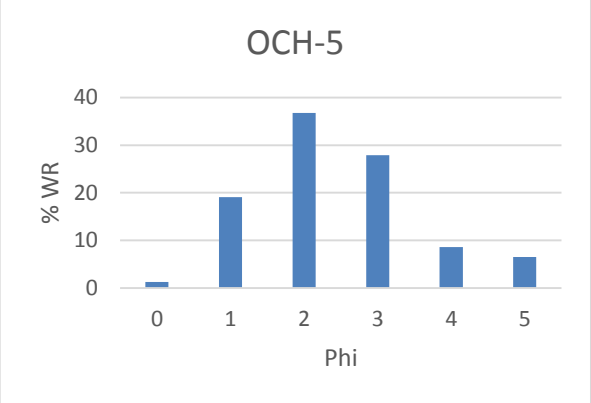

OCH-2b
% WR
50
40
30
20
10
0
-2
-1
1
2
3
4
5
Phi

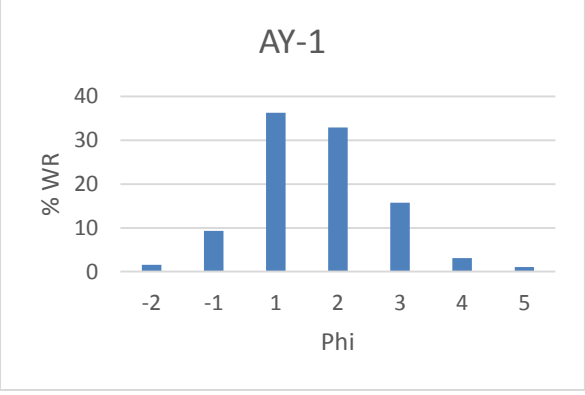

OCH-3a
% WR
50
40
30
20
10
0
-0.59
-0.3
0.6
3.6
4.8
5
Phi

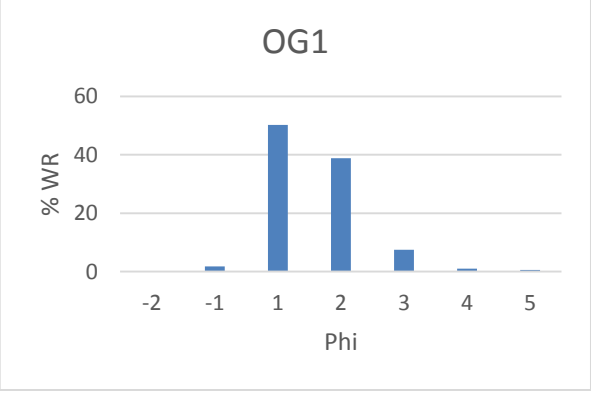

OCH-3b
% WR
80
60
40
20
0
-2
-1
1
2
3
4
5
Phi

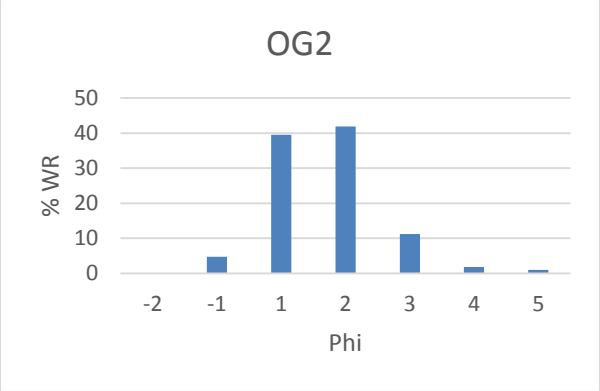

OCH-4a
% WR
50
40
30
20
10
0
-0.59
-0.3
0.6
3.6
4.8
5
Phi

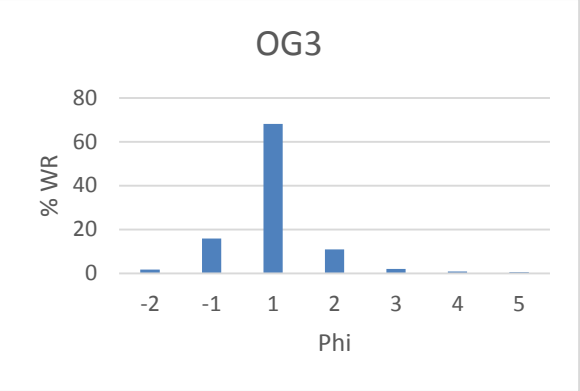

OCH-4b
% WR
80
60
40
20
0
0
1
2
3
4
5
Phi

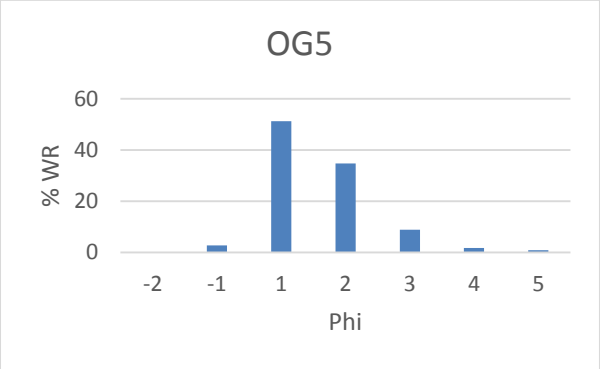

OCH-5
% WR
40
30
20
10
0
0
1
2
3
4
5
Phi

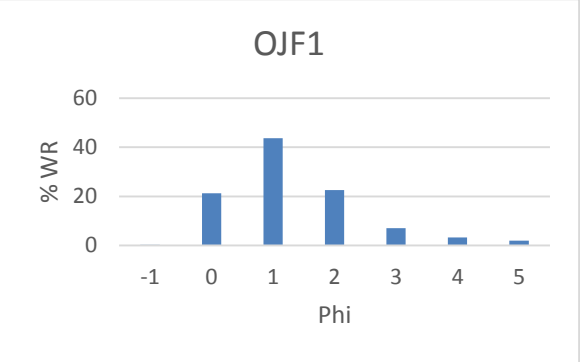

AY-1
% WR
40
30
20
10
0
-2
-1
1
2
3
4
5
Phi

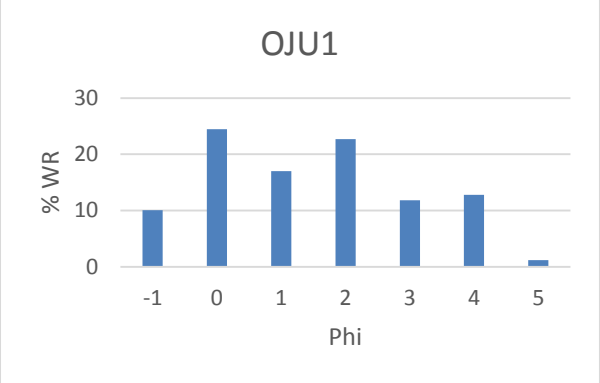

OG1
% WR
60
40
20
0
-2
-1
1
2
3
4
5
Phi

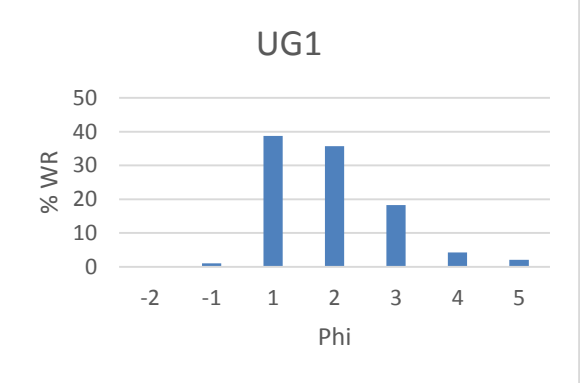

OG2
% WR
50
40
30
20
10
0
-2
-1
1
2
3
4
5
Phi

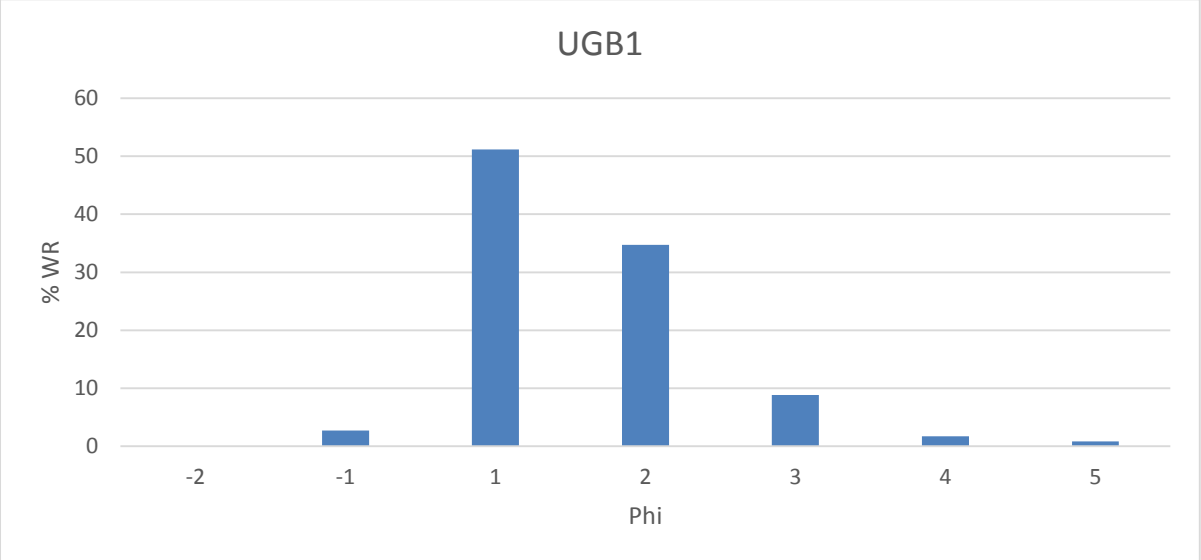

OG3
% WR
80
60
40
20
0
-2
-1
1
2
3
4
5
Phi


OG5
% WR
60
40
20
0
-2
-1
1
2
3
4
5
Phi


OJF1
% WR
60
40
20
0
-1
0
1
2
3
4
5
Phi


OJU1
% WR
30
20
10
0
-1
0
1
2
3
4
5
Phi


UG1
% WR
50
40
30
20
10
0
-2
-1
1
2
3
4
5
Phi


UGB1
% WR
60
50
40
30
20
10
0
-2
-1
1
2
3
4
5
Phi

Appendix III: Calculation of Linear Discriminate Function (Sahu, 1964)

Sample Ay-1

$Y_{1(A:B)} = -3.5688\ M + 3.7016r^2 - 2.0766\ SK + 3.1135\ KG$

$= -3.5688\ (0.92) + 3.7016\ (1.8769) - 2.0766\ (-0.23) + 3.1135\ (0.92)$

$= 7.006$

$Y_{2(B:SM)} = 15.6534\ M + 65.7091\ r^2 + 18.1071\ SK + 18.5043\ KG$

$= 15.6534\ (0.92) + 65.7091\ (1.8769) + 18.1071\ (-0.23) + 18.5043\ (0.92)$

$= 150.590$

$Y_{3(SM:F)} = 0.2852\ M - 8.7604r^2 - 4.8932SK + 0.0482KG$

$= 0.2852\ (0.92) - 8.7604\ (1.8769) - 4.8932(-0.23) + 0.0482(0.92)$

$= -15.010$

Sample ID1(1)

$Y_{1(A:B)} = -3.5688\ M + 3.7016r^2 - 2.0766\ SK + 3.1135\ KG$

$= -3.5688\ (1.28) + 3.7016\ (1.0609) - 2.0766\ (-0.24) + 3.1135\ (1.25)$

$= 3.749$

$Y_{2(B:SM)} = 15.6534\ M + 65.7091\ r^2 + 18.1071\ SK + 18.5043\ KG$

$= 15.6534\ (1.28) + 65.7091\ (1.0609) + 18.1071\ (-0.24) + 18.5043\ (1.25)$

$= 108.532$

$Y_{3(SM:F)} = 0.2852\ M - 8.7604r^2 - 4.8932SK + 0.0482KG$

$= 0.2852\ (1.28) - 8.7604\ (1.0609) - 4.8932(-0.24) + 0.0482(1.25)$

$= -7.694$

Sample ID1(2)

$Y_{1(A:B)} = -3.5688\ M + 3.7016r^2 - 2.0766\ SK + 3.1135\ KG$

$= -3.5688\ (0.57) + 3.7016\ (0.9604) - 2.0766\ (-0.02) + 3.1135\ (0.77)$

$= 3.961$

$Y_{2(B:SM)} = 15.6534\ M + 65.7091\ r^2 + 18.1071\ SK + 18.5043\ KG$

$= 15.6534\ (0.57) + 65.7091\ (0.9604) + 18.1071\ (-0.02) + 18.5043\ (0.77)$

$= 85.916$

$Y_{3(SM:F)} = 0.2852\ M - 8.7604r^2 - 4.8932SK + 0.0482KG$

$= 0.2852\ (0.57) - 8.7604\ (0.9604) - 4.8932(-0.02) + 0.0482(0.77)$

$= -8.116$

Sample ID1(3)

$Y_{1(A:B)} = -3.5688\ M + 3.7016r^2 - 2.0766\ SK + 3.1135\ KG$

$= -3.5688\ (1.6) + 3.7016\ (2.5921) - 2.0766\ (0.1) + 3.1135\ (1.71)$

$= 9.001$

$Y_{2(B:SM)} = 15.6534\ M + 65.7091\ r^2 + 18.1071\ SK + 18.5043\ KG$

$= 15.6534\ (1.6) + 65.7091\ (2.5921) + 18.1071\ (0.1) + 18.5043\ (1.71)$

$= 228.823$

$Y_{3(SM:F)} = 0.2852\ M - 8.7604r^2 - 4.8932SK + 0.0482KG$

$= 0.2852\ (1.6) - 8.7604\ (2.5921) - 4.8932(0.1) + 0.0482(1.71)$

$= -22.658$

Sample ID1(4)

$Y_{1(A:B)} = -3.5688\ M + 3.7016r^2 - 2.0766\ SK + 3.1135\ KG$

$= -3.5688\ (1.5) + 3.7016\ (2.3104) - 2.0766\ (0.06) + 3.1135\ (1.56)$

$= 7.931$

$Y_{2(B:SM)} = 15.6534\ M + 65.7091\ r^2 + 18.1071\ SK + 18.5043\ KG$

$= 15.6534\ (1.5) + 65.7091\ (2.3104) + 18.1071\ (0.06) + 18.5043\ (1.56)$

$= 208.248$

$Y_{3(SM:F)} = 0.2852\ M - 8.7604r^2 - 4.8932SK + 0.0482KG$

$= 0.2852\ (1.5) - 8.7604\ (2.3104) - 4.8932(0.06) + 0.0482(1.56)$

$= -20.031$

Sample OG1

$Y_{1(A:B)} = -3.5688\ M + 3.7016r^2 - 2.0766\ SK + 3.1135\ KG$

$= -3.5688\ (0.8) + 3.7016\ (0.9801) - 2.0766\ (-0.19) + 3.1135\ (0.77)$

$= 3.565$

$Y_{2(B:SM)} = 15.6534\ M + 65.7091\ r^2 + 18.1071\ SK + 18.5043\ KG$

$= 15.6534\ (0.8) + 65.7091(0.9801) + 18.1071\ (-0.19) + 18.5043\ (0.77)$

$= 87.732$

$Y_{3(SM:F)} = 0.2852\ M - 8.7604r^2 - 4.8932SK + 0.0482KG$

$= 0.2852\ (0.8) - 8.7604\ (0.9801) - 4.8932(-0.19) + 0.0482(0.77)$

$= -7.391$

Sample OG2

$Y_{1(A:B)} = -3.5688\ M + 3.7016r^2 - 2.0766\ SK + 3.1135\ KG$

$= -3.5688\ (0.98) + 3.7016\ (1.2321) - 2.0766\ (-0.23) + 3.1135\ (1.04)$

$= 4.779$

$Y_{2(B:SM)} = 15.6534\ M + 65.7091\ r^2 + 18.1071\ SK + 18.5043\ KG$

$= 15.6534\ (0.98) + 65.7091(1.2321) + 18.1071\ (-0.23) + 18.5043\ (1.04)$

$= 111.380$

$Y_{3(SM:F)} = 0.2852\ M - 8.7604r^2 - 4.8932SK + 0.0482KG$

$= 0.2852\ (0.98) - 8.7604\ (1.2321) - 4.8932(-0.23) + 0.0482(1.04)$

$= -9.339$

Sample OG3

$Y_{1(A:B)} = -3.5688\ M + 3.7016r^2 - 2.0766\ SK + 3.1135\ KG$

$= -3.5688\ (-0.02) + 3.7016\ (1.0404) - 2.0766\ (0.04) + 3.1135\ (1.0)$

$= 6.953$

$Y_{2(B:SM)} = 15.6534\ M + 65.7091\ r^2 + 18.1071\ SK + 18.5043\ KG$

$= 15.6534\ (-0.02) + 65.7091(1.0404) + 18.1071\ (0.04) + 18.5043\ (1.0)$

$= 87.279$

$Y_{3(SM:F)} = 0.2852\ M - 8.7604r^2 - 4.8932SK + 0.0482KG$

$= 0.2852\ (-0.02) - 8.7604\ (1.0404) - 4.8932(0.04) + 0.0482(1.0)$

$= -9.268$

Sample OG5

$Y_{1(A:B)} = -3.5688\ M + 3.7016r^2 - 2.0766\ SK + 3.1135\ KG$

$= -3.5688\ (0.85) + 3.7016\ (1.0) - 2.0766\ (-0.14) + 3.1135\ (0.82)$

$= 3.512$

$Y_{2(B:SM)} = 15.6534\ M + 65.7091\ r^2 + 18.1071\ SK + 18.5043\ KG$

$= 15.6534\ (0.85) + 65.7091(1.0) + 18.1071\ (-0.14) + 18.5043\ (0.82)$

$= 91.653$

$Y_{3(SM:F)} = 0.2852\ M - 8.7604r^2 - 4.8932SK + 0.0482KG$

$= 0.2852\ (0.85) - 8.7604\ (1.0) - 4.8932(-0.14) + 0.0482(0.82)$

$= -7.793$

Sample OJF1

$Y_{1(A:B)} = -3.5688\ M + 3.7016r^2 - 2.0766\ SK + 3.1135\ KG$

$= -3.5688\ (0.20) + 3.7016\ (2.3104) - 2.0766\ (-0.095) + 3.1135\ (1.45)$

$= 13.978$

$Y_{2(B:SM)} = 15.6534\ M + 65.7091\ r^2 + 18.1071\ SK + 18.5043\ KG$

$= 15.6534\ (0.20) + 65.7091(2.3104) + 18.1071\ (-0.095) + 18.5043\ (1.45)$

$= 180.056$

$Y_{3(SM:F)} = 0.2852\ M - 8.7604r^2 - 4.8932SK + 0.0482KG$

= 0.2852 (0.20) − 8.7604 (2.3104) − 4.8932(−0.095) + 0.0482(1.45)

= −19.648

Sample OJU1

$Y_{1(A:B)} = -3.5688\ M + 3.7016r^2 - 2.0766\ SK + 3.1135\ KG$

$= -3.5688\ (0.80) + 3.7016\ (3.8809) - 2.0766\ (-1.1) + 3.1135\ (0.73)$

$= 21.778$

$Y_{2(B:SM)} = 15.6534\ M + 65.7091\ r^2 + 18.1071\ SK + 18.5043\ KG$

$= 15.6534\ (0.80) + 65.7091(3.8809) + 18.1071\ (-1.1) + 18.5043\ (0.73)$

$= 261.123$

$Y_{3(SM:F)} = 0.2852\ M - 8.7604r^2 - 4.8932SK + 0.0482KG$

$= 0.2852\ (0.80) - 8.7604\ (3.8809) - 4.8932(-1.1) + 0.0482(0.73)$

$= -28.352$

Sample UG1

$Y_{1(A:B)} = -3.5688\ M + 3.7016r^2 - 2.0766\ SK + 3.1135\ KG$

$= -3.5688\ (1.20) + 3.7016\ (1.4884) - 2.0766\ (-0.07) + 3.1135\ (0.64)$

$= 3.365$

$Y_{2(B:SM)} = 15.6534\ M + 65.7091\ r^2 + 18.1071\ SK + 18.5043\ KG$

$= 15.6534\ (1.20) + 65.7091(1.4884) + 18.1071\ (-0.07) + 18.5043\ (0.64)$

$= 127.161$

$Y_{3(SM:F)} = 0.2852\ M - 8.7604r^2 - 4.8932SK + 0.0482KG$

$= 0.2852\ (1.20) - 8.7604\ (1.4884) - 4.8932(-0.07) + 0.0482(0.64)$

$= -12.323$

Sample UGB1

$Y_{1(A:B)} = -3.5688\ M + 3.7016r^2 - 2.0766\ SK + 3.1135\ KG$

$= -3.5688\ (0.85) + 3.7016\ (1.0) - 2.0766\ (-1.14) + 3.1135\ (0.82)$

$= 5.589$

$Y_{2(B:SM)} = 15.6534\ M + 65.7091\ r^2 + 18.1071\ SK + 18.5043\ KG$

$= 15.6534\ (0.85) + 65.7091(1.0) + 18.1071\ (-1.14) + 18.5043\ (0.82)$

$= 73.546$

$Y_{3(SM:F)} = 0.2852\ M - 8.7604r^2 - 4.8932SK + 0.0482KG$

$= 0.2852\ (0.85) - 8.7604\ (1.0) - 4.8932(-1.14) + 0.0482(0.82)$

$= -2.900$

Sample ID1-1b

$Y_{1(A:B)} = -3.5688\ M + 3.7016r^2 - 2.0766\ SK + 3.1135\ KG$

$= -3.5688\ (0.57) + 3.7016\ (0.7225) - 2.0766\ (0.04) + 3.1135\ (0.80)$

$= 3.047926$

$Y_{2(B:SM)} = 15.6534\ M + 65.7091\ r^2 + 18.1071\ SK + 18.5043\ KG$

$= 15.6534\ (0.57) + 65.7091(0.7225) + 18.1071\ (0.04) + 18.5043\ (0.80)$

$= 71.924987$

$Y_{3(SM:F)} = 0.2852\ M - 8.7604r^2 - 4.8932SK + 0.0482KG$

$= 0.2852\ (0.57) - 8.7604\ (0.7225) - 4.8932(0.04) + 0.0482(0.80)$

$= -6.323993$

Sample OCH-1a

$Y_{1(A:B)} = -3.5688\ M + 3.7016r^2 - 2.0766\ SK + 3.1135\ KG$

$= -3.5688\ (1.20) + 3.7016\ (1.4884) - 2.0766\ (-0.07) + 3.1135\ (0.64)$

$= 3.365$

$Y_{2(B:SM)} = 15.6534\ M + 65.7091\ r^2 + 18.1071\ SK + 18.5043\ KG$

$= 15.6534\ (1.20) + 65.7091(1.4884) + 18.1071\ (-0.07) + 18.5043\ (0.64)$

$= 127.161$

$Y_{3(SM:F)} = 0.2852\ M - 8.7604r^2 - 4.8932SK + 0.0482KG$

$= 0.2852\ (1.20) - 8.7604\ (1.4884) - 4.8932(-0.07) + 0.0482(0.64)$

$= -12.323$

Sample OCH-1b

$Y_{1(A:B)} = -3.5688\ M + 3.7016r^2 - 2.0766\ SK + 3.1135\ KG$

$= -3.5688\ (1.700) + 3.7016\ (0.5184) - 2.0766\ (0.00826) + 3.1135\ (0.94)$

$= -1.2385133$

$Y_{2(B:SM)} = 15.6534\ M + 65.7091\ r^2 + 18.1071\ SK + 18.5043\ KG$

$= 15.6534\ (1.700) + 65.7091(0.5184) + 18.1071\ (0.00826) + 18.5043\ (0.94)$

$= 78.217984$

$Y_{3(SM:F)} = 0.2852\ M - 8.7604r^2 - 4.8932SK + 0.0482KG$

$= 0.2852\ (1.700) - 8.7604\ (0.5184) - 4.8932(0.00826) + 0.0482(0.94)$

$= -4.0516612$

Sample OCH-2a

$Y_{1(A:B)} = -3.5688\ M + 3.7016r^2 - 2.0766\ SK + 3.1135\ KG$

$= -3.5688\ (2.513) + 3.7016\ (0.3339439) - 2.0766\ (0.2522686) + 3.1135\ (0.4527259)$

$= -6.8465666$

$Y_{2(B:SM)} = 15.6534\ M + 65.7091\ r^2 + 18.1071\ SK + 18.5043\ KG$

$= 15.6534\ (2.513) + 65.7091(0.3339439) + 18.1071\ (0.2522686) + 18.5043\ (0.4527259)$

$= 74.225376$

$Y_{3(SM:F)} = 0.2852\ M - 8.7604r^2 - 4.8932SK + 0.0482KG$

$= 0.2852\ (2.513) - 8.7604\ (0.3339439) - 4.8932(0.2522686) + 0.0482(0.4527259)$

$= 3.421353868$

Sample OCH-2b

$Y_{1(A:B)} = -3.5688\ M + 3.7016r^2 - 2.0766\ SK + 3.1135\ KG$

$= -3.5688\ (1.681) + 3.7016\ (1.1025) - 2.0766\ (-0.170) + 3.1135\ (1.22)$

$= 2.2333532$

$Y_{2(B:SM)} = 15.6534\ M + 65.7091\ r^2 + 18.1071\ SK + 18.5043\ KG$

$= 15.6534\ (1.681) + 65.7091(1.1025) + 18.1071\ (-0.170) + 18.5043\ (1.22)$

$= 118.25468$

$Y_{3(SM:F)} = 0.2852\ M - 8.7604r^2 - 4.8932SK + 0.0482KG$

$= 0.2852\ (1.681) - 8.7604\ (1.1025) - 4.8932(-0.170) + 0.0482(1.22)$

$= -8.2882718$

Sample OCH-3a

$Y_{1(A:B)} = -3.5688\ M + 3.7016r^2 - 2.0766\ SK + 3.1135\ KG$

$= -3.5688\ (2.050) + 3.7016\ (3.9382402) - 2.0766\ (0.0588) + 3.1135\ (0.7319)$

$= 9.41841645$

$Y_{2(B:SM)} = 15.6534\ M + 65.7091\ r^2 + 18.1071\ SK + 18.5043\ KG$

$= 15.6534\ (2.050) + 65.7091(3.9382402) + 18.1071\ (0.0588) + 18.5043\ (0.7319)$

$= 306.058166$

$Y_{3(SM:F)} = 0.2852\ M - 8.7604r^2 - 4.8932SK + 0.0482KG$

$= 0.2852\ (2.050) - 8.7604\ (3.9382402) - 4.8932(0.0588) + 0.0482(0.7319)$

$= -34.168341$

Sample OCH-3b

$Y_{1(A:B)} = -3.5688\ M + 3.7016r^2 - 2.0766\ SK + 3.1135\ KG$

$= -3.5688\ (2.00) + 3.7016\ (0.5184) - 2.0766\ (0.09) + 3.1135\ (0.94)$

$= -2.4788946$

$Y_{2(B:SM)} = 15.6534\ M + 65.7091\ r^2 + 18.1071\ SK + 18.5043\ KG$

= 15.6534 (2.00) + 65.7091(0.5184) + 18.1071 (0.09) + 18.5043 (0.94)

= 84.394078

$Y_{3(SM:F)}$ = 0.2852 M − 8.7604r^2− 4.8932SK + 0.0482KG

= 0.2852 (2.00) − 8.7604 (1.0) − 4.8932(0.09) + 0.0482(0.94)

= -4.3660714

Sample OCH-4a

$Y_{1(A:B)}$ = −3.5688 M + 3.7016r^2−2.0766 SK+ 3.1135 KG

= −3.5688 (1.96) + 3.7016 (3.6416089) − 2.0766 (0.1195) + 3.1135 (0.7295)

= 6.2367778

$Y_{2(B:SM)}$ = 15.6534 M + 65.7091 r^2 + 18.1071 SK + 18.5043 KG

= 15.6534 (1.96) + 65.7091(3.6416089) + 18.1071 (0.1195) + 18.5043 (0.7295)

= 285.630388

$Y_{3(SM:F)}$ = 0.2852 M − 8.7604r^2− 4.8932SK + 0.0482KG

= 0.2852 (1.96) − 8.7604 (3.6416089) − 4.8932(0.1195) + 0.0482(0.7295)

= −32.870155

Sample OCH-4b

$Y_{1(A:B)}$ = −3.5688 M + 3.7016r^2−2.0766 SK+ 3.1135 KG

= −3.5688 (0.31) + 3.7016 (0.4356) − 2.0766 (0.99) + 3.1135 (2.87)

= 7.386002

$Y_{2(B:SM)}$ = 15.6534 M + 65.7091 r^2 + 18.1071 SK + 18.5043 KG

= 15.6534 (0.31) + 65.7091(0.4356) + 18.1071 (0.99) + 18.5043 (2.87)

= 104.50881

$Y_{3(SM:F)}$ = 0.2852 M − 8.7604r^2− 4.8932SK + 0.0482KG

= 0.2852 (0.31) − 8.7604 (0.4356) − 4.8932(0.99) + 0.0482(2.87)

= −8.4335522

Sample OCH-5

$Y_{1(A:B)}$ = −3.5688 M + 3.7016r^2−2.0766 SK+ 3.1135 KG

= −3.5688 (1.87) + 3.7016 (1.3225) − 2.0766 (0.25) + 3.1135 (1.15)

= 1.283085

$Y_{2(B:SM)}$ = 15.6534 M + 65.7091 r^2 + 18.1071 SK + 18.5043 KG

= 15.6534 (1.87) + 65.7091(1.3225) + 18.1071 (0.25) + 18.5043 (1.15)

= 141.97887

$Y_{3(SM:F)}$ = 0.2852 M − 8.7604r^2− 4.8932SK + 0.0482KG

$$= 0.2852\,(1.87) - 8.7604\,(1.3225) - 4.8932(0.25) + 0.0482(1.15)$$

$$= -12.220175.$$